

UNCLASSIFIED

AD NUMBER
ADB275131
NEW LIMITATION CHANGE
TO Approved for public release, distribution unlimited
FROM Distribution authorized to U.S. Gov't. agencies only; Proprietary Info.; Jul 2001. Other requests shall be referred to U.S. Army Medical Research and Materiel Command, 504 Scott St., Ft. Detrick, MD 21702-5012.
AUTHORITY
USAMRCM ltr, 29 May 2002

THIS PAGE IS UNCLASSIFIED

AD _____

Award Number: DAMD17-96-1-6088

TITLE: Identification of Two Candidate Tumor Suppressor Genes on Chromosome 17p13.3: Assessment of Their Roles in Breast and Ovarian Carcinogenesis

PRINCIPAL INVESTIGATOR: Andrew K Godwin, Ph.D.

CONTRACTING ORGANIZATION: Fox Chase Cancer Center
Philadelphia, Pennsylvania 19111

REPORT DATE: July 2001

TYPE OF REPORT: Final

PREPARED FOR: U.S. Army Medical Research and Materiel Command
Fort Detrick, Maryland 21702-5012

DISTRIBUTION STATEMENT: Distribution authorized to U.S. Government agencies only (proprietary information, Jul 01). Other requests for this document shall be referred to U.S. Army Medical Research and Materiel Command, 504 Scott Street, Fort Detrick, Maryland 21702-5012.

The views, opinions and/or findings contained in this report are those of the author(s) and should not be construed as an official Department of the Army position, policy or decision unless so designated by other documentation.

20020215 033

NOTICE

USING GOVERNMENT DRAWINGS, SPECIFICATIONS, OR OTHER DATA INCLUDED IN THIS DOCUMENT FOR ANY PURPOSE OTHER THAN GOVERNMENT PROCUREMENT DOES NOT IN ANY WAY OBLIGATE THE U.S. GOVERNMENT. THE FACT THAT THE GOVERNMENT FORMULATED OR SUPPLIED THE DRAWINGS, SPECIFICATIONS, OR OTHER DATA DOES NOT LICENSE THE HOLDER OR ANY OTHER PERSON OR CORPORATION; OR CONVEY ANY RIGHTS OR PERMISSION TO MANUFACTURE, USE, OR SELL ANY PATENTED INVENTION THAT MAY RELATE TO THEM..

LIMITED RIGHTS LEGEND

Award Number: DAMD17-96-1-6088
Organization: Fox Chase Cancer Center

Those portions of the technical data contained in this report marked as limited rights data shall not, without the written permission of the above contractor, be (a) released or disclosed outside the government, (b) used by the Government for manufacture or, in the case of computer software documentation, for preparing the same or similar computer software, or (c) used by a party other than the Government, except that the Government may release or disclose technical data to persons outside the Government, or permit the use of technical data by such persons, if (i) such release, disclosure, or use is necessary for emergency repair or overhaul or (ii) is a release or disclosure of technical data (other than detailed manufacturing or process data) to, or use of such data by, a foreign government that is in the interest of the Government and is required for evaluational or informational purposes, provided in either case that such release, disclosure or use is made subject to a prohibition that the person to whom the data is released or disclosed may not further use, release or disclose such data, and the contractor or subcontractor or subcontractor asserting the restriction is notified of such release, disclosure or use. This legend, together with the indications of the portions of this data which are subject to such limitations, shall be included on any reproduction hereof which includes any part of the portions subject to such limitations.

THIS TECHNICAL REPORT HAS BEEN REVIEWED AND IS APPROVED FOR PUBLICATION.

Nydingha Charan Mishra
01/14/2002

REPORT DOCUMENTATION PAGE

Form Approved
OMB No. 074-0188

Public reporting burden for this collection of information is estimated to average 1 hour per response, including the time for reviewing instructions, searching existing data sources, gathering and maintaining the data needed, and completing and reviewing this collection of information. Send comments regarding this burden estimate or any other aspect of this collection of information, including suggestions for reducing this burden to Washington Headquarters Services, Directorate for Information Operations and Reports, 1215 Jefferson Davis Highway, Suite 1204, Arlington, VA 22202-4302, and to the Office of Management and Budget, Paperwork Reduction Project (0704-0188), Washington, DC 20503

1. AGENCY USE ONLY (Leave blank)		2. REPORT DATE July 2001	3. REPORT TYPE AND DATES COVERED Final (01 Jul 96 - 30 Jun 01)	
4. TITLE AND SUBTITLE Identification of Two Candidate Tumor Suppressor Genes on Chromosome 17p13.3: Assessment of Their Roles in Breast and Ovarian Carcinogenesis			5. FUNDING NUMBERS DAMD17-96-1-6088	
6. AUTHOR(S) Andrew K Godwin, Ph.D.				
7. PERFORMING ORGANIZATION NAME(S) AND ADDRESS(ES) Fox Chase Cancer Center Philadelphia, Pennsylvania 19111 E-Mail: A_Godwin@fcc.edu			8. PERFORMING ORGANIZATION REPORT NUMBER	
9. SPONSORING / MONITORING AGENCY NAME(S) AND ADDRESS(ES) U.S. Army Medical Research and Materiel Command Fort Detrick, Maryland 21702-5012			10. SPONSORING / MONITORING AGENCY REPORT NUMBER	
11. SUPPLEMENTARY NOTES				
12a. DISTRIBUTION / AVAILABILITY STATEMENT Distribution authorized to U.S. Government agencies only (proprietary information, Jul 01). Other requests for this document shall be referred to U.S. Army Medical Research and Materiel Command, 504 Scott Street, Fort Detrick, Maryland 21702-5012.				12b. DISTRIBUTION CODE
13. ABSTRACT (Maximum 200 Words) OVCA1 and OVCA2 were first identified by us as candidate tumor suppressor genes, due to the fact that they map to a critical region of frequent allelic loss in breast and ovarian cancer at 17p13.3. Our studies have shown that OVCA1 is mutated in some tumor cell lines, and its protein levels are decreased or lost in nearly 40% of breast and ovarian adenocarcinomas, while OVCA2 appears to be unaffected. Expression of low levels of exogenous OVCA1 results in dramatic growth suppression and decreased levels of cyclin D1. We used a yeast-2-hybrid screen to identify OVCA1-associating proteins. One such protein, RBM8, was identified. Amino acid sequence indicates that RBM8 is a new member of an RNA-binding motif (RBM) family which is highly conserved evolutionarily. RBM8, also know as Y14 has been shown to be a shuttling protein that preferentially associates with spliced mRNA in the nucleus and remains associated with newly exported mRNA in the cytoplasm. Mutational analysis revealed no somatic mutations in ovarian tumor, however, our current studies suggest that RBM8 is involved in mRNA export and that its levels may be significantly upregulated in most transformed cells. Overall, our studies indicate that altered expression and/or post-translational modifications of OVCA1 is associated with the development of breast and ovarian tumors and suggest a potentially new mechanism for the inactivation of tumor suppressors in cancer.				
14. SUBJECT TERMS Breast Cancer, Ovarian Cancer, RNA Binding Protein, Tumor Suppressor				15. NUMBER OF PAGES 96
				16. PRICE CODE
17. SECURITY CLASSIFICATION OF REPORT Unclassified	18. SECURITY CLASSIFICATION OF THIS PAGE Unclassified	19. SECURITY CLASSIFICATION OF ABSTRACT Unclassified	20. LIMITATION OF ABSTRACT Unlimited	

Table of Contents

Cover 1

SF 298 **2**

Introduction **4**

Body **4**

Key Research Accomplishments **19**

Reportable Outcomes **20**

Conclusions **23**

References **25**

Personnel **33**

Appendices **34**

4. INTRODUCTION:

Breast cancer is the second most common form of cancer in women, striking 1 out of 8 women in their lifetime. Ovarian cancer strikes fewer women but is generally at an advanced stage at the time of detection. Both diseases are controlled by multiple genetic defects, suggesting the involvement of many different genes, including tumor suppressors. According to the two-hit model of Knudson, both alleles encoding for a tumor suppressor must be lost or inactivated in order for cancer to develop. Based on this model, loss of heterozygosity (LOH) of alleles from tumor tissue has been used to suggest the presence of potential tumor suppressor genes.

The short arm of chromosome 17 is one of the most frequently altered regions in human breast and ovarian cancer. One locus of high allelic loss is at 17p13.1, and contains the tumor suppressor gene, *TP53*. However, we and others have shown a second region of LOH distal to the *TP53* gene, at 17p13.3, in breast tumors and ovarian tumors. Genomic abnormalities involving 17p13.3 has also been reported in primitive neuroectodermal tumors, carcinoma of the cervix uteri, medulloblastoma, osteosarcoma, astrocytoma (22), and acute myeloid leukemia and myelodysplastic syndromes, suggesting that a gene(s) on 17p13.3 may play a role in the development of a wide variety of neoplasms, including breast and ovarian cancer.

We have previously defined a minimum region of allelic loss (MRAL) on chromosome 17p13.3 in genomic DNA from ovarian tumors and breast tumors. Positional cloning and sequencing techniques revealed two genes in the MRAL, referred to as *OVCA1* and *OVCA2*, which overlap one another in the MRAL, and have one exon in common. Since translation of *OVCA1* does not proceed into the shared exon, the genes encode for completely distinct proteins. The function of *OVCA1* and *OVCA2* are unknown and their potential role in breast and ovarian oncogenesis has been a major focus of our studies.

5. BODY:

Relevant data that are referenced in this final report are contained in the manuscripts included in the appendices. Other significant data which has yet to be published are included below or have previously been reported in one of the four past annual progress reports.

6.1. Overview of Project

The original proposal focused on determining the role of *OVCA1* in breast and ovarian carcinogenesis. We proposed to evaluate the potential role of *OVCA1* in the development of ovarian cancer by 1) determining the

frequency at which mutations occur in this gene in an extensive panel of ovarian tumors using Single Strand Conformation Polymorphism (SSCP), and direct sequencing, and 2) evaluating its ability to suppress clonal outgrowth when introduced by transfection into tumor cell lines that express reduced levels of OVCA1. Since this locus is also involved in breast cancer, we performed mutational analyses on a large panel of breast tumors as well. We also initiated studies to determine the function of OVCA1 by establishing the subcellular location of this protein using antibodies generated against OVCA1 and by identifying potentially important protein interactions by two-yeast hybrid trap methods. Overall, these studies provided insights into the potential role of OVCA1 in the pathogenesis of sporadic breast and ovarian cancer.

We accomplished all of the original aims and have made additional progress which is relevant. We have continued our efforts to understand the function of OVCA1 by further characterizing its protein interactors and have been attempting to derive Ovca1 +/- ES cells, all in the absence of funding for the past 15 months. We are dedicated to the pursuit of the function of this protein and propose in this offering to determine the biological and biochemical functions of OVCA1 by focusing primarily on its interaction with RBM8A, a novel, yet highly conserved nuclear RNA binding protein that has recently been found to interact with newly exported cytoplasmic mRNAs. There is growing evidence that proteins involved in pre-mRNA splicing and mRNA metabolism are intimately involved in the regulation of cell cycle progression, however their roles in tumorigenesis has not been thoroughly explored and will be addressed in this proposal.

6.2 Evidence for a tumor suppressor locus on chromosome 17p13.3

Chromosome 17 aberrations are the most common genetic abnormality in human breast and ovarian cancer and appear to be an early event in tumorigenesis (1-4). There are at least two tumor suppressor genes other than *BRCA1* and *TP53* present on chromosome 17 which are involved in breast cancer proliferation (5-7). A recent study of 1,280 breast tumors found that the frequency of LOH observed on the p arm of chromosome 17 was much higher than that observed on the q arm: two regions on 17p include *TP53* (17p13.1) and a more telomeric region at 17p13.3 that includes D17S5/30 (YNZ22.1) and D17S28 (YNH37.3) were defined (8).

Numerous studies have shown that YNZ22.1 allele imbalance is more common than *TP53* mutation in breast and ovarian cancer (3, 4, 9-20) and surprisingly that LOH of D17S5/30 is independent of alterations involving *TP53* (3, 19-21). Up to two-thirds of breast tumors show LOH at the YNZ22.1 locus (9, 13, 19, 20, 22-24) and this finding has been associated with markers of tumor aggression (8, 19, 25, 26).

In a recent study of ovarian tumors, it was reported that YNZ22.1 had an 80% (37 of 46 informative malignant tumors) rate of LOH on chromosome 17p, and YNH37.3 showed 65% LOH (15 of 23 informative malignant tumors) (27). Loss at either D17S30 or D17S28 was observed in 80% (4 of 5) of carcinomas without metastases (FIGO stage I), and 90% (27 of 30) of high-stage carcinomas (FIGO stage II-IV) (3).

This same region shows frequent loss of heterozygosity in 12 other tumor types including small-cell lung cancers (28-30), colon cancers (31), medulloblastoma (32-35), astrocytoma (36, 37), malignant melanoma (38), hepatocellular carcinoma (39), leukemia and lymphoma (40). In many of these studies changes on chromosome 17p13.3 occur in the absence of alterations involving *TP53*, suggesting that a tumor suppressor gene(s) residing in this region on chromosome 17p13.3 may be involved in the development of many types of cancers.

6.3 *The OVCA locus*

We reported the identification of a common region of allelic loss on 17p13.3 in ovarian cancer defined by the markers D17S28 and D17S5/S30 (41). These two loci span less than 20 kbp (41). We refer to this region as the *OVCA* (Ovarian Cancer) locus. Using various positional cloning methods, we have identified four previously unreported genes, which we provisionally refer to as *OVCA1*, *OVCA2*, *OVCA3*, and *OVCA5* that map to this critical region (41). *OVCA1*, 2 and 3 are ubiquitously expressed, while *OVCA5* is present at very high levels in testis (data not shown). A fifth gene, *OVCA4*, which is just outside this minimal region of allelic loss, has also recently identified by us (data not shown). We have demonstrated some interesting properties of *OVCA1* related to cell growth and tumor suppression, and have focused much of our studies on the characterization of this unique protein.

To date, only two genes have been reported that map within the critical region of allelic loss on chromosome 17p13.3 defined by YNH37.3 and YNZ22.2; *OVCA1* and *OVCA2*. We have shown that over-expression of *OVCA1*, but not *OVCA2* can suppress tumor cell proliferation (42). We continue to be excited about the potential role of *OVCA1* in breast and ovarian carcinogenesis and believe that reduced expression due to allelic loss (e.g., haplo-insufficiency), altered protein stability, aberrant post-translational modifications, and inactivating mutations may all contribute to the development of these and other cancers.

6.4 *Growing evidence that haploinsufficiency plays a role in tumorigenesis*

It has previously been thought that both alleles of a tumor suppressor gene must be inactivated, as expostulated by Knudson's "2-hit" hypothesis (43). As with other hypotheses in biology, it is now clear that the mechanisms for inactivation must be expanded and revised [reviewed in (44)]. One key revision is the

concept of haplo-insufficiency. It has recently been shown in mouse knockout models that *p27/kip1*, *Nf1*, and *Pten* are haplo-insufficient for tumor suppression (45-47). Although low levels of the p27 protein are frequently found in human carcinomas (48-52), it was not possible to establish a causal link between p27 and tumor suppression because only rare instances of homozygous inactivating mutations of the *p27* gene were found (53-56). Yet, both *p27* nullizygous and *p27* heterozygous mice are predisposed to tumors in multiple tissues when challenged with gamma-irradiation or a chemical carcinogen (57). Molecular analyses showed that the remaining wild-type *p27* allele was neither mutated nor silenced (57). Gutmann and colleagues have found an increase in the number of cerebral astrocytes and increased astrocyte proliferation in *Nf1* heterozygous mice as compared to wild-type littermates. Their studies suggest that reduced NF1 expression results in increased astrocyte proliferation that may be sufficient for the development of astrocytic growth abnormalities in patients with NF1 (58). The *PTEN* gene encodes a dual-specificity phosphatase mutated in a variety of human cancers (59-61). *PTEN* germline mutations are found in three related human autosomal dominant disorders, Cowden disease (CD), Lhermitte-Duclos disease (LDD) and Bannayan-Zonana syndrome (BZS), characterized by tumor susceptibility and developmental defects (62-64). It was recently reported that *Pten*^{+/-} mice and chimaeric mice derived from *Pten*^{+/-}-ES cells showed hyperplastic-dysplastic changes in the prostate, skin and colon, which are characteristic of CD, LDD and BZS (45). They also spontaneously developed germ cell, gonadostromal, thyroid and colon tumors, suggesting that *PTEN* haploinsufficiency plays a causal role in CD, LDD, and BZS (45). These studies therefore suggest that there is another class of tumor suppressor genes: genes that when in the haploinsufficient state lead to reduced levels of the protein, thus resulting in tumorigenesis. This is of great significance given that the *OVCA* locus shows LOH in >80% of ovarian tumors and that hemizyosity is the most frequent observed aberration.

6.5 Rationale for studying *OVCA1*

The data presented here and elsewhere, i.e. high rate of allelic loss observed for chromosome 17p13.3 in ovarian tumors, the abnormal expression of *OVCA1* in the majority of breast and ovarian carcinomas, and the observation that an equimolar level of exogenous p50^{*OVCA1*} suppresses the growth rate of tumor cells up to 10-fold and reduces tumorigenicity, suggests that a slight reduction in the level of expression of *OVCA1* or its mislocalization is sufficient for loss of growth regulation. The high rate of loss of one copy of chromosome 17p in breast and ovarian tumors may contribute to carcinogenesis by reducing *OVCA1* to hemizyosity.

6.6 Previous proposal

The original application which proposed to evaluate the potential role of *OVCA1* in the development of breast and ovarian cancer was well received. The specific objectives in our 1996 proposal were to 1) *determine*

the frequency at which mutations occur in the OVCA1 gene in both breast and ovarian cancer. Assess expression of OVCA1 transcripts (both normal and variant) in tumors and tumor cell lines, 2) evaluate the ability of OVCA1 to suppress cellular growth by introducing into tumor cell lines inducible expression vectors carrying the full-length cDNA and determine the effects of OVCA1 inhibition on cell proliferation via antisense DNA, and 3) evaluate the protein levels in breast and ovarian tumors and tumor cell lines using antibodies specific for OVCA1 and OVCA2. Determine the subcellular location and relevant protein interactions of OVCA1. Determine the effect of tumor-specific alterations on OVCA1 function. We have accomplished all of the specific aims in our funded proposal and have greatly surpassed these initial goals as outlined below.

6.7 Overview of chromosome 17p13.3 and OVCA1 in breast and ovarian cancer

We identified a common region of allelic loss between two highly polymorphic DNA markers on 17p13.3, YNH37.3 and YNZ22.1 (4, 41). These two markers were predicted to be anywhere from 2 to 3.5 centimorgans apart (roughly equivalent to 2 to 3.5 megabases). Remarkably, they are in fact separated by less than 20 kbp, suggesting that the recombination frequency between these two markers is quite high. Using standard positional cloning approaches, we identified several previously unreported genes, including *OVCA1* that maps to this critical region. Northern blot analysis revealed that *OVCA1* mRNA was expressed in normal surface epithelial cells of the ovary, but the level of the transcript was significantly reduced or was undetectable in >70% of ovarian tumors and tumor cell (41). *OVCA1* is highly conserved in mammals and also shares significant amino acid sequence identity when compared to proteins from the nematode and yeast. The predicted gene product of *OVCA1* showed 60% and 53% sequence identity over 328 and 367 of the 443 amino acid residues when compared to *Caenorhabditis elegans* and *Saccharomyces cerevisiae* proteins, respectively. If conserved amino acids substitutions are considered, the sequence similarity is increased to 77% and 89%, respectively (41). No known functional domains match *OVCA1*, indicating that it is a member of a novel class of proteins with an uncharacterized biochemical function. Based on evolutionary distances it appears that *OVCA1* may be a member of a novel family of proteins with two subfamilies. Searches of protein databases and translated ESTs identified significant sequence identity between the N-terminal portion of *OVCA1* and the yeast diphthamide biosynthesis protein 2, *dph2*, suggesting that *OVCA1* may have a yet undefined enzymatic activity. We have subsequently cloned what we believe is the human homolog of *dph2*, referred to as *hDPH2L2*, and found it to be distinct from *OVCA1* (65). We have recently shown that *OVCA1* is abnormally expressed in the majority of breast and ovarian tumors and have shown that exogenous expression of *OVCA1* can suppress tumor growth *in vitro* and tumor formation *in vivo*. Overall, we employed several approaches to evaluate the potential role of *OVCA1* in the development of breast and ovarian cancer. Much of these data have been published and are included in the Appendix.

6.8 Mutation analysis

Mutational Analysis of *OVCA1* by SSCP. SSCP and sequence analyses were conducted on 50 ovarian tumors independent of LOH status for markers on 17p13.3, and 20 breast tumors demonstrating allelic loss for *OVCA1* and retention of *TP53*. Multiple sequence variants were identified throughout the gene (42). Of note, we did detect single somatic mutations (not present in corresponding constitutive DNA samples) in introns 6, 10, and 11 when screening breast and ovarian tumors (unpublished data). All were single nucleotide deletions.

We identified several somatically acquired alterations which suggested that aberrant splicing of *OVCA1* might be involved in carcinogenesis. A sequence alteration in intron 12 near the 5'-splice site was detected in four independent ovarian tumor cell lines, but not in the corresponding constitutional DNA for two of the individuals (the other two DNAs were not available). This variation has not been observed in the germline of our control population. RT-PCR analysis of these tumor cell line RNAs revealed expression of an alternatively spliced transcript of *OVCA1* (data not shown). However, the 50 kDa protein encoded by the modified transcripts is not predicted to be altered (since it occurs after stop codon in exon 12), therefore, the significance of this acquired mutation was not readily apparent. We have recently shown that this splice site mutation may lead to aberrant splicing and modify the reading frame of the p85^{OVCA1} (see Defining the origin of the p70/p85^{OVCA1} proteins in this section).

Interestingly, we identified two non-conservative amino acid substitutions, Ala34Asp and Arg389Ser. Each alteration was detected in the germline of a woman with breast cancer and with a strong family history of the disease. In both cases the missense mutation/rare polymorphism was retained in the corresponding breast tumor DNA and showed reduction to homozygosity (data not shown). Evaluation of more than 200 control chromosomes have failed to detect these sequence variants. The probands do not have unusual ancestries, indicating that the sequence alterations are unlikely to be related to a specific ethnic group. Unfortunately, these individuals are now deceased and we did not receive informed consent from the patient to approach other family members. Both of these probands have tested negative for germline mutations in *BRCA1* and *BRCA2* (Godwin, unpublished data). This is of potential relevance given that recent estimates predict that mutations in *BRCA1* and *BRCA2* account for between 30 to 40% of families with 4 to 5 breast cancers, suggesting that other breast cancer predisposing genes exist (66, 67). In the experiments described below we evaluated the affect of these mutations on cell growth and found that both *OVCA1* mutants reduced abilities to suppress tumor cell growth as compared to wild-type *OVCA1* (see below).

6.9 Tumor suppressor activity

Suppression of Clonal Outgrowth by OVCA1. Attempts to generate cell lines that stably over-expressed OVCA1 were generally unsuccessful. The few clones that did express OVCA1 expressed only low levels of the protein. This phenomenon was consistently observed in a number of different cell types [RAT-1, U2OS, MCF-7, HIO118, and T-47D cells; see (42)]. To quantitate this effect, equimolar amounts (2.5-5 pmol) of a mammalian expression vector containing an amino terminal HA tagged OVCA1 (pcDNA3-*HAOVCA1*) and an empty expression vector (pcDNA3) were transfected into the ovarian cancer cell line, A2780. The A2780 cell line was chosen because it is a well-characterized ovarian tumor line that expresses low levels of p50^{OVCA1} and no detectable p85^{OVCA1}. Evaluation of colony formation in the presence of G418 consistently showed a 50% to 60% reduction in colony number by the *OVCA1* construct as compared to the control construct. This effect was observed in 8 independent transfection experiments and was similar to the level of suppression observed for *TP53* transfection experiments and was independent of plasmid DNA purity and was observed if either equivalent molar amounts or microgram amounts of plasmid were transfected. Furthermore, experiments in which an expression vector containing the gene encoding for the β -galactosidase protein were co-transfected with *OVCA1* indicate that the reduction in clonal outgrowth is not an artifact due to differences in transfection efficiency (data not shown). In comparison, cells that constitutively over-express OVCA2 were numerous (similar to plasmid only control) and easy to establish (data not shown). The fact that cosmids containing ~40 kbp DNA that included the entire minimum region of allelic loss (i.e., *OVCA1* and *OVCA2*) are capable of suppressing clonal outgrowth to a similar extent suggest that *OVCA1* is most likely the gene responsible for this phenotype [(41) and Godwin, unpublished data].

Growth Kinetics of Stable Transfectants. To verify that the suppression effect was due to exogenous OVCA1 expression, seven colonies from pcDNA3 vector control transfected cells and 15 colonies from pcDNA3-*HAOVCA1* transfected cells were amplified following selection for 10 days. All colonies selected from pcDNA3 vector control plates expanded and formed stable cultures. In contrast, only 9 of 15 colonies selected from pcDNA3-*HAOVCA1* transfected cells expanded to form a stable culture. Western blot analysis revealed that there was approximately equimolar expression of exogenous and endogenous OVCA1 in only 4 of 9 stable pcDNA3/*HA-OVCA1* clones (OV-4, OV-5, OV-9, OV-13) (see Appendix, Bruening et al., 1999). The other five cell clones failed to express any detectable levels of HA-OVCA1.

Of the HA-OVCA1 transfectants with exogenous expression, no differences in morphological features were observed when compared to parental A2780 cells (data not shown). However, independent clones, OV-5, OV-13, OV-9 displayed an approximate 8-fold, 10-fold, and 4-fold reduction in growth when compared to

expression vector controls and parental A2780 cells, respectively. We calculated that A2780 cells double only 2-2.5 times during a 24 hour period, while OV-5, OV-9 and OV-13 double approximately 1-1.5 times. Consistent with the reduced growth rate, the clones stably expressing OVCA1 have a dramatic reduction in cyclin D levels. Expression of OVCA1 also dramatically inhibits tumor growth *in vivo*. By week 4 the A2780 vector control line had metastasized to the liver and lung and the animals were euthanized, whereas no palpable tumors were evident for animals injected with OV-4. Interestingly, by week five palpable tumors were detected in OV-4 animals and these tumors rapidly progressed. Evaluation of tumor tissue from these animals found no evidence of the OVCA1/HA protein, indicating that the tumors arose from revertants.

OVCA1 Mutations found in breast cancer patients fail to suppress tumor growth. We evaluated whether the A34D and S389R missense mutations affected the ability of OVCA1 to suppress growth *in vitro*. The two mutations were introduced into the pcDNA3-OVCA1HA expression plasmid. Both mutant proteins expressed equally well in transient transfection assays (data not shown). Protein containing the A34D or the S389R mutation and vector alone were not able to suppress tumor cell growth *in vitro* as well as OVCA1/HA (wild-type) or TP53 (wild-type) in a transient assay. Interestingly, expression of a mutant form of OVCA1 (OVCA1nuc) that is targeted to the nucleus enhances cell growth as compared to vector controls. We are aware that many genes cause toxic or detrimental effects when overexpressed and have shown that the human embryonic kidney 293 cells show no adverse effect when OVCA1 is overexpressed (42). Moreover, the A34D mutant OVCA1, and the S389R to a lesser extent do not appear to suppress growth and OVCA1nuc actually enhances growth. Thus, we feel that we have shown that the growth suppressive effects seen are indeed specific for OVCA1 and not due to nonspecific effects.

6.10 Subcellular localization

Anti-OVCA1 Antibodies. We have generated antibodies to both the amino- and carboxy-terminus of OVCA1. This is summarized in **Table 1**. Both N- and C-terminal antibodies are able to recognize bacterially expressed and *in vitro* translated OVCA1 by Western blotting (data not shown). In addition, these antibodies are able to recognize proteins of ~50 kDa in whole cell lysates from the ovarian tumor cell line A2780. Recognition of this 50 kDa protein can be competed with a molar excess of the antigenic peptide, indicating that the antibodies recognize the authentic OVCA1 protein (data not shown). In addition to the 50 kDa protein, antibodies detect proteins of approximately 85 kDa in extracts prepared from a variety of sources, including

normal human tissues and primary cultures of human ovarian surface epithelial (HOSE) cells (42). The

Table 1. OVCA1 antibodies

Ab	Epitope	Proteins Rec.
TJ132	a.a. 20-31	p50, p70, p85, OVCA1HA, <i>in vitro</i> translated
FC21	a.a. 330-443	p48*, p70, p85, OVCA1HA, <i>in vitro</i> translated
FC22	a.a. 330-443	p48*, p70, p85, OVCA1HA, <i>in vitro</i> translated

*=unmodified form, see below

amino-terminal antibody TJ132 recognizes a protein with a molecular weight of about 70 kDa. Recent evidence suggests that the 70 and 85 kDa forms are proteins encoded by alternatively spliced form of OVCA1 (see below).

Subcellular localization of OVCA1. To assist in understanding the function of OVCA1, its subcellular localization was determined. COS-1 cells were transfected with either an empty vector or with pcDNA3-OVCA1HA. Immunostaining with an anti-HA antibody (Y-11; Santa Cruz) indicates that OVCA1 is localized to punctate bodies. These bodies are scattered throughout the cell, and are heavily clustered around the nucleus. A similar pattern was obtained in immortalized HOSE cells transfected with pcDNA3-OVCA1HA, and when the cells were immunostained with the specific anti-OVCA1 antibody, TJ132 (data not shown). To further confirm the localization, OVCA1 was fused to the carboxyl terminus of the green fluorescent protein (GFP). COS-1 cells expressing the GFP-OVCA1 fusion again demonstrated a punctate, primarily perinuclear localization of the protein (Bruening and Godwin, unpublished data).

Fractionation studies confirmed that the 50 kDa OVCA1 protein is located throughout the cell. The 50 kDa form was found in nuclear, cytoplasmic, and membrane fractions. Extraction of OVCA1 using a variety of buffers indicated that p50 exists in both a soluble and insoluble form. However, the 70 kDa and 85 kDa species appear to be exclusively located within the nucleus.

Expression of OVCA1 in breast and ovarian tumors: There has been some questions regarding the role of OVCA1 in breast and ovarian cancer. Therefore, we analyzed tumor extracts and found that the p85/p70 form was absent in the majority of tumors analyzed (100% of breast tumors, 85% of ovarian tumors), while p50 levels were absent or reduced (by at least 50%) in extracts prepared from breast (39%; 18/46) and ovarian (36%; 21/59) tumors when compared to extracts from primary cultures of mammary or ovarian surface epithelial cells, respectively (42).

In order to further analyze the expression of OVCA1, we performed immunohistochemistry on normal ovaries and benign and malignant ovarian tumors using N- and C-terminal OVCA1 antibodies. In epithelial cells of normal ovaries and ovarian tumors of low malignant potential, strong nuclear and cytoplasmic staining in the epithelial cells was observed using both antibodies. In contrast, 90% (9/10) of ovarian carcinomas showed little or no cytoplasmic staining using the N-terminal antibody. However, varying intensities of nuclear staining (high/medium in 5/9 tumors and light staining in 4/9 tumors) was observed. Interestingly, no nuclear staining or cytoplasmic staining was observed with the C-terminal antibodies (both FC21 and 22). In addition to OVCA1,

all sections are simultaneously stained with antibodies to OVCA2, cytokeratin, Ki-67, and BRCA1 to insure that our immunohistochemical techniques are appropriate. Overall, by immunohistochemistry, we determined that OVCA1 was abnormally expressed in the majority of ovarian adenocarcinomas as compared to normal epithelium. We have also found in some tumors, which still express OVCA1 by Western blotting, that the protein may be mislocalized to the nucleus.

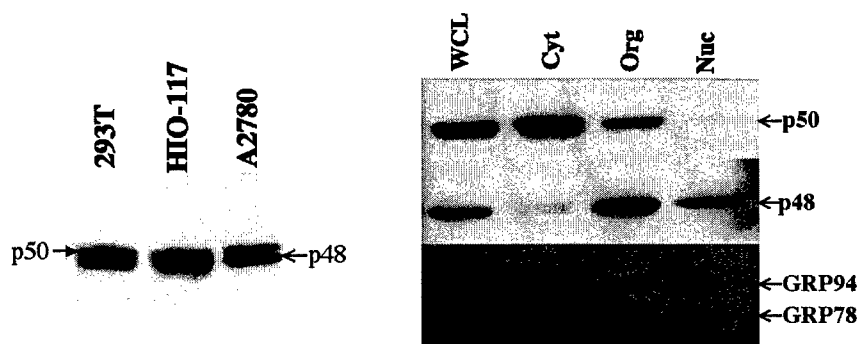


Figure 1. Extracts from 293T, HIO-117 (HOSE cell line), and A2780 cells were evaluated for expression of OVCA1 using a combination of TJ132 and FC22. When evaluated alone, the antibodies detect single bands, right panel. A2780 cells were fractionated and the various protein extracts were evaluated by Western blotting. p50 was detected using TJ132 and p48 was detected using FC22. GRP94 and GRP78 were detected using a monoclonal antibody (KDEL). WCL, whole cell lysate; Cyt, cytoplasm; Org, organelles; and Nuc, nucleus.

Posttranslational modification of OVCA1: We were struck by the observation that TJ132 (N-terminal antibody), but not FC21 or FC22 (C-terminal) antibodies were able to detect protein in both normal and tumor cells by immunohistochemistry. FC22 detected protein staining in only normal ovarian surface epithelial cells and the epithelial component of LMPs, yet truncating mutations were not detected in these samples. This led us to re-evaluate the proteins that were being expressed in these tumors and were being detected differentially by the two antibodies. On closer evaluation we found that each antibody detects a specific form of OVCA1 and that the different forms (p50 and p48) localize differently based on more careful cell fractionation studies (**Figure 1** and **Table 1**). Interestingly, p48 expression pattern is nearly identical to GRP78 (a confirmed OVCA1 interactor), whereas p50 is primarily located in the cytoplasm or associated with detergent insoluble organelles. As indicated above, both antibodies are capable of detecting *in vitro* translated OVCA1 (data not shown), suggesting that the protein may be posttranslationally modified. To address this question, we evaluated cell extracts by two-dimensional gel electrophoresis followed by Western blot analysis. As shown in **Figure 2**, the proteins are extensively modified in the tumor cell extracts as compared to normal control, resulting in nearly the complete absence of immunoreactive p48 (FC22) as observed by immunohistochemistry. Preliminary studies have ruled out phosphorylation as the major posttranslational event which contributes to the dramatic shift in pI. We have recently purified large quantities of OVCA1 following expressing in insect

cells (in collaboration with Dr. R. Raftigionis, FCCC) and will evaluate the protein by mass spectroscopy (in collaboration with Dr. A. Yeung, FCCC).

Defining the origin of the p70/p85^{OVCA1} proteins:

Using RT-PCR approaches we recently identified a transcript in fetal brain that differed from the p50 cDNA in that 49 additional nucleotides were included at the end of exon 10. This alteration leads to a change in reading frame and is predicted to extend the protein 194 additional amino acids. This protein is predicted to be >70 kDa in M.W. and shares 165 amino acids in common with OVCA2. As predicted, this alternatively spliced form would not be detectable by Northern blot analysis, however using RT-PCR approaches, we have been able to

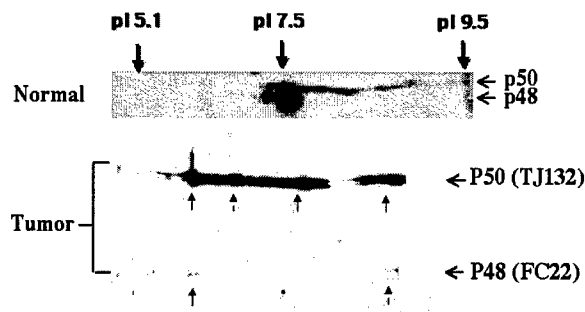


Figure 2. Two-dimensional gel electrophoresis analysis of OVCA1 (p50 and p48 forms) in protein extracts from normal and ovarian tumor cells. Upper filter was stained with sequentially with TJ132 and then FC22, whereas the lower filters with stained individually.

detect the alternatively spliced form in all the mortal SV40 HOSE cell lines and normal tissues tested. In most of these samples both transcripts are at readily detectable levels. We have reconstructed the OVCA1 p50 transcript to contain the additional 49 nucleotides and have shown that the protein migrates as a 70 kDa and an 85 kDa band by Western blot analysis (Bruening and Godwin unpublished data). Our initial results suggest that p70 may be the result of the extended exon 10 clone and that the origin of p85 is a postrationally modified form of p70. Interestingly, the somatic mutation in exon 12 (IVS12+1G>A) that was detected in 4 individual tumor cell lines is predicted to lead to a truncated protein.

6.11. Proteins that associate with OVCA1

Yeast two hybrid/interaction trap (IT) and OVCA1 protein interactors. We used a yeast two-hybrid screen to identify cDNAs from a human fetal brain library encoding proteins that were able to interact with OVCA1. The IT system has the advantage of permitting protein interactions under physiological conditions at physiologic levels (68). Therefore, we established two baits for OVCA1, one including amino acids 2 to 161 (N-terminal bait) and another including amino acids 225 to 443 (C-terminal bait). Using the N-terminal bait of OVCA1, no strong interactors were detected. The C-terminus bait of OVCA1 yielded the only protein interactors. A total of 3.5×10^5 primary transformants were screened, resulting in the identification of 28 clones coding for 4 OVCA1 interactor candidates. The most redundant clone, initially referred to as *BOV-1* (Binder of OVCA1-1), but later renamed to RBM8A, accounted for 54% (15/28) of the total clones isolated.

The second most redundant cDNA found encoded for the glucose-regulated protein 78 (GRP78). Members of the HSP70 protein family have been reported to bind non-specifically to baits in some two-yeast hybrid interactor hunts (E. Golemis, personal communication), however, this clone passed both the low and high stringency tests and failed to interact with a series of other baits, including C-terminal truncated OVCA1, OVCA2, TP53, CDK4, and biocoid (data not shown). Two additional candidate OVCA1 binders were identified and both cDNAs encoded for previously uncharacterized proteins (data not included).

Northern analysis of BOV-1. The expression pattern of *BOV-1* mRNA was evaluated by multiple tissue Northern blotting. Three major mRNA species were detected, *BOV-1a*, *1b*, and *1c*, of ~1 kb, ~3.2 kb, ~5.8 kb, respectively. While these species were expressed in all tissues to varying degrees, the 1-kb transcript was most abundant in testis, heart, placenta, spleen, thymus, and lymphocytes (**Figure 3**). The three mRNA species could also be detected in mammalian cell lines to varying degrees (data not shown).

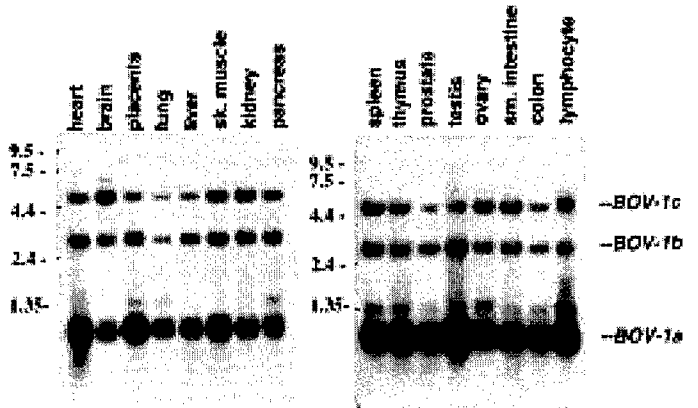


Figure 3. Tissue expression pattern of *BOV-1* mRNA. Blots containing 5 μ g of polyA⁺ selected mRNA from each of the indicated human tissues were hybridized with a ~800 bp *BOV-1a/b* cDNA clone. Size standards are in kilobases.

Cloning of BOV-1. To aid in the characterization of *BOV-1*, we isolated thirty cDNA clones from a

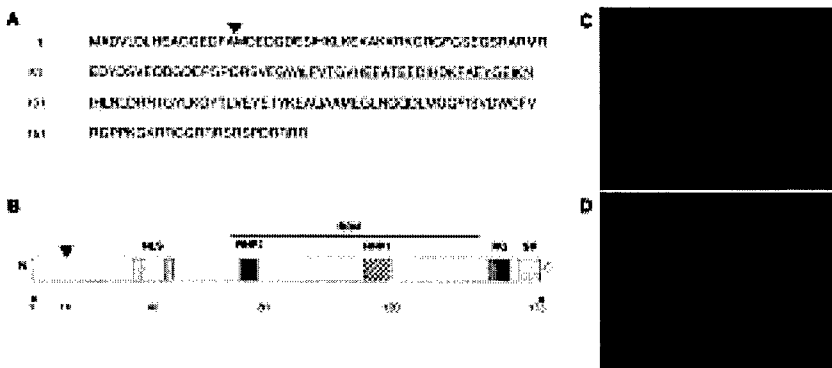


Figure 4. RBM8A structural features (A-B). **A.** The predicted primary sequence of the protein encoded by *BOV-1a/b* cDNA is shown, and the RNA-recognition motif (RRM) is underlined. The arrow indicates the methionine where protein encoded by *BOV-1c* is predicted to start. **B.** A schematic diagram highlighting structural domains of *BOV-1a/b* is presented in the lower panel. The RRM and both RNP1 (residues 113-120) and RNP2 (residues 74-79) consensus sequences are indicated. A putative bipartite nuclear localization signal (NLS) is predicted to be present at the N-terminus of *BOV-1a/b*. The diagram also shows the arginine-glycine-rich (RG) box (residues 151-162) and a serine-arginine-rich (SR) domain (residues 163-173) identified in the C-terminus of *BOV-1a/b*. The protein encoded by *BOV-1c* is predicted to be 16 amino acids shorter than *BOV-1a/b*. The arrow indicates the methionine where protein encoded by *RBM8B* is predicted to start. **C-D.** Immunolocalization of *BOV-1a/b* in COS-1 cells. COS-1 cells were transiently transfected with pcDNA3/T7-*BOV-1*. Forty eight hours after transfection, cells were fixed and stained with a mouse monoclonal anti-T7 tag antibody (Novagen, Madison, WI), followed by staining with FITC-conjugated anti-mouse antibody (Jackson Immunochemicals) (**C**) and counter-staining

abundant ~1 kb transcript) represents the entire coding region identified through the yeast two-hybrid screen, and that *BOV-1b* results from the use of an alternative polyadenylation signal (Accession number AF231511).

Based on initial sequence analysis, it appears that *BOV-1c* may be the product of an alternative exon splicing and the use of the alternative polyadenylation signal (Accession number AF231512).

The cDNA encoding for *BOV-1a* consists of an open reading frame of 173 amino acids. The cDNA for

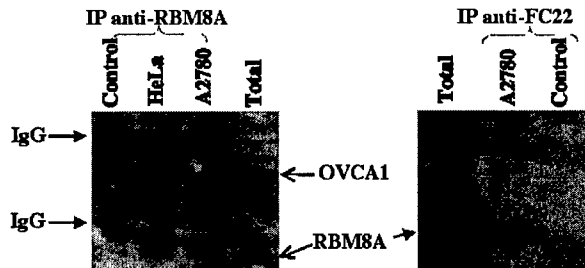


Figure 5. Co-immunoprecipitation of OVCA1 and RBM8A. Left panel, anti-RBM8A monoclonal antibodies were used to co-immunoprecipitate p48^{OVCA1} (FC22). The filter was stained with both anti-RBM8A and anti-FC22 antibodies. p48^{OVCA1} was detected in both A2780 and HeLa extracts. Right panel, anti-OVCA1 polyclonal antibodies (FC22) were used to co-immunoprecipitate RBM8A. The p50^{OVCA1} (TJ132) form was not detected in either case (data not shown).

BOV-1b differs from *BOV-1a* in that the 3'-UTR is substantially longer, 2,236 bp versus 161 bp, respectively. The cDNA encoding for *BOV-1c* consists of 3,074bp of 5'-UTR, an ORF of 158 amino acids, and a 3'-UTR of 2,238 bp. At the nucleotide level *BOV-1b* and *BOV-1c* cDNAs are identical except for the 5'-UTRs (compare accession numbers AF231511 and AF231512).

The predicted proteins encoded by *BOV-1c* differs from *BOV-1a/b* in that the protein is predicted to be 15 amino acids shorter (see

Figure 4; translation of protein encoded by *BOV-1c* is predicted to start at the second methionine, but includes an additional amino acid at codon 27), otherwise the proteins are identical. *BOV-1a/b* and *BOV-1c* proteins predicted molecular weights are 20 kDa and 18kDa, and their isoelectric points occur at pH 5.78 and pH 7.62, respectively. Comparison of 12 of the 14 *BOV-1* cDNA clones identified a sequence variant involving codon 43 (GAA) of *BOV-1a/b* (or codon 27 of *BOV-1c*). In 66.7% (8/12) of the clones, this additional codon was present. These transcripts would be predicted to encode for a protein of 174 amino acids (*BOV-1a/b*). In comparison, this polymorphism was not detected in any of the *BOV-1c* cDNA clones.

6.12 Intracellular association of OVCA1 and RBM8

Having identified potential partners for OVCA1 using a yeast two-hybrid screen, and having identified a novel RNA binding motif protein, we wished to validate these associations in mammalian cells. To do so, we immunoprecipitated OVCA1 with antibodies to RBM8A. As shown in **Figure 5**, anti-RBM8/Y14 (monoclonals derived from GST-tagged Y14 that was provided by Dr. G. Dreyfuss) antibodies coimmunoprecipitated OVCA1 (p48^{OVCA1} form only) from an ovarian cancer cell line, A2780 and HeLa cells. In comparison, anti-OVCA1 (FC22) immunoprecipitated RBM8A, but only weakly.

Chromosomal mapping of BOV-1 cDNA. We mapped the chromosomal location of *BOV-1* by FISH using the 5.8 kb cDNA probe, corresponding to the *BOV-1c* transcript. Of the 51 signals observed, 24 (47%) hybridized specifically at 5q13-14 in 19 of the 20 metaphase spreads scored. In 11 of 20 (55%) metaphase spreads, signals were also detected on chromosome 14, specifically at 14q22-23. Sixteen (31%) of the 51 signals observed mapped to 14q22-23, indicating that two closely related genes may exist at these two sites (**Figure 6**). Finally, we noted that six metaphases showed weak hybridization (single signals) in the 1qh region.

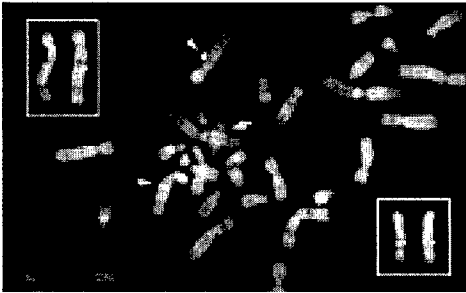


Figure 6. Chromosomal localization of *BOV-1a/b* and *BOV-1c* by FISH. Partial metaphase spread showing specific hybridization signals at chromosome 5q13-14 (arrowheads). Arrow indicates specific hybridization signals at chromosome 14q22-23. Insets: Left, *BOV-1c*-specific hybridization at 5q13-14 to individual chromosomes from other metaphases. Right, *BOV-1c*-specific hybridization at 14q22-23 to individual chromosomes from other metaphases.

Nucleotide Sequence Analysis of BOV-1 cDNAs. Comparison analysis of *BOV-1a/b* using the BLASTN program demonstrated 99% nucleotide homology (score=898; E value 0.0) to a human EST from a colon carcinoma (HCC) cell line cDNA library (Accession number AA30779).

Comparison of 5'-UTR of the *BOV-1c* cDNA with the GenBank

databases demonstrated 99.4% nucleotide homology over 314 nt (in the reverse orientation) to human integrin binding protein Del-1 (Del1) mRNA (1712-1399 nt of Del1 and 2668-2981 nt of *BOV-1c*) (Accession number U70312 versus AF231512). The 3'-UTR for both *BOV-1b* and *BOV-1c* also shared nucleotide identity with a

human cDNA (Accession number AL049219) (score=496; E=1.0x10⁻¹³⁷) identified in fetal brain.

Based on comparison of the cDNA sequence for *BOV-1a/b* and our genomic sequence data, the *BOV-1a/b* gene appears to contain 6 exons, whereas *BOV-1c* is intronless. Based on our mapping and sequence data, approved names for *BOV-1a/b* and *BOV-1c* have recently been assigned by the Human Gene Nomenclature Committee and are *RBM8A* and *RBM8B*, respectively.

Protein sequence analysis and subcellular localization of BOV-1. The deduced primary amino acid sequence of *RBM8A* and *RBM8B* indicates the presence of one copy of an RNA-binding domain (RBD) in the central region (amino acid residues 71-148 or 55-132, respectively), also known as RNA-recognition motif (RRM) (Figure 15, A-B). This RRM contains one set of the two consensus nucleic acid binding motifs, RNP-1 (a.a. 113-120 for *RBM8A* and a.a. 97-104 for *RBM8B*) and RNP-2 (a.a. 74-79 for *RBM8A* and a.a. 58-63 for *RBM8B*), which are characteristic of the heterogeneous nuclear ribonucleoprotein (hnRNP) family of proteins. The *RBM8A* and *RBM8B* amino acid sequence also contains a putative bipartite nuclear localization signal (NLS) (69) at the N-terminus (a.a. 33-51 for *RBM8A* and a.a. 17-35 for *RBM8B*) and a stretch rich in glycine

residues (not shown). Interestingly, the C-terminus of the RBM8A and RBM8B proteins (residues 151-173 and 135-157, respectively) show significant homology to the serine- arginine-rich (SR) domain of the splicing factor SC35 (70), as well as a domain rich in glycine and arginine (residues 151-162 for RBM8A and residues 135-146 for RBM8B), reminiscent of the RG box described in human nucleolin (71). In addition, we analyzed the intracellular distribution of RBM8A by immunofluorescence analysis. Immunolocalization experiments using COS-1 cells transfected with a T7-tagged RBM8A expression vector indicates that full-length RBM8A is predominantly in the nucleoplasm and in nuclear speckles. Lower but significant cytoplasmic staining is also observed.

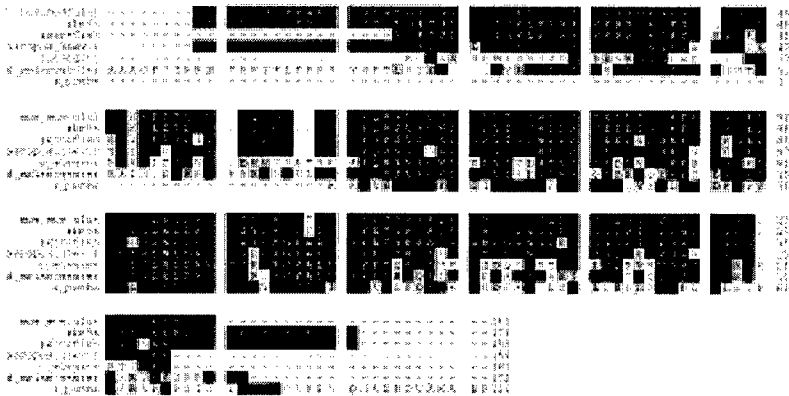


Figure 7. RBM8A protein sequence alignment with hypothetical proteins identified in *M. musculus* (100%identity), *zebrafish* (93.7%/98.7%), *X. laevis* (91.2%/95.6%), *Drosophila melanogaster* (63%/76%), *C. elegans* (60.5%/75.3%), and *S. pombe* (48.8%/64.5%), using the UWGCG PileUp program. Percentages of identity/similarity relative to RBM8A are indicated in parenthesis. GenBank™ accession numbers: AL0022712, AI943400, AW200013, AC006074, CAA83626, and AL021813, respectively. White letters in darkened boxes indicate identical residues. Shading indicates conserved residues.

RBM8 proteins appear to be highly conserved evolutionarily (Figure 7). Sequence analysis of the predicted RBM8A and RBM8B coding sequence using both FastA and TBLASTN algorithms revealed that *M. musculus*, *zebrafish*, *X. laevis*, *Drosophila melanogaster*, *C. elegans*, and *S. pombe* encode hypothetical proteins remarkably similar to RBM8A and RBM8B at the amino acid level.

RBM8 protein model. To gain more information on the RNA binding properties of RBM8A we built a three-dimensional model of the RRM domain of RBM8A. Sequence analysis using PSI-BLAST indicated that there were 18 possible template structures in 6 families in the Protein Data Bank that could be used to build the RRM domain of RBM8. We chose two of these, the sex-lethal protein from *Drosophila* (Sxl, PDB entry 1b7f) (72) and the polyA binding protein (PABP, PDB entry 1cvj) (73), since both of these sequence could be aligned with RBM8A without insertions or deletions. The resulting sequence alignment is shown in Salicioni et al, 2000 (see appended manuscript). Also, both structures contained RNA so that interactions between RBM8A and RNA could also be modeled.

We built models of RBM8A from both of these structures using the sidechain conformation prediction program SCWRL (74). A superposition of the backbones of these two models is shown in Figure 5b. The root-mean-square deviation of the backbones is 0.82 Å. The sequence identity between Sxl and PABP is 31 %, while the sequence identity between RBM8 and Sxl is 24% and between RBM8A and PABP is 27%. Since these

sequence identities are similar, we expect that the model of the RRM of RBM8A is quite accurate, with an RMS comparable to the Sxl-PABP RMS of 0.82 Å.

We show the model of RBM8A based on Sxl (see Salicioni et al, 2000 in appendices). Residues that bind to RNA are indicated in the Figure. These include F75, T77, H102, R107, F111, Y115, L117, and P142. Some of these residues are identical or similar in Sxl and/or PABP, which may indicate similar interactions between these sidechains and RNA. For example, RBM8A F75 is a tyrosine in PABP and forms an aromatic ring stacking interaction with an adenine in the RNA. In Sxl this residue is an isoleucine, making a hydrophobic interaction with a uracil base. RBM8A Y115 is a tyrosine in both Sxl and PABP, making a ring stacking interaction with an adenine in PABP and a hydrogen bond to a uracil ring carbonyl in Sxl. RBM8A Y111 is also tyrosine in Sxl that makes a hydrogen bond with a uracil carbonyl in Sxl. While it is not possible to predict the RNA binding sequence for RBM8A from the model, it is clear that many of the residues typical of RNA-protein interactions in this family of proteins are contained in the RNA binding site of RBM8A. Since many of these interactions make contact with RNA bases, mutations of these residues are likely to alter the binding affinity of RBM8A for its natural RNA ligand. Our work provides a starting point for further biochemical and genetic studies of the RBM8 protein family and the biological relevance of its interaction with OVCA1 in the context of abnormal RNA splicing and downstream events including mRNA export, translation, stability, and localization in breast and ovarian tumorigenesis.

6. KEY RESEARCH ACCOMPLISHMENTS:

- Cloned OVCA1 and OVCA2, two evolutionarily conserved genes.
- Found that OVCA1 was mutated in the germline of two breast cancer syndrome families that had previously tested negative for *BRCA1* or *BRCA2* mutations.
- Found that somatic mutations in *OVCA1* were present in a limited number of ovarian tumors showing LOH of the *OVCA* locus.
- Showed that OVCA1 levels are reduced in breast and ovarian tumors and that OVCA1 may be modified in some ovarian carcinomas as compared to normal ovarian epithelium and benign or LMP ovarian tumors.
- Determined that several OVCA1 mutants fail to suppress tumor cell growth *in vitro*, indicating potential domains that may be of functional significance.
- Derived antibodies to OVCA1 (both N- and C-terminal) that work for Western blotting, immunohistochemistry and immunoprecipitation.

- Derived antibodies to OVCA2 (both N- and C-terminal) that work for Western blotting, immunohistochemistry and immunoprecipitation.
- Derived inducible OVCA1 cell lines.
- Identified other genes within the *OVCA* locus.
- Cloned and sequenced the mouse *Ovca* locus.
- Reported the identification and structural analysis of human RBM8/Y14: a highly conserved RNA-binding motif protein that interact with OVCA1.
- Identified that GRP 78 interacts with a C-terminal bait of OVCA1 in a yeast two-hybrid trap system.
- Created a knockout vector for the *Ovca* locus in mice.
- Initiated screening for chimeras.

7. **REPORTABLE ACCOMPLISHMENTS** (related to the tasks outlined in the approved SOW):

*-Copy of the manuscript is included in the appendices.

Publications:

*Schultz, D.C., Vanderveer, L., Berman, D.B., Wong, A.J., and Godwin, A.K. Identification of two candidate tumor suppressor genes on chromosome 17p13.3. *Cancer Res*, 56:1997-2002, 1996.

*Schultz, D.C., Balasara, B., Testa, J.R., and Godwin, A.K. Cloning and localization of a human diphthamide biosynthesis-like protein gene, *hDPH2L2*. *Genomics*, 52:186-191, 1998.

*Oleykowski, C.A., Bronson-Myllins, C.R., Godwin, A.K., Yeung, A.T. Mutation detection using a novel plant endonuclease. *Nucleic Acid Research*, 26:4597-4602, 1998.

*Bruening, W. Prowse, A.H., Schultz, D.C., Holgado-Madruga, M., Wong, A., Godwin, A.K. Expression of OVCA1, a candidate tumor suppressor gene, is reduced in tumors and inhibits growth of ovarian cancer cells. *Cancer Research*, 59:4973-4983, 1999.

*Salicioni, A.M., Xi, M., Vanderveer, L.A., Balsara, B. Testa, J.R., Dunbrack, R.L., and Godwin, A.K. Identification and structural analysis of human RBM8A and RBM8B: two highly conserved RNA-binding motif proteins that interact with OVCA1, a candidate tumor suppressor. *Genomics*, 69:54-62, 2000.

Invited Reviews and Chapter During the Funded Period:

Boente, M.P., Godwin, A.K., Hogan, W.M., Kohler, M.F., Berchuck, A., Hamilton, T.C., and Young, R.C. Early Ovarian Cancer. *Current Problems in Cancer* (2):81-140, 1996.

Hamilton, T.C., Miller, P.D. Getts, L.A., and Godwin, A.K. The use of retroviral-like elements to detect genetic differences between normal and transformed rat ovarian surface epithelial cells. In *Ovarian Cancer 4*, edited by F. Sharp, T. Blackett, J. Berek. Chapman & Hall, London, 1996.

Godwin, A.K., Schultz, D.C., Hamilton, T.C., and Knudson, A.G. Oncogenes and Tumor Suppressor Genes gynecologic malignancies. In Hoskins, W.J., Perez, C.A., Young, R.C. (eds): *Gynecologic Oncology: Principles and Practice*, pp. 107-148, 1997.

Lynch, H.T., Casey, M.J., Lynch, J., White, T.E.C., and Godwin, A.K. Genetics and Ovarian Carcinoma In Ozols (ed): *Seminars in Oncology*, 25:265-281, 1998.

Hamilton, T.C., Johnson, S.W., and Godwin, A.K. The molecular biology of gynecological malignancies. In: *Diagnostic and Therapeutic Advances in Gynecologic Oncology*, Ozols RF (ed). Kluwer Academic Publishers, Boston, pp. 103-114, 1998.

Broccoli, D., and Godwin, A.K. Telomere length changes in Human Cancer. In *Methods in Molecular Biology: The Molecular Analysis of Cancer*. Eds J. Boulton & C. Fidler. The Humana Press, (In press, 2001).

Prowse, A. Frolov, A., and Godwin, A.K. The genetics of ovarian cancer. *American Cancer Society Atlas of Clinical Oncology*. B.C. Decker Inc., Publisher (In press, 2001).

Bove, B, Dunbrack, R., Godwin, A.K. *BRCA1, BRCA2, and Hereditary Breast Cancer*. *Breast Cancer: Prognosis, Treatment and Prevention* Marcel Dekker Inc., Publisher (In press, 2001).

Raftogianis, R.B., Godwin, A.K. The impact of protein interaction technologies on cancer biology and pharmacogenetics, Ed E. Golemis. The Cold Spring Harbor, (Submitted, 2001).

Papers Under Review/Preparation:

*Prowse, A.H., Vanderveer, L., R. Dunbrack, Godwin, A.K. *OVCA2*, not *OVCA1/DPH2L* may be down-regulated during retinoid-induced differentiation and apoptosis. Submitted to Int. J. Cancer, 2001.

Bruening, W., Schultz, D.C., Godwin, A.K. *OVCA1*, a candidate tumor suppressor, is transiently stabilized during the decision to enter G0 phase. Submitted, JBC, 2001.

Prowse, A.H., Bruening, B., Godwin, A.K. Post-translational Modifications of *OVCA1* Contribute to Ovarian Carcinogenesis. (Manuscript in preparation, 2001).

Abstracts/Meetings:

Schultz, D.C., A.H. Prowse, A.H., Godwin, A.K. Characterization of *OVCA1*, a novel tumor suppressor: evidence for a role in the development of human epithelial tumors. *American Journal of Human Genetics* 61:443, 1997.

Prowse, A.H., Bruening, W., Schultz, D.C., Godwin, A.K.. Characterization of *OVCA1*, a novel tumor suppressor: evidence for a role in the development of human epithelial tumors. *Proceedings of American Association of Cancer Research* 39: 4234, 1998.

Prowse, A.H., Bruening, W., Godwin, A.K. *OVCA1*, a novel tumor suppressor, is aberrantly expressed in ovarian carcinomas. *American Journal of Human Genetics* 65: 1781, 1999.

Salicioni, A.M., Bruening, W., Vanderveer, L., Godwin, A.K. Functional characterization of *OVCA1*, a putative tumor suppressor. *Am. J. Hum. Genet* 65:1797, 1999.

Prowse, A.H., Bruening, B., Godwin, A.K. *OVCA1*, a candidate ovarian cancer gene, is aberrantly expressed in ovarian carcinomas. (The Fifth Annual Postdoctoral Research Conference, Philadelphia, 2000, oral presentation, award for best presentation).

Prowse, A.H., Bruening, B., Godwin, A.K. Post-translational Modifications of *OVCA1* Contribute to Ovarian Carcinogenesis. *American Human Genetics Society*, 2000.

Prowse, A.H., Salicioni, A.M., Dunbrack, R., Godwin, A.K. OVCA1, a candidate tumor suppressor, interacts with RBM8: a highly conserved RNA-binding protein. Second International Conference: Proteins that Bind RNA, Austin, TX, pg 116:97, March 4-8, 2001.

Patents obtained during the course of the grant:

Godwin, A.K. Gene Associated with Suppression of Tumor Development. U.S. Patent Number: 5,801,041, awarded on September 1, 1998.

Godwin, A.K. Novel Gene Associated with Suppression of Tumor Development. U.S. Patent Number 5,821,338 awarded on October 13, 1998.

Degrees Obtained that were Supported by This Award:

David Schultz, Ph.D. from Lehigh University

8. CONCLUSIONS:

In order for future therapies to be developed for the fight against cancer it is important to understand the basic molecular mechanisms that give rise to a specific cancer type. The fundamental mechanisms underlying the genetic basis of cancer are slowly being defined and involve alterations in genes which have been classified into three general categories: (i) protooncogenes are involved in growth promotion and the defects leading to cancer are a gain of function; (ii) tumor suppressor genes are negative regulators of growth and a loss of function gives rise to cancer; and (iii) DNA repair genes are involved in maintaining the fidelity of the genome and altered function can lead to increase rates of mutations in both classes of cancer-causing genes. Cancer is a multistep process that involves alterations in many specific genes. The normal cell has multiple independent mechanisms that regulate its growth and differentiation and several separate events are required to override these control mechanisms. Progress is now being made in isolating these genes and the proteins they encode for, determining the normal cellular functions of the proteins and in investigating the mechanisms of tumorigenesis.

Breast cancer is a very common disease, causing about 10% of deaths in women in the Western World, while ovarian cancer is the number one gynecologic killer in the United States with over 25,000 diagnosed cases and nearly 14,000 deaths in 2000. Molecular genetic analysis of these tumors has revealed many genetic aberrations that may represent important steps in tumor development. To understand the genetic pathways

underlying breast and ovarian tumor development, it is necessary to identify the genes affected by these genetic aberrations and establish any correlations between disruption of their function and tumor phenotype.

Chromosome 17 frequently shows loss of heterozygosity (LOH) in both breast and ovarian carcinomas. In addition, re-introduction of chromosome 17 fragments into breast cancer cell lines has been shown to suppress tumorigenicity. Therefore, inactivation of tumor suppressor genes on chromosome 17 appears to be a critical event in the pathogenesis of breast cancer as well as other cancers. Although *TP53* at chromosome 17p13.1 is involved in the pathogenesis of breast and ovarian cancer, our LOH mapping studies in breast and ovarian carcinomas have defined a region distal to *TP53*, at 17p13.3, thought to harbor a tumor suppressor gene (Godwin *et al.*, 1994, Schultz *et al.*, 1996). New genes, *OVCA1* and *OVCA2*, have been identified on chromosome 17p13.3, in this critical region of allelic loss (Schultz *et al.*, 1996). *OVCA1* is composed of 12 coding exons and one non-coding exon, while *OVCA2* is composed of two exons: a unique exon 1, and an exon 2 which comprises part of the 3' untranslated region of *OVCA1*. Thus, the two genes are overlapping, but their protein products are completely distinct.

Much of our focus during the past few years has been on trying to uncover clues about the function of *OVCA1*. We have found that *OVCA1* is highly conserved and exists in at least three forms; a 48, a 50, and an 85-kDa protein. Evidence suggests that the 85-kDa form is encoded by an alternatively spliced form of *OVCA1* and that the 48- and 50-kDa forms are the result of posttranslational modifications. Subcellular fractionation studies indicate that p50^{*OVCA1*} localizes primarily to the cytoplasm whereas p48^{*OVCA1*} is predominantly found in the organelle fraction with some in the nuclear fraction. Western blot analysis revealed that p50^{*OVCA1*} levels are reduced or are absent in >30% of tumors examined when compared to extracts from normal cells and tissues, and that p85^{*OVCA1*} is rarely detected in tumors. Somatic mutations have been detected, but are rare in *OVCA1*. Furthermore, two germline missense mutations have been found in breast cancer-prone women who have tested negative for a *BRCA1* or a *BRCA2* mutation. Attempts to create breast and ovarian cell lines that stably over-express the p50 form of *OVCA1* have generally been unsuccessful. The clones that do express exogenous p50^{*OVCA1*} do so at very low levels, and have dramatically reduced rates of proliferation, an increased proportion of the cells in the G₁ fraction of the cell cycle, and decreased levels of cyclin D, which may be caused by an accelerated rate of cyclin D degradation (Bruening, W., *et al.*, 1999). Reversion of these cells to a more rapid growth phenotype is accompanied by complete loss of expression of exogenous *OVCA1*. Screens for proteins that potentially interact with *OVCA1* have uncovered several known and some unidentified proteins, including a novel RNA binding protein (BOV-1/RBM8/) (Salicioni, A.M., *et al.*, 2000). RBM8, also known as Y14 has recently been shown to be a highly conserved RNA-binding motif protein that preferentially associates with

spliced mRNA in the nucleus and then remains associated with newly exported mRNA in the cytoplasm as a shuttling protein. It also exists in a complex with a number of proteins, including the splicing associated factors SRm160, DEK, RNPS1 and the mRNA export factor REF/Aly. This complex is deposited 20-24 nucleotides upstream of mRNA exon-exon junctions. RBM8/Y14 can also bind the mRNA export factor TAP. Recent studies have shown that splicing promotes efficient mRNA export and it has been hypothesized that splicing can promote the removal of nuclear retention factors and the formation of more efficient export complexes. The RBM8/Y14 complex is an excellent candidate for such an export complex since both REF/Aly and TAP have been shown to be involved in mRNA export. It is also possible that the RBM8/Y14 complex may be involved in nonsense-mediated mRNA decay (NMD), a process whereby nonsense transcripts are recognized and efficiently degraded by the cell, by "marking" the positions of exon-exon junctions. It is intriguing to speculate that aberrant expression/localization of proteins such as RBM8 and its interactors may result in the inappropriately marked mRNAs in the cytoplasm. This could result in abnormal decay of mutant transcripts, and in turn expression of mutant proteins that contribute to tumorigenesis. The significance of these observations and the role of RBM8/Y14 in carcinogenesis needs to be evaluated.

Our studies continue to suggest that OVCA1 has certain properties that are in common with a number of tumor suppressors. We have found that exogenous expression of OVCA1 can inhibit tumor cell growth and that expression of the protein is altered in both breast and ovarian tumors. Yet through our studies, we have not been able to establish a likely function for OVCA1. Therefore, we have initiated studies in mice to evaluate the effect(s) of altering OVCA1 (and in some cases OVCA2) expression on normal growth and development. By establishing such models, we should be better able to identify the function(s) of this very unique, but highly conserved protein. Unfortunately, this work will not be pursued any further until new funds are obtained.

9. REFERENCES:

1. Godwin, A. K., Schultz, D. C., Hamilton, T. C., and Knudson, A. G. Oncogenes and Tumor Suppressor Genes. *In*: W. J. Hoskins, C. A. Perez, and R. C. Young (eds.), *Gynecologic Oncology: principles and practice*, pp. 107-148. Philadelphia: J. B. Lippencot Company, 1997.
2. Murphy, D., McHardy, P., Coutts, J., Mallon, E., George, W., Kaye, S., Brown, R., and Keith, W. Interphase cytogenetic analysis of erbB2 and topoII alpha co-amplification in invasive breast cancer and polysomy of 17 in ductal carcinoma *in situ*., *Int. J. Cancer*. 64: 18-26, 1995.
3. Phillips, N., Ziegler, M., Radford, D., Fair, K., Steinbrueck, T., Xynos, F., and Donis-Keller, H. Allelic deletion on chromosome 17p13.3 in early ovarian cancer., *Cancer Res*. 56: 606-611, 1996.

4. Godwin, A. K., Vanderveer, L., Schultz, D. C., Lynch, H. T., Altomare, D. A., Buetow, K. H., Daly, M., Getts, L. A., Masny, A., Rosenblum, N., Hogan, M., Ozols, R. F., and Hamilton, T. C. A common region of deletion on chromosome 17q in both sporadic and familial epithelial ovarian tumors distal to BRCA1, *American Journal of Human Genetics*. 55: 666-677, 1994.
5. Theile, M., Hartmann, S., Scherthan, H., Arnold, W., Deppert, W., Frege, R., Glaab, F., Haensch, W., and Scherneck, S. Suppression of tumorigenicity of breast cancer cells by transfer of human chromosome 17 does not require transferred BRCA1 and p53 genes., *Oncogene*. 10: 439-447, 1995.
6. Casey, G., Plummer, S., Hoeltge, G., Scanlon, D., Fasching, D., Fasching, C., and Stanbridge, E. Functional evidence for a breast cancer growth suppressor gene on chromosome 17., *Hum Mol Genet*. 2: 1921-1927, 1993.
7. Negrini, M., Sabbioni, S., Haldar, S., Possati, L., Castagnoli, A., Corallini, A., Barbanti-Brodano, G., and Croce, C. Tumour and growth suppression of breast cancer cells by chromosome 17-associated functions., *Cancer Research*. 54: 1818-1824, 1994.
8. Phelan, C., Borg, A., Cuny, M., Crichton, D., Baldersson, T., Andersen, T., Caligo, M., Lidereau, R., Lindblom, A., Seitz, S., Kelsell, D., Hamann, U., Rio, P., Thorlacius, S., Papp, J., Olah, E., Ponder, B., Bignon, Y.-J., Scherneck, S., Barkardottir, R., Borresen-Dale, A.-L., Eyfjord, J., Theillet, C., Thompson, A., Devilee, P., and Larsson, C. Consortium study on 1280 breast carcinomas: Allelic loss on chromosome 17 targets subregions associated with family history and clinical parameters., *Cancer Res*. 58: 1004-1012, 1998.
9. Stack, M., Jones, D., White, G., Liscia, D., Venesio, T., Casey, G., Crichton, D., Varley, J., Mitchell, E., Heighway, J., and Santibanez-Koref, M. Detailed mapping and loss of heterozygosity analysis suggests a suppressor locus involved in sporadic breast cancer within a distal region of chromosome band 17p13.3., *Hum Mol Genet*. 4: 2047-2055, 1995.
10. Matsumura, K., Kallioniemi, A., Kallioniemi, O., Chen, L., Smith, H., Pinkel, D., Gray, J., and Waldman, F. Deletion of chromosome 17p loci in breast cancer cells detected by fluorescence *in situ* hybridization., *Cancer Res*. 52: 3474-3477, 1992.
11. Niederacher, D., Picard, F., van Roeyen, C., An, H.-X., Bender, H., and Beckmann, M. Patterns of allelic loss on chromosome 17 in sporadic breast carcinomas detected by fluorescent-labeled microsatellite analysis., *Genes Chromosom Cancer*. 18: 181-192, 1997.
12. Merlo, G., Vesesio, T., Bernardi, A., Cropp, C., Diella, F., Cappa, A., Callahan, R., and Liscia, D. Evidence for a second tumor suppressor gene on 17p linked to high S-phase index in primary human breast carcinomas., *Cancer Genet Cytogenet*. 76: 106-111, 1994.

13. Harada, Y., Katagiri, T., Ito, I., Akiyama, F., Sakamoto, G., Kasumi, F., Nakamura, Y., and Emi, M. Genetic studies of 457 breast cancers., *Cancer*. 74: 2281-2286, 1994.
14. Devilee, P., Cornelisse, C., Kuipers-Dijkshoorn, N., Jonker, C., and Pearson, P. Loss of heterozygosity on 17p in human breast carcinomas: defining the smallest common region of deletion., *Cytogenet Cell Genet*. 53: 52-54, 1990.
15. Sato, T., Tanigami, A., Yamakawa, K., Akiyama, F., Kasumi, F., Sakamoto, G., and Nakamura, Y. Allelotype of breast cancer: Cumulative allele losses promote progression in primary breast cancer, *Cancer Research*. 50: 7184-7189, 1990.
16. Sato, T., Akiyama, F., Sakamoto, G., Kasumi, F., and Nakamura, Y. Accumulation of genetic alterations and progression of primary breast cancer, *Cancer Research*. 51: 5794-5799, 1991.
17. Sato, T., Saito, H., Morita, R., Koi, S., Lee, J. H., and Nakamura, Y. Allelotype of human ovarian cancer, *Cancer Research*. 51: 5118-5122, 1991.
18. Lindblom, A., Skoog, L., Andersen, T., Rotstein, S., Nordenskjold, M., and Larsson, C. Four separate regions on chromosome 17 show loss of heterozygosity in familial breast carcinomas., *Hum Genet*. 91: 6-12, 1993.
19. Thompson, A., Crichton, D., Elton, R., Clay, M., Chetty, U., and Steel, C. Allelic imbalance at chromosome 17p13.3 (YNZ22) in breast cancer is independent of p53 mutation or p53 overexpression and is associated with poor prognosis at medium-term follow-up., *Br J Cancer*. 77: 797-800, 1998.
20. Cornelis, R., van Vliet, M., Vos, C., Cleton-Jansen, A.-M., van de Vijver, M., Peterse, J., Khan, P., Borresen, A.-L., Cornelisse, C., and Devilee, P. Evidence for a gene on 17p13.3, distal to TP53, as a target for allele loss in breast tumors without p53 mutations., *Cancer Res*. 54: 4200-4206, 1994.
21. Lizard-Nacol, S., Riedinger, J.-M., Lizard, G., Glasser, A.-L., Coudray, N., Chaplain, G., and Guerrin, J. Loss of heterozygosity at the *TP53* gene: Independent occurrence from genetic instability events in node-negative breast cancer., *Int. J Cancer*. 72: 500-603, 1997.
22. Mackay, J., Elder, P., Steel, C., Forrest, A., and Evans, H. Allele loss on short arm of chromosome 17 in breast cancers., *The Lancet* 1384-1385, 1988.
23. Devilee, P., Pearson, P., and Cornelisse, C. Allele losses in breast cancer., *The Lancet* 154, 1989.
24. Singh, S., Simon, M., Meybohm, I., Jantke, I., Jonat, W., Maass, H., and Goedde, H. Human breast cancer: frequent p53 allele loss and protein overexpression., *Hum Genet*. 90: 635-640, 1993.
25. Ito, I., Yoshimoto, M., Iwase, T., Watanabe, S., Katagiri, T., Harada, Y., Kasumi, F., Yasuda, S., Mitomi, T., Emi, M., and Nakamura, Y. Association of genetic alterations on chromosome 17 and loss of hormone receptors in breast cancer., *Br J Cancer*. 71: 438-441, 1995.

26. Nagai, M. A., Medeiros, A., Brentani, M. M., Marques, L. A., Mazoyer, S., and Mulligan, L. M. Five distinct deleted regions on chromosome 17 defining different subsets of human primary breast tumor, *Oncogene*. 52: 448-453, 1995.
27. Phillips, N., Ziegler, M., Saha, B., and Xynos, F. Allelic loss on chromosome 17 in human ovarian cancer., *Int J Cancer*. 54: 85-91, 1993.
28. Marchetti, A., Buttitta, F., Merlo, G., Diella, F., Pellegrini, S., Pepe, S., Macchiarini, P., Chella, A., Angeletti, A., Callahan, R., Bistocchi, M., and Squartini, F. *p53* alterations in non-small cell lung cancers correlate with metastatic involvement of hilar and mediastinal lymph nodes., *Cancer Res*. 53: 2846-2851, 1993.
29. Takahashi, T., Nau, M. M., Chiba, I., and al., e. *p53*; a frequent target for genetic abnormalities in lung cancer., *Science*. 246: 491-494, 1989.
30. Konishi, H., Takahashi, T., Kozaki, K., Yatabe, Y., Mitsudomi, T., Fujii, Y., Sugiura, T., Matsuda, H., Takahashi, T., and Takahashi, T. Detailed deletion mapping suggests the involvement of a tumor suppressor gene at 17p13.3, distal to *p53*, in the pathogenesis of lung cancers., *Oncogene*. 17: 2095-2100, 1998.
31. Baker, S., Fearon, E., Nigro, J., Hamilton, S., Preisinger, A., Jessup, J., vanTuinen, P., Ledbetter, D., Barker, D., Nakamura, Y., White, R., and Vogelstein, B. Chromosome 17 deletions and *p53* gene mutations in colorectal carcinomas., *Science*. 244: 217-221, 1989.
32. Saylor, R., Sidransky, D., Friedman, H. S., Bigner, S. H., Bigner, D. D., Vogelstein, B., and Brodeur, G. M. Infrequent *p53* gene mutations in medulloblastomas, *Cancer Research*. 51: 4721-4723, 1991.
33. McDonald, J., Daneshvar, L., Willert, J., Matsumara, K., Waldman, F., and Cogen, P. Physical mapping of chromosome 17p13.3 in the region of a putative tumor suppressor gene important in medulloblastoma., *Genomics*. 23: 229-232, 1994.
34. Scheurlen, W., Krauss, J., and Kuhl, J. No preferential loss of one parental allele of chromosome 17p13.3 in childhood medulloblastoma., *Int J Cancer*. 63: 372-374, 1995.
35. Cogen, P., Daneshvar, L., Metzger, A., Duyk, G., Edwards, M., and Sheffield, V. Involvement of multiple chromosome 17p loci in medulloblastoma tumorigenesis., *Am J Hum Genet*. 50: 584-589, 1992.
36. Chattopadhyay, P., Rathore, A., Mathur, M., Sarkar, C., Mahapatra, S., and Sinha, S. Loss of heterozygosity of a locus on 17p13.3, independent of *p53*, is associated with higher grades of astrocytic tumours., *Oncogene* 871-875, 1997.
37. Saxena, A., Clark, W., Robertson, J., Ikejiri, B., Oldfield, E., and Ali, I. Evidence for the involvement of a potential second tumor suppressor gene on chromosome 17 distinct from *p53* in malignant astrocytomas., *Cancer Res*. 52: 6716-6721, 1992.

38. Tomlinson, I., Gammack, A., Stickland, J., Mann, G., MacKie, R., Kefford, R., and McGee, J. D. Loss of heterozygosity in malignant melanoma at loci on chromosomes 11 and 17 implicated in the pathogenesis of other cancers., *Genes Chromosom Cancer*. 7: 169-172, 1993.
39. Nishida, N., Fukuda, Y., Kokuryu, H., Toguchida, J., Yandell, D., Ikenega, M., Imura, H., and Ishizaki, K. Role and mutational heterogeneity of the *p53* gene in hepatocellular carcinoma., *Cancer Res*. 53: 368-372, 1993.
40. Sankar, M., Tanaka, K., Kumaravel, T., Arif, M., Shintani, T., Yagi, S., Kyo, T., Dohy, H., and Kamada, N. Identification of a commonly deleted region at 17p13.3 in leukemia and lymphoma associated with 17p abnormality., *Leukemia*. 12: 510-516, 1998.
41. Schultz, D. C., Vanderveer, L., Berman, D. B., Hamilton, T. C., Wong, A. J., and Godwin, A. K. Identification of two candidate tumor suppressor genes on chromosome 17p13.3, *Cancer Res*. 56: 1997-2002 but not to mitogenic activators such as PDGF or EGF, results in a marked cytoplasmic accumulation of hnRNP A1, concomitant with an increase in its phosphorylation. These effects are mediated by the MKK(3/6)-p38 pathway, and moreover, p38 activation is necessary and sufficient for the induction of hnRNP A1 cytoplasmic accumulation. The stress-induced increase in the cytoplasmic levels of hnRNP A/B proteins and the concomitant decrease in their nuclear abundance are paralleled by changes in the alternative splicing pattern of an adenovirus E1A pre-mRNA splicing reporter. These results suggest the intriguing possibility that signaling mechanisms regulate pre-mRNA splicing in vivo by influencing the subcellular distribution of splicing factors., 1996.
42. Bruening, W., Prowse, A. H., Schultz, D. C., Holgado-Madruga, M., Wong, A., and Godwin, A. K. Expression of OVCA1, a candidate tumor suppressor, is reduced in tumors and inhibits growth of ovarian cancer cells, *Cancer Res*. 59: 4973-83, 1999.
43. Knudson, A. Mutation and cancer: statistical study of retinoblastoma., *Proc Natl Acad Sci U S A*. 68: 820-823, 1971.
44. Cook, W. D. and McCaw, B. J. Accommodating haploinsufficient tumour suppressor genes in Knudson's model, *Oncogene*. 19: 3434-3438, 2000.
45. DiCristofano, A., Kotsi, P., Peng, Y., Cordon-Cardo, C., Elkon, K., and Pandolfi, P. Impaired fas response and autoimmunity in *Pten*^{+/-} mice., *Science*. 285: 2122-2125, 1999.
46. Fero, M., Rivkin, M., Tasch, M., Porter, P., Carow, C., Firpo, E., Polyak, K., Tsai, L., Broudy, V., Perlmutter, R., Kaushansky, K., and Roberts, J. A syndrome of multiorgan hyperplasia with features of gigantism, tumorigenesis, and female sterility in p27(Kip1)-deficient mice., *Cell*. 85: 733-744, 1996.

47. Gutmann, D., Loehr, A., Zhang, Y., Kim, J., Henkemeyer, M., and Cashen, A. Haploinsufficiency for the neurofibromatosis 1 (NF1) tumor suppressor results in increased astrocyte proliferation., *Oncogene*. 18: 4450-4459, 1999.
48. Yang, R., Naitoh, J., Murphy, M., Wang, H., Phillipson, J., deKernion, J., Loda, M., and Reiter, R. Low p27 expression predicts poor disease-free survival in patients with prostate cancer., *J Urol*. 159: 941-945, 1988.
49. Yasui, W., Kudo, Y., Semba, S., Yokozaki, H., and Tahara, E. Reduced expression of cyclin-dependent kinase inhibitor p27Kip1 is associated with advanced stage and invasiveness of gastric carcinomas., *Jpn J Cancer Res*. 88: 625-629, 1997.
50. Esposito, V., Baldi, A., DeLuca, A., Groger, A., Loda, M., Giordano, G., Caputi, M., Baldi, F., Pagano, M., and Giordano, A. Prognostic role of the cyclin-dependent kinase inhibitor p27 in non-small cell lung cancer., *Cancer Res*. 57: 3381-3385, 1997.
51. Loda, M., Cukor, B., Tam, S., Lavin, P., Fiorentino, M., Draetta, G., Jessup, J., and Pagano, M. Increased proteasome-dependent degradation of the cyclin-dependent kinase inhibitor p27 in aggressive colorectal carcinomas., *Nat Med*. 3: 231-234, 1997.
52. Porter, P., Malone, K., Heagerty, P., Alexander, G., Gatti, L., Firpo, E., Darling, J., and Roberts, J. Expression of cell-cycle regulators p27Kip1 and cyclin E, alone and in combination, correlate with survival in young breast cancer patients., *Nat Med*. 3: 222-225, 1997.
53. Spirin, K., Simpson, J., Takeuchi, S., Kawamata, N., Miller, C., and Koeffler, H. p27/Kip1 mutation found in breast cancer., *Cancer Res*. 56: 2400-2404, 1996.
54. Kawamata, N., Morosetti, R., Miller, C., Park, D., Spirin, K., Nakamaki, T., Takeuchi, S., Hatta, Y., Simpson, J., and Wilczynski, S. e. a. Molecular analysis of the cyclin-dependent kinase inhibitor gene p27/Kip1 in human malignancies., *Cancer Res*. 55: 2266-2269, 1995.
55. Morosetti, R., Kawamata, N., Gombart, A., Miller, C., Hatta, Y., Hiramata, T., Said, J., Tomonaga, M., and Koeffler, H. Alterations of the p27KIP1 gene in non-Hodgkin's lymphomas and adult T-cell leukemia/lymphoma., *Blood*. 86: 1924-1930, 1995.
56. Pietenpol, J., Bohlander, S., Sato, Y., Papadopoulos, N., Liu, B., Friedman, C., Trask, B., Roberts, J., Kinzler, K., and Rowley, J. e. a. Assignment of the human p27Kip1 gene to 12p13 and its analysis in leukemias., *Cancer Res*. 55: 1206-1210, 1995.
57. Fero, M., Randel, E., Gurley, K., Roberts, J., and Kemp, C. The murine gene p27 Kip1 is haploinsufficient for tumour suppression., *Nature*. 396: 177-180, 1998.

58. Gutmann, D. H., Loehr, A., Zhang, Y., Kim, J., Henkemeyer, M., and Cashen, A. Haploinsufficiency for the neurofibromatosis 1 (NF1) tumor suppressor results in increased astrocyte proliferation, *Oncogene*. *18*: 4450-4459, 1999.
59. Li, J., Yen, C., Liaw, D., Podsypanina, K., Bose, S., Wang, S., Puc, J., Miliareis, C., Rodgers, L., McCombie, R., Bigner, S., Giovanella, B., Ittmann, M., Tycko, B., Hibshoosh, H., Wigler, M., and Parsons, R. PTEN, a putative protein tyrosine phosphatase gene mutated in human brain, breast, and prostate cancer., *Science*. *275*: 1943-1947, 1997.
60. Steck, P., Pershouse, M., Jasser, S., Yung, W., Lin, H., Ligon, A., Langford, L., Baumgard, M., Hattier, T., Davis, T., Frye, C., Hu, R., Swedlund, B., Teng, D., and Tavtigian, S. Identification of a candidate tumour suppressor gene, MMAC1, at chromosome 10q23.3 that is mutated in multiple advanced cancers., *Nat Genet*. *15*: 356-362, 1997.
61. Gulberg, P., Straten, P., Birck, A., Ahrenkiel, V., Kirkin, A., and Zeuthen, J. Disruption of the MMAC1/PTEN gene by deletion or mutation is a frequent event in malignant melanoma., *Cancer Res*. *57*: 3660-3663, 1997.
62. Liaw, Marsh, D., Li, J., Dahia, P., Wang, S., Ahrenkiel, V., Kirkin, A., and Zeuthen, J. Germline mutations of the PTEN gene in Cowden disease, an inherited breast and thyroid cancer syndrome., *Nat Genet*. *16*: 64-67, 1997.
63. Marsh, D., Coulon, V., Lunetta, K., Rocca-Serra, P., Dahia, P., Zheng, Z., Liaw, D., Caron, S., Duboue, B., Lin, A., Richardson, A., Bonnetblanc, J., Bressieux, J., Cabarrot-Moreau, A., Chompret, A., Demange, L., Eeles, R., Yahanda, A., Fearon, E., Fricker, J., Gorlin, R., Hodgson, S., Huson, S., Lacombe, D., and Eng, C. e. a. Mutation spectrum and genotype-phenotype analyses in Cowden disease and Bannayan-Zonana syndrome, two hamartoma syndromes with germline PTEN mutation., *Hum Mol Genet*. *7*: 507-515, 1998.
64. Nelen, M., van Staveren, W., Peeters, E., Hassel, M., Gorlin, R., Hamm, H., Lindboe, C., Fryns, J., Sijmons, R., Woods, D., Mariman, E., Padberg, G., and Kremer, H. Germline mutations in the PTEN/MMAC1 gene in patients with Cowden disease., *Hum Mol Genet*. *6*: 1383-1387, 1997.
65. Schultz, D. C., Balasara, B. R., Testa, J. R., and Godwin, A. K. Cloning and localization of a human diphthamide biosynthesis-like protein-2 gene, *DPH2L2*., *Genomics*. *52*: 186-191, 1998.
66. Peto, J., Collins, N., Barfoot, R., Seal, S., Warren, W., Rahman, N., Easton, D. F., Evans, C., Deacon, J., and Stratton, M. R. Prevalance of BRCA1 and BRCA2 gene mutations in patients with early-onset breast cancer, *JNCI*. *91*: 943-949, 1999.
67. Ford, D., Easton, D. F., Bishop, D. T., Narod, S. A., and Goldgar, D. E. BRCA1-mutation carriers; Breast cancer linkage consortium, *Lancet*. *343*: 692-695, 1994.

68. Golemis, E. and Serebriiskii, I. Two-hybrid system/interaction trap. *In*: D. Spector, R. Goldman, and L. Leinwand (eds.), *Cells, a laboratory manual*, pp. 69.1-69.40. Cold Spring Harbor, NY: CSHL Press, 1998.
69. Robbins, J., Dilworth, S. M., Laskey, R. A., and Dingwall, C. Two interdependent basic domains in nucleoplasmin nuclear targeting sequence: identification of a class of bipartite nuclear targeting sequence, *Cell*. 64: 615-23, 1991.
70. Fu, X. D. and Maniatis, T. Isolation of a complementary DNA that encodes the mammalian splicing factor SC35, *Science*. 256: 535-8, 1992.
71. Nigg, E. Nucleocytoplasmic transport: signals, mechanisms and regulation, *Nature*. 386: 779-, 1997.
72. Handa, N., Nureki, O., Kurimoto, K., Kim, I., Sakamoto, H., Shimura, Y., Muto, Y., and Yokoyama, S. Structural basis for recognition of the tra mRNA precursor by the Sex-lethal protein, *Nature*. 398: 579-85, 1999.
73. Deo, R. C., Bonanno, J. B., Sonenberg, N., and Burley, S. K. Recognition of polyadenylate RNA by the poly(A)-binding protein, *Cell*. 98: 835-45, 1999.
74. Bower, M. J., Cohen, F. E., and Dunbrack, R. L., Jr. Prediction of protein side-chain rotamers from a backbone-dependent rotamer library: a new homology modeling tool, *J Mol Biol*. 267: 1268-82, 1997.
75. Crowder, S. M., Kanaar, R., Rio, D. C., and Alber, T. Absence of interdomain contacts in the crystal structure of the RNA recognition motifs of Sex-lethal, *Proc Natl Acad Sci U S A*. 96: 4892-7, 1999.
76. Kataoka, N., Yong, J., Kim, V. N., Velazquez, F., Perkinson, R. A., Wang, F., and Dreyfuss, G. Pre-mRNA splicing imprints mRNA in the nucleus with a novel RNA-binding protein that persists in the cytoplasm, *Mol. Cell*. 6: 673-682, 2000.
77. Salicioni, A. M., Xi, M., Vanderveer, L. A., Balsara, B., Testa, J. R., Dunbrack, J., R.L., and Godwin, A. K. Identification and structural analysis of human RBM8A and RBM8B: Two highly conserved RNA-binding motif proteins that interact with OVCA1, a candidate tumor suppressor, *Genomics*. 69: 54-62, 2000.

10. PERSONNEL

Andrew Godwin, Principal Investigator

Ana Maria Salicioni, Postdoctoral Associate

Amanda Prowse, Postdoctoral Associate

Lisa Vanderveer, Technical Specialist

11. APPENDICES:

"Identification of two candidate tumor suppressor genes on chromosome 17p13.3: Assessment of their roles in breast and ovarian carcinogenesis"

1. Manuscripts:

- a. Schultz, D.C., Vanderveer, L., Berman, D.B., Wong, A.J., and Godwin, A.K. Identification of two candidate tumor suppressor genes on chromosome 17p13.3. *Cancer Res*, 56:1997-2002, 1996.
- b. Schultz, D.C., Balasara, B., Testa, J.R., and Godwin, A.K. Cloning and localization of a human diphthamide biosynthesis-like protein gene, *hDPH2L2*. *Genomics*, 52:186-191, 1998.
- c. Oleykowski, C.A., Bronson-Mullins, C.R., Godwin, A.K., Yeung, A.T. Mutation detection using a novel plant endonuclease. *Nucleic Acid Research*, 26:4597-4602, 1998.
- d. Bruening, W. Prowse, A.H., Schultz, D.C., Holgado-Madruga, M., Wong, A., Godwin, A.K. Expression of OVCA1, a candidate tumor suppressor gene, is reduced in tumors and inhibits growth of ovarian cancer cells. *Cancer Research*, 59:4973-4983, 1999.
- e. Salicioni, A.M., Xi, M., Vanderveer, L.A., Balsara, B. Testa, J.R., Dunbrack, R.L., and Godwin, A.K. Identification and structural analysis of human RBM8A and RBM8B: two highly conserved RNA-binding motif proteins that interact with OVCA1, a candidate tumor suppressor. *Genomics*, 69:54-62, 2000.
- f. Prowse, A.H., Vanderveer, L., R. Dunbrack, Godwin, A.K. *OVCA2*, not *OVCA1/DPH2L* may be down-regulated during retinoid-induced differentiation and apoptosis. Submitted to *Int. J. Cancer*, 2001.

Identification of Two Candidate Tumor Suppressor Genes on Chromosome 17p13.3¹

David C. Schultz,² Lisa Vanderveer,² David B. Berman, Thomas C. Hamilton, Albert J. Wong, and Andrew K. Godwin³

Department of Medical Oncology, Fox Chase Cancer Center, Philadelphia, Pennsylvania 19111 [D. C. S., L. V., D. B. B., T. C. H., A. K. G.], and Department of Microbiology and Immunology, Jefferson Cancer Institute, Thomas Jefferson University, Philadelphia, Pennsylvania 19107 [A. J. W.]

Abstract

A second tumor suppressor locus on 17p that is distinct from *TP53* has been identified in brain, breast, lung, and ovarian tumors. Using allelic loss mapping and positional cloning methods, we have recently identified two novel genes, which we refer to as *OVCA1* and *OVCA2*, that map to 17p13.3. The two genes are ubiquitously expressed and encode proteins of 443 and 227 amino acids, respectively, with no known functional motifs. Sequence comparison of *OVCA1* and *OVCA2* revealed extensive sequence identity and similarity to hypothetical proteins from *Saccharomyces cerevisiae*, *Caenorhabditis elegans*, and *Rattus species*. Northern blot analysis reveals that *OVCA1* and *OVCA2* mRNA were expressed in normal surface epithelial cells of the ovary, but the level of this transcript is significantly reduced or is undetectable in 92% (11/12) of the ovarian tumors and tumor cell lines analyzed. The location, high degree of amino acid conservation, and reduced expression in ovarian tumors and tumor cell lines suggest that decreased expression of these two genes contributes to ovarian tumorigenesis and should be considered candidate tumor suppressor genes.

Introduction

The molecular basis of ovarian cancer is rapidly being defined (1). The inactivation of multiple tumor suppressor genes seems to be important in the etiology of ovarian cancers. One strategy of locating putative tumor suppressor genes is to survey tumors for high rates of LOH.⁴ The combined data from four separate allelotyping studies of ovarian cancers demonstrate the observation of allelic loss for polymorphic DNA markers on nearly every chromosome arm. Furthermore, these studies revealed that >30% of the tumors studied showed LOH on chromosomes 6, 9, 13q, 17, 18q, 19p, 22q, and Xp (2-5). Additional studies indicate that chromosome 17 is clearly the most frequently altered chromosome in ovarian carcinomas (6-9).

The ovarian carcinomas surveyed for LOH have been largely high stage, and allelic loss in at least some of the arms listed above may not be causally related to carcinogenesis or metastasis. Furthermore, high-stage ovarian carcinomas tend to have more numerical chromosome abnormalities, which can confound attempts to distinguish between candidate tumor suppressor genes on the same deleted chromosome. Chromosome 17 has a number of potential cancer causing genes, including *TP53* at 17p13.1, the *BRCA1* gene at 17q21, prohibitin and *NM23* at 17q23-24, and the proto-oncogene *ERBB2* at 17q21. Recently, it has been shown that alterations at 17p13.3 may be an

important early event in stage I ovarian carcinomas and tumors of low malignant potential (7). Interestingly, in tumors of low malignant potential, allelic losses at 17p13.3 were not accompanied by LOH at *TP53*, suggesting there is a more distal tumor suppressor gene whose loss of function is required for early tumorigenesis. This same region has shown frequent LOH in breast cancers (10, 11), primitive neuroectodermal tumors (12), carcinoma of the cervix uteri (13), medulloblastoma (14, 15), osteosarcoma (16), and astrocytoma (17), suggesting that this tumor suppressor gene(s) residing on chromosome 17p13.3 is involved in the development of many types of cancers. We have found a high rate of allelic loss on 17p13.3 in our cohort of ovarian tumors and have identified a minimum region of allelic loss. Using positional cloning methods, we report the identification of two genes located within this critical region on 17p13.3 that show loss of expression and are candidates for being the tumor suppressor gene.

Materials and Methods

Tumor Samples and Cell lines. Ovarian tumor specimens were collected from consenting patients undergoing surgery for ovarian cancer at the American Oncological Hospital and the Lankenau Hospital in Philadelphia, or were obtained from the Gynecological Oncology Group/Cooperative Human Tissue Network Ovarian Tissue Bank (Columbus, OH). Ovarian cancer cell lines and human ovarian surface epithelial cells were maintained as described previously (18).

Isolation of DNA and RNA from Tumors and Matched Blood Samples. Preparation of RNA for Northern blot analysis, DNA isolation for Southern blot analysis, and LOH studies have been previously described by us (8, 18).

PCR Analysis of STRPs. STRPs were typed in a PCR-based assay containing 15-30 ng genomic DNA, 10 mM Tris-HCl (pH 8.3), 50 mM KCl, 1.5 mM MgCl₂, 0.001% gelatin, 0.4 μM each primer, dCTP, dGTP, and TTP each at 16 μM, dATP at 2 μM, 0.65 μCi [α -³²S]dATP (DuPont/New England Nuclear), 5% DMSO, and 0.25 units Amplitaq DNA polymerase (Perkin Elmer/Cetus) in a final volume of 5 μl. Following an initial denaturation step at 94°C for 4 min, DNA was amplified through 20 cycles consisting of 5 s denaturing at 94°C, 1 min annealing at 68°C-0.5°C/cycle, and 1 min extension at 72°C. The samples were then subjected to an additional 25 cycles consisting of 5 s denaturation at 94°C, 1 min at 58°C, and 1 min extension at 72°C and a final extension at 72°C for 5 min. PCR products were diluted 1:1 in 90% formamide, 20 mM EDTA, 0.3% bromophenol blue, 0.3% xylene cyanol, denatured at 94°C for 5 min and 4 μl loaded onto a 6% denaturing polyacrylamide gel, and electrophoresed at 90 W in 1× TBE (1× = 0.09 M Tris, 0.09 M boric acid, and 0.002 M EDTA). After electrophoresis, gels were dried at 70°C under vacuum and exposed to Kodak XAR-5 film for 24 to 28 h. Polymorphisms used to map a minimum region of allelic loss are as follows: *D17S34*, *D17S926*, *D17S849*, *D17S28*, *AKG2-1*, *D17S5*, *D17S786*, *D17S796*, *D17S513*, and *TP53* (19-22). The simple tandem repeat polymorphism *AKG2-1* was identified in our laboratory during the construction of a physical map of 17p13.3. The primers used were 5'-TCC TGC TCT GCA ACA GTG AC-3' (sense) and 5'-CAG CCC CTG TCT GAT TC-3' (antisense).

Genomic Library Screening. Cosmid clones were isolated from a genomic human placental cosmid library (Stratagene). Duplicate lifts from each plate were made to GeneScreen NEF-978x hybridization membranes (Dupont). Membranes were hybridized with [α -³²P]dATP random primed *D17S5* (YNZ22.2) and *D17S28* (YNH37.3) as probes. Hybridization and washing conditions have been described previously (8).

Received 2/8/96; accepted 3/18/96.

The costs of publication of this article were defrayed in part by the payment of page charges. This article must therefore be hereby marked *advertisement* in accordance with 18 U.S.C. Section 1734 solely to indicate this fact.

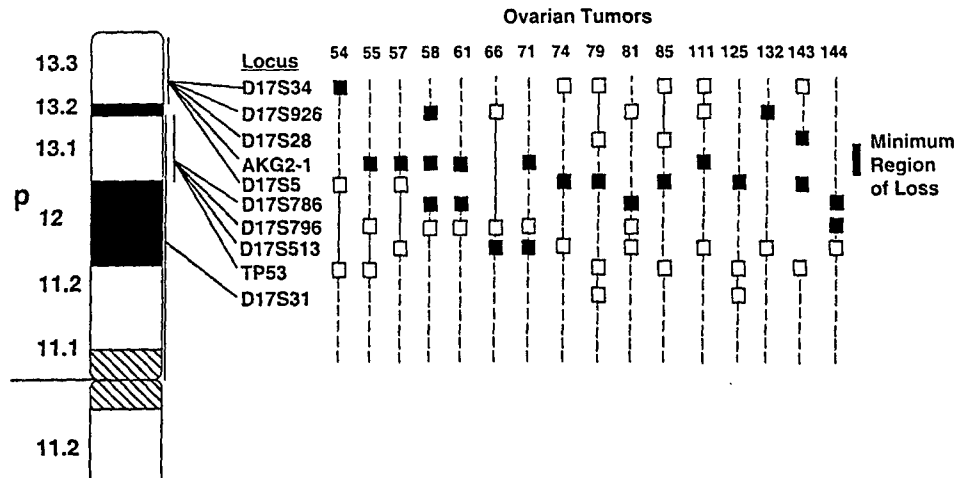
¹ This work was supported in part by NIH Grant RO1 CA60643 (A. K. G.), the Hoxie Harrison Smith Foundation, the Mary Smith Charitable Lead Trust, Butler Family Fund, Emile Zola Chapter of Brith Shalom Women, and the Ladies Auxiliary to the Veterans of Foreign Wars of the United States of America.

² These authors contributed equally to this work.

³ To whom requests for reprints should be addressed, at Department of Medical Oncology, Fox Chase Cancer Center, 7701 Burholme Avenue, Philadelphia, PA 19111. Phone: (215) 728-2557; Fax: (215) 728-2741.

⁴ The abbreviations used are: LOH, loss of heterozygosity; kbp, kilobase pair; STRP, simple tandem repeat polymorphism; EF-2, elongation factor 2.

Fig. 1. Allelic loss patterns of ovarian tumors for the short arm of chromosome 17. DNA samples from normal blood and ovarian tumor tissue were typed with STRPs from 17p. For each tumor, all informative loci are shown. ■, constitutional heterozygosity with LOH; □, constitutional heterozygosity with no LOH; blank spaces, uninformative. With the assumption that alleles in all regions between loci showing allelic loss are lost, solid lines indicate retained regions of chromosome 17p and open areas represent regions of allelic loss. - - -, regions that are uncertain in tumors with LOH for some loci.



Exon Trapping. Exon sequences were isolated from *Bam*H/*Hg*III- and *Pst*I-digested cosmid 7-2 DNA shotgun subcloned into the pSPL3 vector and transfected into Cos-1 cells. Total RNA was isolated 48 h posttransfection, reverse transcribed (18), and amplified using sequence-specific primers according to the manufacturer's instructions (Life Technologies, Inc.). Potential exon sequences were subcloned into pGEM-T (Promega), and the inserts were sequenced using vector primers by the single-stranded dideoxy method (United States Biochemical). Reaction products were analyzed on a 6% acrylamide/7 M urea gel. Sequencing results were analyzed by the GCG program. Exons were mapped by hybridizing trapped sequences to *Eco*RI-digested cosmid 7-2 DNA. Exons were analyzed by hybridization to Southern "zoo" blots and total RNA Northern blots.

cDNA Cloning and Northern Blot Analysis. A 1.6-kbp *Eco*RI fragment from cosmid 7-2 was used to screen to 1×10^6 plaques from an oligo(dT)-primed fetal brain cDNA library (Stratagene) or a library made from the A2780 ovarian cancer cell line. Sequencing of the cDNA clones was performed as described above with vector primers or primers derived from the obtained sequence. The complete nucleotide sequence of *OVCA1* and *OVCA2* will be submitted to the Genbank nucleotide sequence data base. Intron/exon boundaries were determined by sequencing cosmid clone 7-2 using a Model 373A automated fluorescence-based cycle sequencer (Applied Biosystems) and Taq dye terminator chemistry. Expression patterns and transcript sizes of cDNA clones were determined by hybridization of plasmid inserts to commercially available multiple-tissue Northern blots (Clontech).

Results

Definition of a Minimum Region of Allelic Loss on 17p13.3. Using DNA isolated from ovarian tumors, including Caucasian, Hispanic, and African-American patients of varying ages, we typed ovarian carcinomas for LOH on chromosome 17p using 10 highly polymorphic markers (Fig. 1). Forty-one (60%) of 68 informative ovarian tumors exhibited LOH, a frequency consistent with previous measurements. No correlations could be made between LOH and histopathological parameters such as subtype, stage, or grade. A common region of allelic loss was defined to be distal to YNZ22 (*D17S5*) and proximal to YNH37.3 (*D17S28*; Fig. 1). The predicted genetic distance between these two markers has been estimated to be approximately 3.5 cM (23). We have found that this region spans less than 30 kbp, which is in agreement with the results of Ledbetter *et al.* (19).

Isolation of Candidate Cancer Gene Sequences. Cosmid clones surrounding and including these two loci were isolated from a human placental DNA cosmid library, and several strategies were employed to evaluate these clones for potential expressed sequences. Cosmid clones containing genomic inserts spanning the limited region of allelic loss were introduced into the ovarian cancer cell line A2780

along with the bacterial *TnSneo* gene (an aminoglycoside 3' phosphotransferase) expressed from the SV40 early promoter (pKOneo). Evaluation of clonal outgrowth in the presence of geneticin (G418) revealed that cosmid clones 7-2 and 2-1 were the most effective in suppressing clonal outgrowth as compared to control cosmids (data not shown). This data suggested that a growth suppressor gene(s) is likely to be contained within these cosmids, and, moreover, this growth suppressor gene maps to the minimum region of allelic loss. Evaluation of clones 2-1 and 7-2 for expressed sequences by exon amplification identified a 65-bp exon which mapped to a 1.6-kbp *Eco*RI DNA fragment. Hybridization of the 65-bp fragment at low stringency to a zoo blot revealed conservation among other mammals (data not shown). Sequencing of the 1.6-kbp *Eco*RI fragment revealed a second potential open reading frame of 152 bp that was 122 bp away from the putative 65-bp exon.

Screening of a human fetal brain cDNA library using the 1.6-kbp genomic *Eco*RI fragment as the probe yielded six positive clones. Only two of the six clones (fb67-1 and 77-1) hybridized to any of the clones of the 17p13.3 cosmid "contig," indicating the presence of a potential family of genes.⁵ Sequence analysis of clones fb67-1 and fb77-1 revealed a 1350-bp open reading frame and an 847-bp of the 3' untranslated region, including a polyadenylation signal 19-bp 5' to the poly(A) tail. To identify the initiation codon, we employed an "anchored" PCR. Thirty-five additional nucleotides were identified, including 18 bases of the 5' untranslated region and two potential initiation codons. We provisionally refer to this gene as *OVCA1*, for ovarian cancer gene 1. The reading frame using the first AUG encodes a 443-amino acid protein with a predicted M_r ~50,000 which has been verified by *in vitro* translation, bacterial expression, and Western blot analysis (data not shown).

Characterization of *OVCA1* and *OVCA2*. Hybridization of Northern blots containing poly(A)⁺ RNA from different human tissues with the full-length *OVCA1* cDNA revealed two distinct transcripts of approximately 2.3 kb and 1.1 kb that were ubiquitously expressed (Fig. 2A). Isolation of a cDNA clone for the smaller transcript from an ovarian tumor cell line library revealed that this transcript was composed of the last 828 bp of *OVCA1* and 184 bp of the unique sequence. We refer to this transcript as *OVCA2* (ovarian cancer gene 2). Furthermore, Northern blot analysis of ovarian tumors and tumor cell lines revealed that the 2.3-kb *OVCA1* mRNA was expressed in normal surface epithelial cells of the ovary, but the level of the 2.3-kb transcript was significantly reduced or was undetectable

⁵ A. K. Godwin, unpublished data.

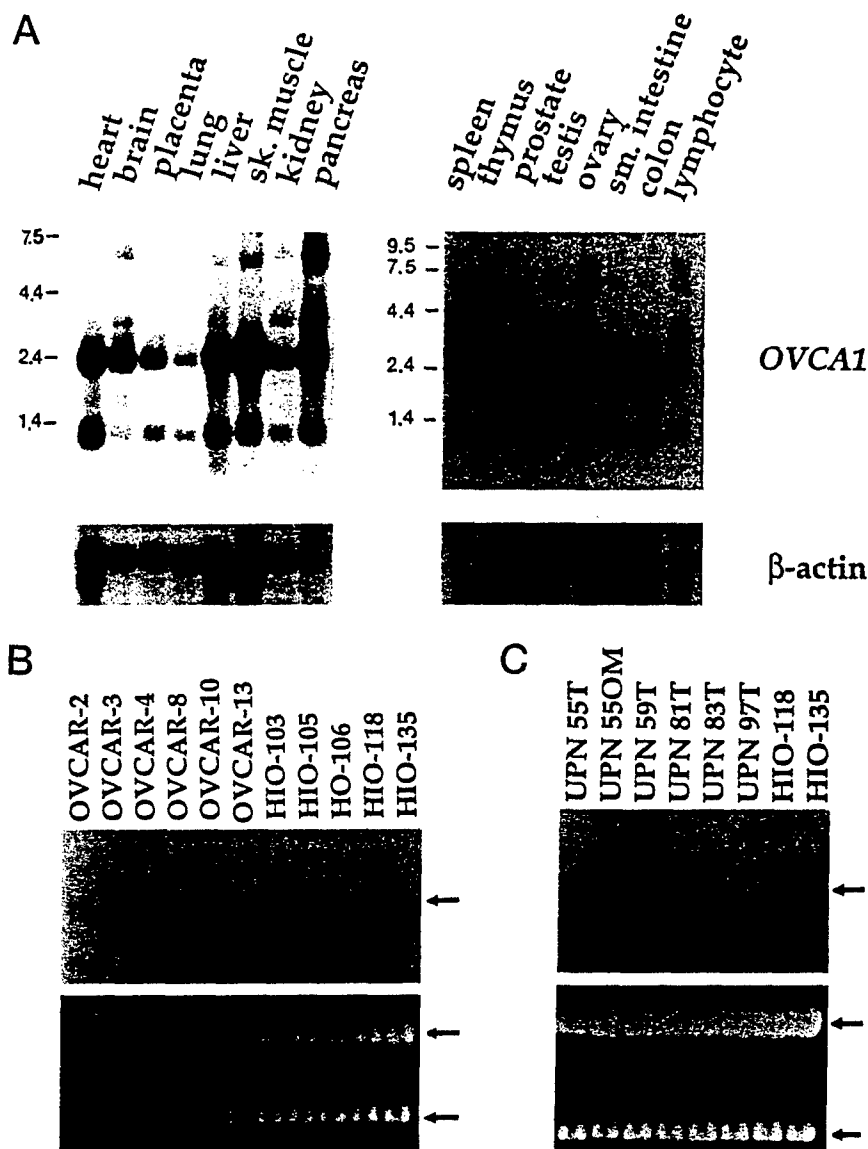


Fig. 2. A, tissue expression pattern of *OVCA1* and *OVCA2*. Blots containing 5 μ g poly(A)⁺-selected mRNA from the indicated human tissues were hybridized with a full-length *OVCA1* cDNA fragment. Note that the tissues are heterogeneous and the percentage of relevant epithelial cells in the ovary can be variable. Size standards are in kb. Lower panel, blots were reprobated with β -actin. The heart and skeletal muscle express two forms of β -actin, a 1.8-kb and a 2.0-kb transcript. B, Northern blot analysis of *OVCA1*-specific RNA in ovarian tumor cell lines (*OVCAR*). C, fresh ovarian tumors (*UPN*) as compared to normal ovarian surface epithelial cells (*HIO* or *HO*). Lower panels, ethidium bromide-stained gel prior to blotting; the position of the 28S and 18S rRNA is indicated.

in the majority (11/12) of the ovarian tumors and tumor cell lines evaluated ($P < 0.01$; Fig. 2, B and C). Similarly, RNA levels for *OVCA2* were also reduced in these same samples (data not shown).

Restriction mapping of genomic clones using cDNA probes and sequence comparison between cDNA and genomic clones indicated that *OVCA1* has 13 exons, 12 which are coding, and spans approximately 20-kbp of genomic DNA. The entire *OVCA1* and *OVCA2* cDNA sequences are present in the insert of cosmids 7-2 and 2-1, the same cosmids demonstrating the most significant clonal outgrowth in the *in vitro* suppression assay. The position of the 13 exons of *OVCA1* and the 2 exons of *OVCA2* relative to the common region of allelic loss defined by DNA markers *D17S5* and *D17S28* is shown in Figure 3. Furthermore, the transcriptional orientation of *OVCA1* is from telomere to centromere with the transcriptional start site of *OVCA1* telomeric to *D17S28*. The unique sequence of *OVCA2* has been positioned in the intron between exons 12 and 13 of *OVCA1* (Fig. 3).

Hybridization of genomic DNA samples from several different species with a full-length *OVCA1* cDNA fragment revealed strongly hybridizing fragments in tissue from humans, bovine, cat, dog, equine, monkey, mouse, porcine, rat, and yeast. These results suggested that *OVCA1* was highly conserved in mammals (data not shown). Basic local alignment search tool (BLAST) searches of the Genbank and

SwissProt data bases revealed extensive sequence identity at the nucleotide and the amino acid level to two recently identified sequences from *Caenorhabditis elegans* and *Saccharomyces cerevisiae* (Fig. 4A). The predicted gene product of *OVCA1* showed 60% and 53% sequence identity over 328 and 367 of the 443-amino acid residues when compared to the nematode and yeast proteins, respectively. If conserved amino acids substitutions are considered, the sequence similarity is increased to 77 and 89%, respectively. Because they were identified as the result of nematode and yeast genome sequencing projects, the function of these two predicted proteins is at the present time unknown. The fact that the *OVCA1* protein is so highly conserved at the amino acid level with organisms lower on the phylogenetic tree argues that it possesses an important cellular function.

The predicted gene product of *OVCA2* is a 227-amino acid protein with an approximate M_r 24,000, as determined by expression in bacteria (data not shown). Blast searches of the *OVCA2* gene identified extensive sequence identity at the 5' end of this gene with a recently identified expressed sequence tag from the *Rattus species* (24). *OVCA2* was observed to be 76% identical over 104 amino acids to the predicted rat gene product and 80% similar when conserved amino acids are considered (Fig. 4B).

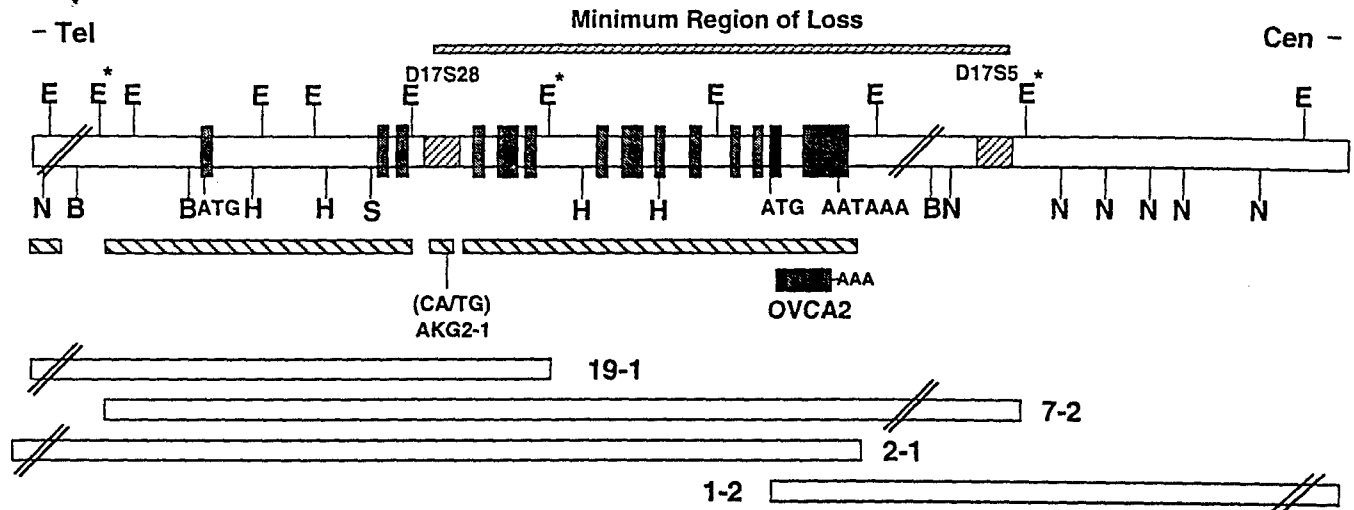


Fig. 3. Schematic of chromosome 17p13.3 containing the *OVCA1* and *OVCA2* genes. Stippled boxes, open reading frame of *OVCA1*; black box, unique exon of *OVCA2*. Cosmid clones, used to identify *OVCA1* and *OVCA2*, which span the minimum region of allelic loss in ovarian cancer are indicated. The position of *D17S5* and *D17S28* and one of the four newly identified (CA-GT)_n repeat polymorphisms are indicated relative to *OVCA1*. Lower hatched boxes, regions of genomic DNA that have been sequenced. B, *Bss*HII; E, *Eco*RI; H, *Hind*III; N, *Not*I; S, *Sfi*I; *, site in the vector.

A

ovca1	MRRQVMA...	ALVVS	GAAEQGGRDG	PGRGRAPRGR	VANQIPPEIL	42
yik3	MSGSTESKKQ	PRRRFIGRKS	GNSNNDKLT	TT	VAENGN E I I H	KQKSRIALGR	SVNHVPEDIL	60
cec14b1	0
ovca1	KNPQLQAATR	VLPSNYNFEI	PKTIWRFOQA	QAKKVALOMP	EGLLLFACTI	VDILERFTEA	102	
yik3	NDKELNEAK	LLPSNYNFEI	HKTWNIRKY	NAKRVALOMP	EGLLIYSLII	SDILEQFCGV	120	
cec14b1MITF	QLPSNYTPEM	PKTIWKIRST	ESKYVALOFP	EGLIMYACVI	ADILERKATGC	54	
ovca1	EVMVMGDVTV	GACCVDDFTA	RALGADFLVH	YGHSCLPMD	TSAQDERVLY	VFVDIRIDTT	162	
yik3	ETLVMGDVSV	GACCVDDFTA	RALDCDFLVH	YAHSCLVPID	VT..KTKVLY	VFVTHIQED	178	
cec14b1	DTVIMGDVTV	GACCVDDFTA	KSMGCDLHV	YGHSCLVPIQ	NT.DGTAMLY	VF.....	105	
ovca1	HLLDSLRLTF	PPATALALVS	TIOFVSTLOA	AAQELKAE..	..YRMSVPOC	KPLSPGEVLG	218	
yik3	HIKTLQKNR	PKGSRIATFG	TIOFNPAVHS	VRDKLLNDEE	HMLYTIIPQI	KPLSRGEVLG	238	
cec14b1GKRLVVVS	TMOFIPSLQ	LRTTETNKDD	S.IRIDIPOC	KPLSPGEVLG	152	
ovca1	CTSPRLSRE.	VFAVYVLGDG	RFHLESVMI	NPNVPAKRYD	PYSKVL SREH	YDHQRMQAAF	277	
yik3	CTSERLDKEQ	YDAMVFIIGDG	RFHLESAMI	NPEIPAFKYD	PYNRKE TREG	YDQKQHEVVR	298	
cec14b1	CTSPRLDASK	YDAIVYVLGDG	RFHLESIMH	NPEIEAFQYD	PYSRKL TRE F	YDHDLMRKRN	212	
ovca1	QEAIATARSA	KS WGLILGTL	GROGSPKILE	HLESRLRADG	LSFVRLLLSE	IFPSKLSSTSP	337	
yik3	AEATEVARKG	KVFGLILGAL	GROGNLNTVK	NLEKNLIAAG	KTVVKIILSE	WFPOKLMAMD	358	
cec14b1	IGSIEIARKC	TFGLIQGTL	GROGNLKVVE	ELEAQLERK	KKFLRVL LSE	IFPEKLAMFP	272	
ovca1	EVDVWVOVAC	PRLSIDWGTA	FPKPLLTPEE	AAVAL.RRDS	WQPP.VPMD.F	385	
yik3	QEDVWVOVAC	PRLSIDWGYA	FNKPPLTPEE	ASVLLKKDVM	FSEKYYPMD.Y	408	
cec14b1	EVD CWVOVAC	PRLSIDWGTQ	FPKPLLYPEE	LAVAL.DNVS	EKFRCLQLTG	QWTIIRMIPW	331	
ovca1	YAGSSLGPT	VNHG.....QDRR	PHAPGRPARG	KVQEGSARPP	423	
yik3	YEAKEYGR.GETP	KHAIE.....	425	
cec14b1	VLGRIIMKRT	VRNGRNGNLI	LLSKPKIHSR	ELSYFNEEKA	KRIGERFEGG	KLAKKVHKS I	391	
ovca1	SAVACEDCSC	RDEKVAPLAP	443	
yik3	425	
cec14b1	EQLKRHD PDV	QISTEPTKYL	LVSNS SILCG	VSLEELEE I F	LPLDELAEFI	VYPNKRSSYSF	451	

B

ovca2	MAAQRPLRVL	CLAGFRQSER	GFREKTGALR	KALRGRAELV	CLSGPHVPD	PPGPEGARSD	60
ratovca2VL	CLAGFRQSER	GFREKTGALR	KALRGHAEV	CLSGPHPVTE	AAASEGAGTD	52
ovca2	FGSCPPPEEOP	RGWVFSQEQA	DVFSALEEPA	VCRGLEESLG	MVAQALNRLG	FDGLLGFSQ	120
ratovca2	SGPFSPEEOP	RGWVFE EEA	DVFSALEEPT	VCRGLEEAAL E	TVAOALDKLG	AE.....	104

Fig. 4. A, comparison of the predicted amino acid sequence of the *OVCA1* protein with the hypothetical *S. cerevisiae* protein YIK3, chromosome IX cosmid 9150, and *C. elegans* cosmid C14B1 predicted proteins. B, comparison of the predicted amino acid sequence of the *OVCA2* protein with the predicted protein of EST110891 *Rattus norvegicus*. Identical amino acids are in black; conservative amino acids are shaded in gray. Gaps introduced for maximum alignment are marked with dots. Numbers on the right, amino acid position for each of the predicted proteins. Arrowheads, approximate position of exon/intron boundaries of *OVCA1* (A) and *OVCA2* (B).

Discussion

Molecular analyses of ovarian carcinomas has implicated one or more tumor suppressor genes on chromosome 17 (3, 6–9). To date, only a limited number of sporadic ovarian cancers have been found to possess mutations in the *BRCA1* gene (25, 26). Furthermore, evidence of allelic loss on chromosome 17p often coincides with mutations in *TP53* at 17p13.1. In ovarian carcinomas, mutations in *TP53* occur in advanced stage tumors when compared to either benign lesions, borderline tumors, or low grade carcinomas (27). We report in this study that 60% of sporadic ovarian tumors show LOH for markers distal to *TP53*, and that many retain *TP53* at 17p13.1 and the *BRCA1* locus at 17q21. This frequency is in agreement with a similar study in which tumors of low malignant potential and low-stage carcinomas demonstrated allelic loss for markers at 17p13.3 (7–9). These data suggest that in addition to the *TP53* gene at 17p13.3, at least one additional tumor suppressor gene resides on chromosome 17p.

Mapping of minimum regions of allelic loss have been helpful in defining chromosomal regions in which a tumor suppressor gene may reside (e.g., *DCC*, *CDKN2*, and *DPC4*) and allow positional cloning strategies to be initiated. These methods have allowed us to identify *OVCA1* and *OVCA2*. Sequence analysis of *OVCA1* and *OVCA2* identified no known functional domains; however, *OVCA1* showed significant sequence identity and similarity to a yeast and nematode sequence (Fig. 4).

The predicted protein for the *C. elegans* clone CEC14B1, which displays significant similarity to *OVCA1*, has sequence similarities to diphtheria toxin resistance like protein (28). In yeast, diphtheria resistance mutants form at least five complementation groups, and the enzymes corresponding to two of the complementation groups have been cloned (29). To a lesser extent, *OVCA1* is 20% identical and 50% similar in amino acid sequence to the yeast diphthamide biosynthesis protein DPH2. Diphthamide, is the result of posttranslationally modified histidine found almost exclusively in the eukaryotic translation EF-2. ADP ribosylation of diphthamide by bacterial exotoxins or by endogenous ADP ribosyltransferases inhibits EF-2 from translocating the growing peptide and ultimately arrests translation (30). However, *OVCA1* is more similar to the yeast and nematode proteins of unknown function (YIK3 and CEC14B1) than to the yeast DPH2. Therefore, *OVCA1* is likely not to be the homologue of DPH2, but could represent a human homologue for the other complementation groups in the diphthamide biosynthesis pathway or possess a similar role in a different biosynthetic pathway.

Northern blot analysis performed on fresh ovarian tumors and tumor cell lines indicates that the expression of *OVCA1* and *OVCA2* are decreased as compared to normal human ovarian surface epithelial cells (Fig. 2, B and C; data not shown). It is conceivable that mutations in upstream regulatory sequences may be the predominate mode of inactivation of these candidate tumor suppressor genes. For example, a nucleotide transversion near the exon/intron boundary of exon 12 was detected in the germ line of an individual diagnosed with ovarian cancer at age 45 years, and this change was homozygous in the tumor (data not shown). Studies are under way to determine whether this alteration affects the expression of *OVCA2* in the tumor, since the C to A transversion destroys a Sp1 site in the promoter of *OVCA2* (data not shown). This alteration has not been observed in >50 constitutional DNA samples collected from unaffected individuals. In addition to genetic changes, epigenetic changes such as *de novo* methylation of promoter CpG islands may also result in the inactivation of the retained allele. Silencing of gene transcription in association with hypermethylation of normally unmethylated 5'-CpG islands has been implicated as the major mechanism for the inactivation of the tumor

suppressor genes *CDKN2* and *VHL* in sporadic disease (31, 32). It has previously been shown that the region of 17p13.3 that contains *OVCA1* and *OVCA2* is aberrantly hypermethylated in colon, lung, neural, renal, and ovarian tumors (33, 34). These changes in methylation patterns could contribute to the decreased level of expression observed in ovarian tumor specimens and tumor cell lines. Preliminary evidence suggests that expression of *OVCA1* and *OVCA2* may be regulated by methylation of a 5'-CpG island.⁶ Furthermore, it was recently reported that a novel zinc finger protein, HIC-1 (hypermethylated in cancer gene 1), is localized to 17p13.3 and its expression found to be dependent on the methylation status of its promoter (35). Although this putative tumor suppressor gene maps outside our minimum region of allelic loss, its inactivation may further contribute to tumorigenesis alone or in combination with *OVCA1* and *OVCA2*.

Mutational analysis of the 13 exons of *OVCA1* and the unique exon to *OVCA2*, including adjacent intron boundaries, is currently being investigated in a large panel of breast, brain, and ovarian tumors. Mutation or deregulation of protein expression of either gene may prove to be causative in tumorigenesis and support the hypothesis that one or both of these genes are tumor suppressor genes. Overall, the chromosomal location, high degree of amino acid conservation, and deregulation of mRNA expression suggest that one or both genes are likely to be involved in the pathogenesis of ovarian cancer as well as other neoplasms such as breast and brain.

Acknowledgments

We thank Drs. W. Michael Hogan, Matthew Boente, Nelly Auersperg, and also Josephine Costalas, Brian Kane, and Alena Schnarr for their invaluable help and contributions to this work.

References

- Godwin, A. K., Schultz, D. C., Hamilton, T. C., and Knudson, A. G. Oncogenes and tumor suppressor genes. In: W. J. Hoskins, C. A. Perez, and R. C. Young (eds.), *Gynecological Oncology: Principles and Practice*. Philadelphia: J. B. Lippincott Company, in press, 1996.
- Sato, T., Saito, H., Morita, R., Koi, S., Lee, J. H., and Nakamura, Y. Allelotype of human ovarian cancer. *Cancer Res.*, 51: 5118–5122, 1991.
- Yang-Feng, T. L., Han, H., Chen, K.-C., Li, S.-b., Claus, E. B., Carcangiu, M. L., Chambers, S. K., Chambers, J. T., and Schwartz, P. E. Allelic loss in ovarian cancer. *Int. J. Cancer*, 54: 546–541, 1993.
- Cliby, W., Ritland, S., Hartman, L., Dodson, M., Halling, K. C., Keeney, G., Podratz, K. C., and Jenkins, R. B. Human epithelial ovarian cancer allelotype. *Cancer Res.*, 53: 2393–2398, 1993.
- Osborne, R. J., and Leech, V. PCR allelotyping of human ovarian cancers. *Br. J. Cancer*, 69: 429–438, 1994.
- Foulkes, W. D., Black, D. M., Stamp, G. W. H., Solomon, E. and Trowsdale, J. Very frequent loss of heterozygosity throughout chromosome 17 in sporadic ovarian carcinoma. *Int. J. Cancer*, 54: 220–225, 1993.
- Phillips, N., Ziegler, M., SaHa, B., and Xynos, F. Allelic loss on chromosome 17 in human ovarian cancer. *Int. J. Cancer*, 54: 85–91, 1993.
- Godwin, A. K., Vanderveer, L., Schultz, D. C., Lynch, H. T., Altomare, D. A., Buetow, K. H., Daly, M., Getts, L. A., Masny, A., Rosenblum, N., Hogan, M., Ozols, R. F., and Hamilton, T. C. A common region of deletion on chromosome 17q in both sporadic and familial epithelial ovarian tumors distal to *BRCA1*. *Am. J. Hum. Genet.*, 55: 666–677, 1994.
- Phillips, N. J., Ziegler, M. R., Radford, D. M., Fair, K. L., Steinbrueck, T., Xynos, F. P., and Donis-Keller, H. Allelic deletion on chromosome 17p13.3 in early ovarian cancer. *Cancer Res.*, 56: 606–611, 1996.
- Coles, C., Thompson, A. M., Elder, P. A., Cohen, B. B., Mackenzie, I. M., Cranston, G., Chetty, U., Mackay, J., MacDonald, M., Nakamura, Y., Hoyheim, B., and Steel, C. M. Evidence implicating at least two genes on chromosome 17p in breast carcinogenesis. *Lancet*, 336: 761–763, 1990.
- Cornelis, R. S., van Vliet, M., Vos, C. B. J., Cleton-Jansen, A.-M., van de Vijver, M. J., Peterse, J. L., Khan, P. M., Borresen, A.-L., Cornelisse, C. J., and Devilee, P. Evidence for a gene on 17p13.3, distal to *TP53* as a target for allele loss in breast tumors without *p53* mutations. *Cancer Res.*, 54: 4200–4206, 1994.
- Biegel, J. A., Burk, C. D., Barr, F. G., and Emanuel, B. S. Evidence for a 17p tumor locus distinct from *p53* in pediatric primitive neuroectodermal tumors. *Cancer Res.*, 52: 3391–3395, 1992.
- Atkin, N. B., and Baker, M. C. Chromosome 17p loss in carcinoma of the cervix uteri. *Cancer Genet. Cytogenet.*, 37: 229–233, 1989.

⁶H. Ling and A. K. Godwin, manuscript in preparation.

14. Çogen, P. H., Daneshvar, L., Metzger, A. K., Duyk, G., Edwards, M. S. B., and Sheffield, V. C. Involvement of multiple chromosome 17p loci in medulloblastoma tumorigenesis. *Am. J. Hum. Genet.*, 50: 584-589, 1992.
15. Saylor, R., Sidransky, D., Friedman, H. S., Bigner, S. H., Bigner, D. D., Vogelstein, B., and Brodeur, G. M. Infrequent *p53* gene mutations in medulloblastomas. *Cancer Res.*, 51: 4721-4723, 1991.
16. Toguchida, J., Ishizaki, K., Nakamura, Y., Sasaki, M. S., Ikenaga, M., Kato, M., Sugimoto, M., Kotoura, Y., and Yamamuro, T. Assignment of a common allele loss in osteosarcoma to the subregion 17p13. *Cancer Res.*, 49: 6247-6251, 1989.
17. Saxena, A., Clark, W. C., Robertson, J. T., Ikejiri, B., Oldfield, E. H., and Ali, I. Evidence for the involvement of a potential second tumor suppressor gene on chromosome 17 distinct from *p53* in malignant astrocytomas. *Cancer Res.*, 52: 6716-6721, 1992.
18. Schultz, D. C., Vanderveer, L., Buetow, K. H., Boente, M. P., Ozols, R. F., Hamilton, T. C., and Godwin, A. K. Characterization of chromosome 9 in human ovarian neoplasia identifies frequent genetic imbalance on 9q and rare alterations involving 9p, including *CDKN2*. *Cancer Res.*, 55: 2150-2157, 1995.
19. Ledbetter, D. H., Ledbetter, S. A., vanTuinen, P., Summers, K. M., Robinson, T. J., Nakamura, Y., Wolff, R., White, R., Barker, D. F., Wallace, M. R., Collins, F. S., and Dobyns, W. B. Molecular dissection of a contiguous gene syndrome: frequent submicroscopic deletions, evolutionary conserved sequences, and a hypomethylated "island" in the Miller-Dieker chromosome region. *Proc. Natl. Acad. Sci. USA*, 86: 5136-5140, 1989.
20. Gypay, G., Morissette, J., Vignal, A., Dib, C., Fizames, C., Millasseau, P., Marc, S., Bernardi, G., Lathrop, M., and Weissenbach, J. The 1993-94 Génethon human genetic linkage map. *Nat. Genet.*, 7: 246-339, 1994.
21. Jones, M., H. and Nakamura, Y. Detection of loss of heterozygosity at the human *TP53* locus using a dinucleotide repeat polymorphism. *Genes Chromosomes & Cancer*, 5: 89-90, 1992.
22. Oliphant, A. R., Wright, E. C., Swensen, J., Gruis, N. A., Goldgar, D., and Skolnick, M. H. Dinucleotide repeat polymorphism at the *D17S513* locus. *Nucleic Acids Res.*, 19: 4794, 1993.
23. Murray, J. C., Buetow, K. H., Weber, J. L., Ludwigsen, S., Scherpbier-Heddema, T., Manion, F., Quillen, J., Sheffield, V. C., Sunden, S., Duyk, G. M., Weissenbach, J., Gyapay, G., Dib, C., Morissette, J., Lathrop, G. M., Vignal, A., White, R., Matsunami, N., Gerken, S., Melis, R., Albertsen, H., Plaetke, R., Odelberg, S., Ward, D., Dausset, J., Cohen, D., and Cunn, H. A comprehensive human linkage map with centiMorgan density. Cooperative Human Linkage Center (CHLC). *Science* (Washington DC), 265: 2049-2054, 1994.
24. Lee, N. H., Weinstock, K. G., Kirkness, E. F., Earle-Hughes, J. A., Fuldner, R. A., Marmaras, S., Glodek, A., Gocayne, J. D., Adams, M. D., Kerlavage, A. R., Fraser, C. M., and Venter, J. C. Comparative expressed sequence tag analysis of differential gene expression profiles in PC-12 cells before and after nerve growth factor treatment. *Proc. Natl. Acad. Sci.*, 92: 8303-8307, 1995.
25. Hosking, L., Trowsdale, J., Nicolai, H., Solomon, E., Foulkes, W., Stamp, G., Signer, E., and Jeffreys, A. A somatic *BRCA1* mutation in an ovarian tumor. *Nat. Genet.*, 9: 343-344, 1995.
26. Merajver, S. D., Pham, T. M., Caduff, R. F., Chen, M., Poy, E. L., Cooney, K. A., Weber, B. L., Collins, F. S., Johnston, C., and Frank, T. S. Somatic mutations in the *BRCA1* gene in sporadic ovarian tumors. *Nat. Genet.*, 9: 439-443, 1995.
27. Zheng, J., Benedict, W. F., Xu, H.-J., Hu, S.-X., Kim, T. M., Velicescu, M., Wan, M., Cofer, K. F., and Dubeau, L. Genetic disparity between morphologically benign cysts contiguous to ovarian adenocarcinomas and solitary cystadenomas. *J. Natl. Cancer Inst.*, 87: 1146-1153, 1995.
28. Wilson, R., Ainscough, R., Andersen, K., Baynes, C., Berks, M., Bonfield, J., Burton, J., Connell, M., Copsey, T., Cooper, J., Coulson, A., Craxton, M., Dear, S., Du, Z., Durbin, R., Favello, A., Fulton, L., Gardner, A., Green, P., Hawkins, T., Hillier, L., Jier, M., Johnston, L., Jones, M., Kershaw, J., Kirsten, J., Laister, N., Latrielle, P., Lightning, J., Lloyd, C., McMurray, A., Mortimore, B., O'Callaghan, M., Parsons, J., Percy, C., Rifken, L., Roopra, A., Saunders, D., Showkneen, R., Smaldon, N., Smith, A., Sonhammer, E., Staden, R., Sulston, J., Thierry-Mieg, J., Thomas, K., Vaudin, M., Vaughan, K., Waterston, R., Watson, A., Weinstock, L., Wilkinson-Sproat, J., and Wohlman, P. 2.2Mb of contiguous nucleotide sequence from chromosome III of *C. elegans*. *Nature* (Lond.), 368: 32-38, 1994.
29. Mattheakis, L. C., Sor, F., and Collier, R. J. Diphthamide synthesis in *Saccharomyces cerevisiae*: structure of the *DPH2* gene. *Gene*, 132: 149-154, 1993.
30. Iglewski, W. J. Cellular ADP-ribosylation of elongation factor 2. *Mol. Cell. Biochem.*, 138: 131-133, 1994.
31. Herman, J. G., Latif, F., Weng, Y., Lerman, M., Zbar, B., Liu, S., Samid, D., Duan, D.-S. R., Gnarr, J. R., Linehan, W. M., and Baylin, S. B. Silencing of the *VHL* tumor-suppressor gene by DNA methylation in renal carcinoma. *Proc. Natl. Acad. Sci. USA*, 91: 9700-9704, 1994.
32. Merlo, A., Herman, J. G., Mao, L., Lee, D. J., Gabrielson, E., Burger, P. C., Baylin, S. B., and Sidransky, D. 5' CpG island methylation is associated with transcriptional silencing of the tumor suppressor *p16/CDKN2/MTS1* in human cancers. *Nat. Med.*, 1: 686-692, 1995.
33. Makos, M., Nelkin, B. D., Chazin, V. R., Cavenee, W. K., Brodeur, G., and Baylin, S. B. DNA hypermethylation is associated with 17p allelic loss in neural tumors. *Cancer Res.*, 53: 2715-2718, 1993.
34. Pieretti, M., Powell, D. E., Gallion, H. H., Conway, P. S., Case, E. A., and Turker, M. S. Hypermethylation at a chromosome 17 "hot spot" is a common event in ovarian cancer. *Hum. Pathol.*, 26: 398-401, 1995.
35. Wales, M. M., Biel, M. A., Deiry, W. E., Nelkin, B. D., Issa, J.-P., Cavenee, W. K., Kuerbitz, S. J., and Baylin, S. B. *p53* activates expression of *HIC-1*, a new candidate tumor suppressor gene on 17p13.3. *Nat. Med.*, 1: 570-577, 1995.

Cloning and Localization of a Human Diphthamide Biosynthesis-like Protein-2 Gene, *DPH2L2*

David C. Schultz,*†¹ Binaifer R. Balasara,* Joseph R. Testa,* and Andrew K. Godwin*†²

*Department of Medical Oncology, Fox Chase Cancer Center, Philadelphia, Pennsylvania 19111; and
†Department of Chemistry, Lehigh University, Bethlehem, Pennsylvania 18015

Received November 17, 1997; accepted May 27, 1998

Sequence analysis of the candidate tumor suppressor *OVCA1* revealed extensive sequence identity and similarity to proteins from a diverse number of species, including the yeast diphthamide biosynthesis protein-2, *dph2*, which suggested that *OVCA1* may be the human homologue to this yeast gene. However, searches of the translated EST database for sequences in common with *dph2* and *OVCA1* uncovered an EST, h52976, with significant amino acid conservation with *dph2*. Isolation of a cDNA clone encompassing the EST by RACE methodologies and sequence analysis indicate the identification of a previously unidentified gene that is ubiquitously expressed and maps to chromosome 1p34. Based on amino acid sequence analysis, the 489-amino-acid protein encoded by this novel gene is distinct from *OVCA1* and is more closely related to the yeast *dph2* gene product. Therefore, we refer to this novel gene as *DPH2L2*, which constitutes one member of a novel gene family that may be involved in diphthamide biosynthesis in humans. © 1998 Academic Press

Press

INTRODUCTION

Diphtheria toxin resistance is best defined in yeast, in which five complementation groups have been defined. Genes complementing two of these groups have been cloned and characterized (Mattheakis *et al.*, 1992, 1993). Both genes are believed to encode enzymes that are integral to the biosynthesis of diphthamide through the posttranslational modification of histidine. Diphthamide is a rare amino acid that is found almost exclusively in the eukaryotic translation elongation factor 2, EF-2. The cellular role of EF-2 is to translocate a growing peptide from the "A" pocket of the ribosome to the "P" pocket through an energy-dependent mechanism, allowing the next codon of a message to be read during the synthesis of a peptide. ADP ribosyla-

tion of cellular proteins by endogenous ribosyltransferases or bacterial toxins has been shown to affect profoundly the activity of these proteins (Iglewski, 1994).

We and others have recently described the positional cloning of *OVCA1/DPH2L1* from a chromosomal region on 17p13.3 that displays high rates of LOH³ in ovarian, breast, and brain tumors (Phillips *et al.*, 1996; Schultz *et al.*, 1996). These sequences have been found to be similar to a diphtheria toxin resistance protein and the yeast diphthamide biosynthesis protein-2. Based on amino acid sequence conservation, a cDNA sequence for a gene related to but distinct from *OVCA1* has been identified. Analysis of the predicted amino acid sequence of this previously unidentified gene suggests that it is more closely related to the yeast *dph2* gene product; hence, it has been referred to as the diphthamide biosynthesis-like protein-2 gene, *DPH2L2*. The high degree of amino acid sequence homology between *OVCA1* and *DPH2L2* suggests that a novel gene family has been uncovered, based on putative functional motifs with uncharacterized biochemical function.

MATERIALS AND METHODS

Northern blot analysis of *DPH2L2*. The expression of *DPH2L2* mRNA in various human tissues was determined by hybridization of an 800-bp *EcoRI/BamHI* fragment from the insert of commercially obtained EST h52976 (Genome Systems, St. Louis, MO) to multiple-tissue Northern blots (Clontech, Palo Alto, CA). Membranes were prehybridized, hybridized, and washed as previously described (Schultz *et al.*, 1996).

Marathon RACE PCR used to clone a *DPH2L2* cDNA. The entire coding region of *DPH2L2* was identified by the PCR amplification of 1 μ l of a human spleen or human thymus Marathon cDNA library (Clontech) with 5'-CCA TCC TAA TAC GAC TCA CTA TAG GGC-3' (AP-1) and either 5'-CGG AGA TCT CCA GTA ATG AGT GAC ACG-3' (5' GSP-1) or 5'-TCC TGC AGT CTC ATT CCT TAG TTC CCG-3' (3' GSP-1) in 40 mM Tricine-KOH, pH 9.2, 15 mM KOAc, 3.5

¹ Current address: Wistar Institute, 3601 Spruce Street, Philadelphia, PA 18014.

² To whom correspondence should be addressed. Telephone: (215) 728-2756. Fax: (215) 728-2741.

³ Abbreviations used: *OVCA1*, ovarian cancer 1 gene; DPH, diphthamide; LOH, loss of heterozygosity; RACE, rapid amplification of cDNA ends; EST, expressed sequence TAG; FISH, fluorescence *in situ* hybridization; AP, anchor primer; GSP, gene-specific primer; PFU, plaque-forming units.

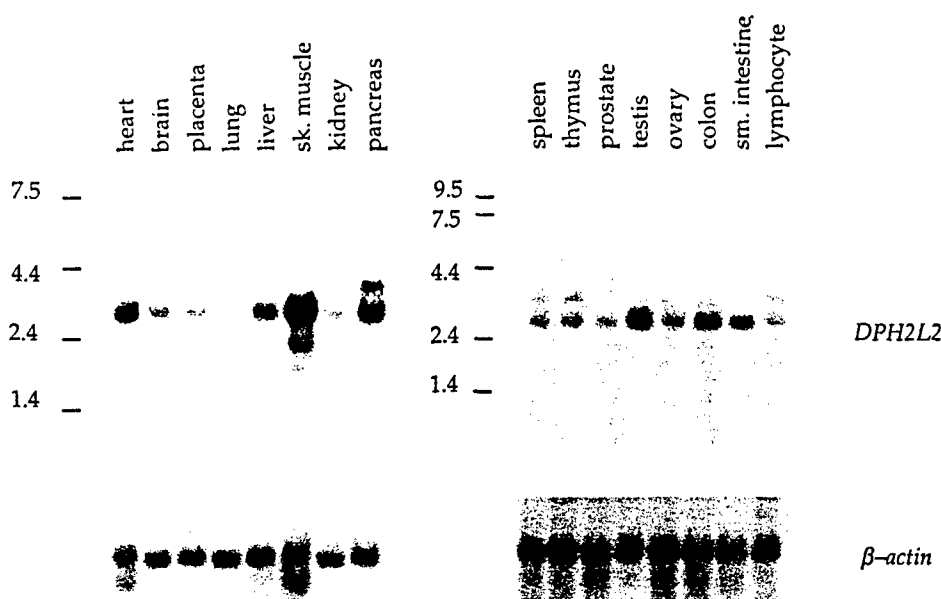


FIG. 1. Tissue expression pattern of *DPH2L2*. Blots containing 5 μ g of poly(A)⁺ selected mRNA from each of the indicated human tissues were hybridized with an internal 800-bp *EcoRI/BamHI* fragment from the insert of EST h52976. Note that the tissues are heterogeneous, and the percentage of relevant epithelial cells in breast and ovary can be variable. Size standards are in kilobases. (**Bottom**) Blots were reprobred with a β -actin cDNA probe. Heart and skeletal muscle express two β -actin transcripts, 1.8 and 2.0 kb in size.

mM Mg(OAc)₂, 75 μ g/ml BSA, 1% glycerol, 0.8 mM Tris-HCl, pH 7.5, 1 mM KCl, 0.5 mM (NH₄)₂SO₄, 2.0 μ M EDTA, 0.1 mM β -mercaptoethanol, 0.005% Thesit, 0.44 μ g of TaqStart antibody (Clontech), 0.5 μ M of each primer, 200 μ M of each dNTP, 5% DMSO, and 0.4 μ l of KlenTaq Advantage DNA polymerase (Clontech) in a final volume of 20 μ l. Following an initial denaturation step at 94°C for 1 min, DNA was amplified through 5 cycles consisting of 5 s of denaturing at 94°C and a 4-min extension at 72°C and 5 additional cycles consisting of 5 s of denaturing at 94°C and a 4-min extension at 70°C. The samples were then subjected to an additional 25 cycles, consisting of 5 s of denaturation at 94°C, and a 4-min extension at 68°C. PCR products were diluted 1:10, and 2 μ l were reamplified by nested PCR with 5'-ACT CAC TAT AGG GCT CGA GCG GC-3' (AP-2) and either 5'-CCC AGG GCC AAC ACA TAG CTA CG-3' (5' GSP-2) or 5'-CTC AGC ACA TGC CCA GTA ATG CG-3' (3' GSP-2) as described above. PCR products were gel purified or directly ligated into 50 ng pGEM-T (Promega, Madison, WI). Colonies with inserts were sequenced in a core sequencing facility at the Fox Chase Cancer Center using a Model 377A automated fluorescence-based cycle sequencer (Applied Biosystems, Foster City, CA) and Taq dye terminator chemistry.

Fluorescence in situ hybridization analysis of *DPH2L2*. Phage clones were isolated from a human placenta genomic DNA λ library, EMBL3 (Clontech). A total of 5×10^5 PFU immobilized on Gene-Screen NEF-978x hybridization membrane (Dupont-NEN, Boston, MA) were hybridized with an [α -³²P]dATP (Dupont-NEN) random prime-labeled 800-bp *EcoRI/BamHI* fragment of EST h52976. Hybridization and washing conditions were as previously described (Godwin *et al.*, 1994). Two independently purified phage DNA clones were biotinylated and hybridized to human metaphase chromosome spreads from phytohemagglutinin-stimulated peripheral blood lymphocytes prepared according to methods previously described (Fan *et al.*, 1990). Cultures were synchronized by treatment with 5-bromodeoxyuridine (0.18 mg/ml, Sigma) for 16 h, followed by release from the block by incubation in fresh medium containing thymidine (2.5 μ g/ml) for 6 h. Metaphase cells were harvested, and chromosome spreads were prepared according to standard procedures.

Fluorescence *in situ* hybridization and detection of immunofluorescence were carried out essentially as described previously (Bell *et al.*, 1995). Biotinylated probes were denatured, preannealed with excess Cot1 DNA, and hybridized overnight at 37°C to metaphase spreads. Hybridization sites were detected with fluorescein-labeled avidin (Oncor) and amplified by the addition of anti-avidin antibody

(Oncor) and a second layer of fluorescein-labeled avidin. The chromosome preparations were counterstained with diamidino-2-phenylindole (DAPI) and observed with a Zeiss Axiophot epifluorescence microscope equipped with a cooled charge-coupled device camera (Photometrics, Tucson AZ) operated by a Macintosh computer workstation. Digitized images of DAPI staining and fluorescein signals were captured, pseudo-colored, and merged using Oncor version 1.6 software.

RESULTS

Following the cloning of a candidate tumor suppressor gene, *OVCA1*, subsequent searches of the EST database revealed an EST, h52976, that was 63% identical to the corresponding nucleotide sequence of *OVCA1*. These data implicated the existence of a gene potentially related to *OVCA1*. To explore further the nature of this similar nucleotide sequence, the EST was commercially obtained from Genome Systems. A 1.2-kbp insert was rescued from the plasmid, and sequence analysis did not identify a polyadenylate tail. Sequence comparison of the EST sequence with sequences in the GenBank or EST databases did not match that of any previously identified transcripts; however, 400 bp of a repetitive line element, MER 20, was identified. Hybridization of an internal 800-bp nonrepetitive DNA probe to poly(A)⁺ selected Northern blots revealed a 2.5-kb transcript that was ubiquitously expressed (Fig. 1). In addition to the expression of the 2.5-kb transcript, an alternative transcript, approximately 3.0 kb, was identified in pancreas, spleen, thymus, and lymphocytes. To obtain the full-length sequence of this novel transcript, a PCR cloning strategy was employed using Marathon stretch cDNA libraries (see Materials and Methods). Sequencing of multiple independent 5' and 3' RACE amplification

1	CGCCCGGCAGG TAGGGGATACTC ACCGGCTGAAGG CCGACTGTGATT CCCCTACCCCC ACAAGGCGATTT TGACCCCTGAG GGCTGCTCTAGA	96
97	GGACTCAGGCC CGAAGCTGTCCC AGGGAGGTCCCC GCTGCATCCCAC CACCCAAGCTGT GCCTCATGGAGT CGATGTTTAGCA GCCCTGCCGAGG	192
1	M E S M F S S P A E A	11
193	CGGCGTGCAGC GAGAGACCGGGG TGCCAGGACTGC TTA CTCTCTCTC CGGACCTGGACG GAGTGTACGAGC TGGAGCGAGTCG CTGGATTGTGCC	288
12	A L Q R E T G V P G L L T P L P D L D G V Y E L E R V A G F V R	43
289	GCGACCTGGGGT GTGAACGAGTTG CTTTGCAGTTCC CTGACCAGCTAT TGGGAGATGCTG TGGCTGTGGCTG CACGACTGGAGG AGACGACAGGGT	384
44	D L G C E R V A L Q F P D Q L L G D A V A V A A R L E E T T G S	75
385	CAAAGATGTTC TTTGGGTGACA CAGCCTACGGCA GCTGCTGCTGG ATGTGCTGGGTG CTGAGCAAGCTG GAGCTCAGGCTC TCATACATTTTG	480
76	K M F I L G D T A Y G S C C V D V L G A E Q A G A Q A L I H F G	107
481	GCCCTGCCTGCT TAAGCCCTCCAG CCCGCCACTGC CCGTTGCCTCG TGCTTTCGTCAA CGTCTGTGGCC TTGGAACCTGT GTCAAGACCTTT	576
108	P A C L S P P A R P L P V A F V L S S T F C G L G T L C Q D L W	139
577	GGGGCCAAAAC CCAGACCCCAA GCGCCTGTGGTG CTGCTGTGAGC CCGCCTGTGCC ATGCCCTGGAGG CTTTGGCTACTC TCCTGCGCCCAC	672
140	G P K P R P Q S A C G A A G E P A C C A H A L E A L A T L L R P R	171
673	GGTACTGGACC TGCTAGTCTCCA GCCCAGCTTTTC CCCAACCAGTGP GTTCCCTGAGTC CAGAGCCTATGC CCCTAGAGCGTT TTGGGCGCCGCT	768
172	Y L D L L V S S P A F P Q P V G S L S P E P M P L E R F G R F	203
769	TCCCCCTGCCC CAGGGAGGCGTC TAGAAGAGTATG GTGCCCTCTATG TAGGGGGCTCTA AGGCCAGCCCTG ACCCAGACCTTG ACCCAGACCTGA	864
204	P L A P G R R L E E Y G A F Y V G G S K A S P D P D L D P D L S	235
865	GTCGGCTGCTCT TGGGGTGGGAC CAGGTCAACCTT TCTCTCTGCT GTCCAGATACAG GGAAGACTCAGG ATGAGGGTGCCC GGGCTGGAGGGC	960
236	R L L L G W A P G Q P F S S C C P D T G K T Q D E G A R A G G L	267
961	TAAGGGCACGAA GACGATATCTGG TAGAGAGGGCCA GAGATGCCCGG TGTTAGGGCTGC TGGCAGGCACAC TGGTGTAGCCC AACCCGTGAGG	1056
268	R A R R R Y L V E R A R D A R V V G L L A G T L A G T L G H R E A	299
1057	CACTGGCCCACT TGCGGAACCTGA CTCAGGTGCTG GCAAGCGTAGCT ATGTGTGGGCC TGGGGCGGCCA CCCCTGCCAAGC TTGCCAATTCC	1152
300	L A H L R N L T Q A A G K R S Y V L A L G R P T P A K L A N F P	331
1153	CTGAGGTGGATG TCTTTGTGCTAT TAGCCTGTCTC TGGGTGCTCTAG CCCCCAGCTTT CTGGTAGCTTCT TCCAGCCTATAC TGGCACCATGTG	1248
332	E V D V F V L L A C P L G A L A P Q L S G S F F Q P I L A P C E	363
1249	AGCTGGAAGCTG CTTGCAACCTG CTTGGCCACCTC CAGGCCTGGCTC CCCACCTCACAC ATTATGCGGACT TATGCTGGCT CTCCTTCCACG	1344
364	L E A A C N P A W P P P G L A P H L T H Y A D L L P G S L P F H V	395
1345	TGGCTCTCCAC CACCTGAGTCAG AGCTGTGGGAAA CCCCAGACGTGT CACTCTACTG GAGATCTCCGAC CCCCACCTGCCT GGAAGTCATCAA	1440
396	A L P P P E S E L W E T P D V S L I T G D L R P P P A W K S S N	427
1441	ATGATCATGGAA GCTTGGCTCTGA ACCCAGGGCCCC AGCTGGAGCTGG CTGAGAGCAGTC CTGCAGTCTCAT TCCTTAGTTCCT GGAGCTGGCAAG	1536
428	D H G S L A L N P R P Q L E L A E S S P A V S F L S S R S W Q G	459
1537	GGCTGGAGCCCC GCCTGGGTGAGA CGCCAGTGACAG AAGCTGTGAGTG GAAGACGAGGGA TTGCCATCGCCT ATGAGGATGAGG GAAGCGGCTGAT	1632
460	L E P R L G Q T P V T E A V S G R R G I A I A Y E D E G S G	489
1633	ACCATGTGGGGC TGGAGACATAGA TGGACTTATGAA TGGCTGCTAGGA CCTTTAGTGCTC CTGCACCAACC TCCCATCCCCCT GCCAAGATCCTT	1728
1729	GAAGGACCTGG AAGGAGGGAGAG CAGGCAGCCCTT CACAGGATAGGA TCCGTCTCTGTC CTGTCTGGCAC TGGCACAAGCTC AGCACATGCCCA	1824
1825	GTAATGCGTGT GTTTGGCTGATG GAATAAAGGGCT TAGGGACTTCCC TGAGGCCTCTGG ACCCATCTGTCT TCCTGAGGGCAG CCCAGGACCTTT	1920
1921	GGCCAATCCAG TTCCCAGGCTGC AGTTGAGGGTCT GTCCTTGTCAA AGGCAGGTGCTA GACAGTCTAGAC CAGGGTTTCTCA AACTCGTACTTG	2016
2017	ACATTTGGGGCC AGATAATTCITT GTTGTGGGGCTG TCTGGTGTATGG TAGGGTCTCAG CAGCATCCCTGG CCTCTGCCCCACT AGACATCAGAAG	2112
2113	CACTCCCCCAGT TGTGACAACCAA AAATATCTCCAG ACCTTGGCAAAT GTTATCTGTGGG GGAAAATTGCC TCAATTGAGAAC CACTGGTCTAGC	2208
2209	TAGACCTGCACT GTCCAGTACAGT AGCCACTAAATA CATGTGGCTAAA CTAAATTAAG TTAATTAAGATT AAAAGCTCAGTT TCTCAGTCACAT	2304
2305	TAGTCATTCAAG TGTTACAGACAG CACATGAGGGGA CAGTGCAGTAC AGGATATGCCAT CATGGCAGAAA TTCTATTGGTTG GACAGTGTGGT	2400
2401	CTATACTGACTC TTATTCTCAGG GAGATCAGCA ACCTAATAAAC CAGATACCTTTT CG 2462	

FIG. 2. The nucleotide and predicted amino acid sequence derived from the composite nucleotide sequence generated from the overlapping sequence of the RACE clones and EST 52976. The start codon (ATG), the stop codon (TGA), and the polyadenylation signal (AATAAA) are indicated. The MER-20 repetitive line element is boxed.

products generated a sequence of 2462 bp (Accession No. AF053003) that was distinct from that described for *OVCA1*. An open reading frame of 1464-bp was identified that would be predicted to produce a protein of 489 amino acids with a predicted molecular mass of approximately 52 kDa. The repetitive line element is located entirely within the 3' untranslated region and spans approximately 800 nucleotides (Fig. 2). We refer to this new gene as *DPH2L2*. Hybridization of the internal nonrepetitive fragment to DNA from 12 different species demonstrated strong cross-hybridization to restriction fragments in all species tested except chicken (data not shown). The 800-bp nonrepetitive

cDNA probe was used to isolate human genomic phage clones (>10 kbp in size) that were used to map the chromosomal location of *DPH2L2* by FISH. Hybridization of two overlapping genomic *DPH2L2* probes to metaphase spreads revealed specific labeling on human chromosome 1. Fluorescent signals were detected on chromosome 1 in 38 of 40 metaphase spreads scored. Altogether, 45% (77/171) of all fluorescence signals hybridized to chromosome 1p, specifically at 1p34 (Fig. 3). The distribution of signals among spreads was as follows: 1 chromatid (9 cells), two chromatids (20 cells), three chromatids (8 cells), and four chromatids (1 cell).

Amino acid sequence analysis revealed that *DPH2L2*

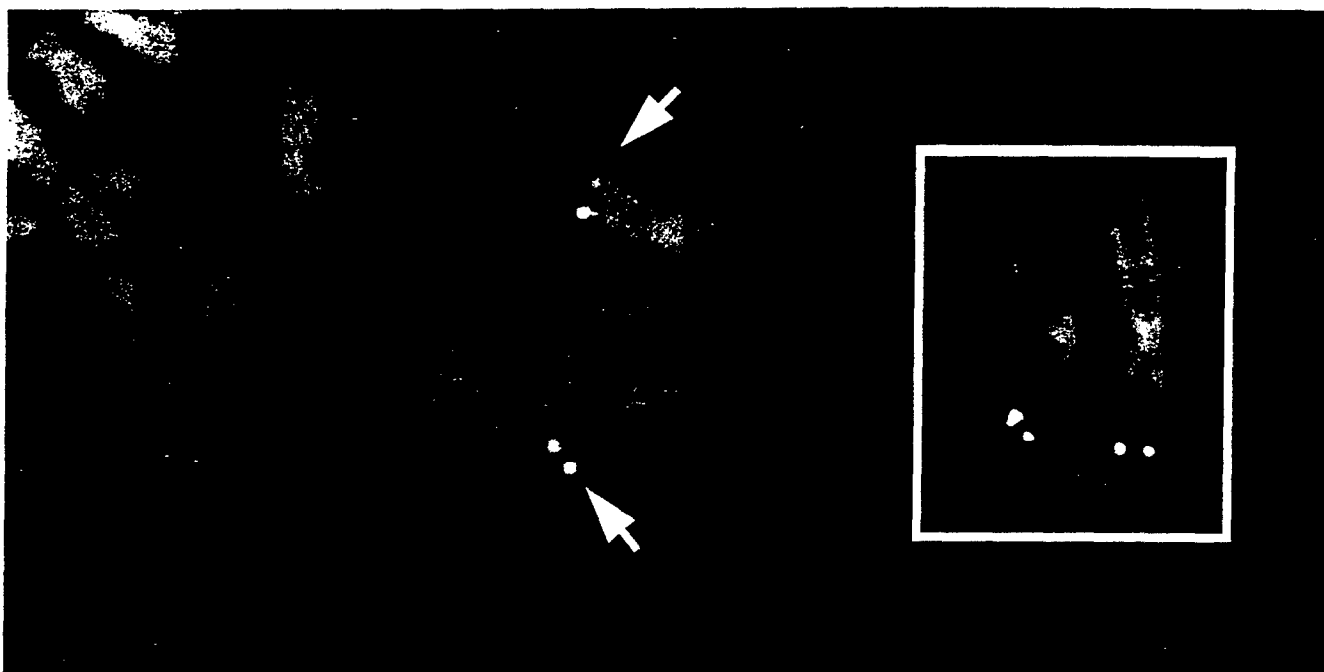


FIG. 3. Chromosomal localization of *DPH2L2* by FISH. Partial metaphase spreads show specific hybridization signals at chromosome band 1p34 (arrows). Photograph represents computer-enhanced, merged images of fluorescein signals (arrows) and DAPI-stained chromosomes. The inset shows similar localization of human *DPH2L2* to two pairs of sister chromatids from independent metaphase spreads.

is 24% identical and 46% similar to OVCA1. In fact, both *DPH2L2* and OVCA1 display significant relationships with proteins from *Saccharomyces cerevisiae*, *Caenorhabditis elegans*, *Drosophila melanogaster*, *Mus musculus*, *Schizosaccharomyces pombe*, *Brugia malayi*, *Arabidopsis thaliana*, *Plasmodium falciparum*, *Methanococcus jannaschii*, and rice, indicating that these proteins may constitute a gene family that is highly conserved throughout evolution (Fig. 4) (Schultz *et al.*, 1996). Because OVCA1 is more closely related to another yeast protein, *yik3* (53% identical and 89% similar), *DPH2L2* may represent the human homologue of the yeast *dph2* protein (28% identical and 50% similar). Although these proteins are highly conserved, no known functional domains match the conserved amino acids, indicating that *DPH2L2* and OVCA1 possess biochemical functions yet to be described. Overall, the fact that *DPH2L2* and OVCA1 are so highly conserved at the amino acid level with organisms lower on the phylogenetic tree argues that each is likely to possess an important cellular function.

DISCUSSION

We have reported the identification and characterization of an evolutionarily conserved candidate tumor suppressor gene in chromosome 17p13.3 (Schultz *et al.*, 1996). Although sequence analysis of OVCA1 revealed no known functional domains, OVCA1 showed significant sequence identity and similarity to sequences present in yeast, nematode, and other species (Fig. 4). The predicted protein for the *C. elegans* clone CEC14B1, *yky5*, which displays significant similarity

to OVCA1, has sequence similarities to a diphtheria toxin resistance-like protein (Wilson *et al.*, 1994). To a lesser extent, OVCA1 is 20% identical and 50% similar in amino acid sequence to the yeast diphthamide biosynthesis protein, *dph2*. However, our results indicate that OVCA1 is more similar to the yeast and nematode proteins of unknown function, *yik3* (89%) and *yky5* (77%), respectively, than to the yeast *dph2* (Schultz *et al.*, 1996).

BLAST analysis of OVCA1 identified significant similarity to proteins present in mice, *Drosophila*, yeast, nematodes, parasites, bacteria, and plants. During the course of these computer searches, we observed that a human EST, h52976, that when translated exhibited 39% identity and 70% similarity to a 108-amino-acid stretch of OVCA1 (amino acids 272 to 380). Cloning of the full-length cDNA corresponding to h52976 identified a novel protein of 489 amino acids distinct from the sequence of OVCA1. Because the sequence of this protein appears to be more closely related to sequences of the yeast *dph2* protein, it has been referred to as *DPH2L2* (Fig. 4).

FISH analysis mapped *DPH2L2* to chromosome 1p34 (Fig. 3). Cytogenetic and allelotyping studies have revealed frequent losses from the 1p34-pter region in meningiomas (Bostrom *et al.*, 1997), pheochromocytomas (Vargas *et al.*, 1997), and malignant peripheral nerve sheath tumors (Mertens *et al.*, 1995). Structural rearrangements of chromosome 1 with breakpoints in 1p34 have been described in human myelodysplasia and marginal zone B-cell lymphoma (Dierlamm *et al.*, 1996). Furthermore, in a review of cytogenetic findings in more than 3000 malignant solid tumors, four regions

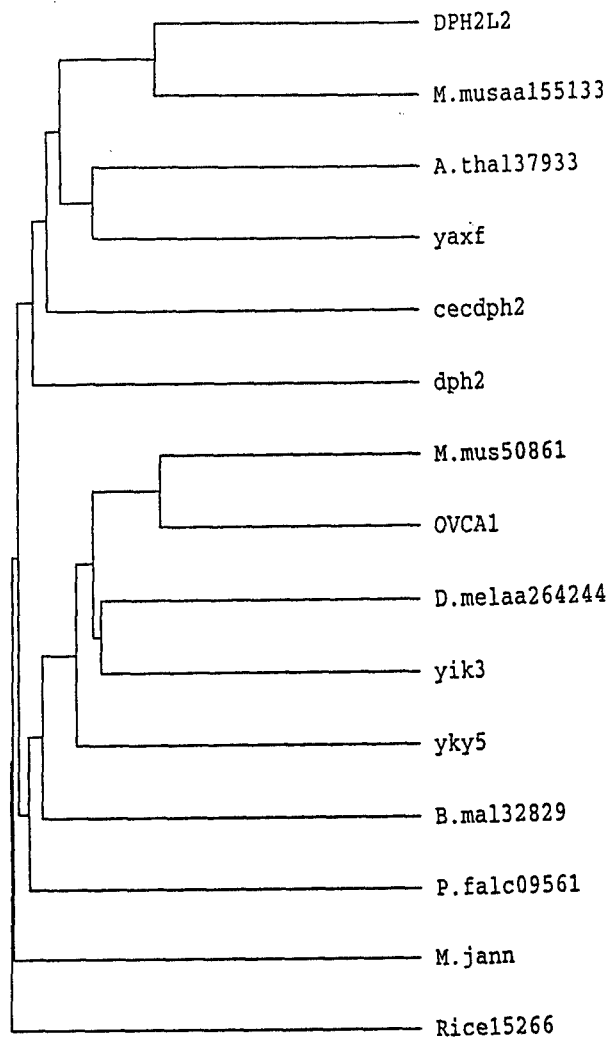


FIG. 4. Dendrogram illustrating the evolutionary relationships between the following predicted amino acid sequences: DPH2L2, dph2, yaxf, cecdph2 (C09G5.2), OVCA1, yik3, yky5, M. jann (U67498), and ESTs 37933 from *A. thaliana*, 50861, and aa155133 from *M. musculus*, aa266244 from *D. melanogaster*, 32829 from *B. malayi*, 09561 from *P. falciparum*, and 15266 from rice. Clustering of related sequences was generated by a progressive, pairwise alignment employed by the PileUp subprogram of the GCG package (Feng and Doolittle, 1987). Distances along the vertical axis are proportional to the difference between sequences; distance along the horizontal axis has no significance.

of deletion within the short arm of chromosome 1 were identified, including one at 1p34 (Mertens *et al.*, 1997). Since alterations of 17p13.3 also are commonly reported in several types of cancer, it is possible that inactivation of genes in this gene family could play a role in tumorigenesis.

Taken collectively, our data suggest that OVCA1 is not the human homologue of dph2. It remains possible that OVCA1 may represent a human homologue for one of the other complementation groups in the diphthamide biosynthesis pathway that have yet to be identified or it may possess a similar role in a different biosynthetic pathway. The fact that the amino acid conservation drops significantly outside the amino one-third of human OVCA1 and yeast

dph2 suggests that these two proteins may share only a common functional motif, with an as yet unidentified function, and not necessarily a common biological function. The cloning of *DPH2L2* will facilitate future studies that aim to address whether OVCA1 and *DPH2L2* can function in the same pathway. To demonstrate further that OVCA1 is most likely not a member of the *DPH* gene family, several haploid yeast strains in which *yik3* has been disrupted have been created. Disruption of *dph2* or *dph5* does not affect the growth or viability of yeast (Mattheakis *et al.*, 1992, 1993). However, disruption of *yik3* was observed to reduce significantly the growth rate of the yeast (Godwin, unpublished data). These preliminary studies suggest that *yik3* is most likely not a member of the *DPH* family. Current efforts are in progress to evaluate whether OVCA1 or *DPH2L2* can complement a *yik3* or a *dph2* knockout, which may help to distinguish the biochemical function of OVCA1 from *DPH2L2*. Furthermore, identification of proteins that interact with *DPH2L2* and OVCA1 by two-hybrid genetic screens might provide some clues to the biochemical function these proteins possess as well as decipher whether they both function in a common cellular pathway.

ACKNOWLEDGMENTS

We thank Lisa Vanderveer for her technical assistance. This work was supported in part by National Institutes of Health Grant RO1 CA70328 (A.K.G.), the Susan G. Komen Foundation (A.K.G.), by the United States Army Medical Research and Materiel Command under DAMD17-96-1-6088 (A.K.G.), by National Institutes of Health Grant CA-06927 (J.R.T.), and by an appropriation from the Commonwealth of Pennsylvania.

REFERENCES

- Bell, D. W., Taguchi, T., Jenkins, N. A., Gilbert, D. J., Copeland, N. G., Gilks, C. B., Zweidler-McKay, P., Grimes, H. L., Tschlis, P. N., and Testa, J. R. (1995). Chromosomal localization, in man and rodents, of a gene (*GFI1*) encoding a novel zinc finger protein reveals a new syntenic region between mouse and man. *Cytogenet. Cell Genet.* **70**: 263-267.
- Bostrom, J., Muhlbauer, A., and Reifenger, G. (1997). Deletion mapping of the short arm of chromosome 1 identifies a common region of deletion distal to D1S496 in human meningiomas. *Acta Neuropathol.* **94**: 479-485.
- Dierlamm, J., Pittaluga, S., Wlodarska, I., Stul, M., Thomas, J., Boogaerts, M., Michaux, L., Driessen, A., Mecucci, C., Cassiman, J. J., *et al.* (1996). Marginal zone B-cell lymphomas of different sites share similar cytogenetic and morphologic features. *Blood* **87**: 299-307.
- Fan, Y. S., Davis, L. M., and Shows, T. B. (1990). Mapping small DNA sequences by fluorescence in situ hybridization directly on banded metaphase chromosomes. *Proc. Natl. Acad. Sci. USA* **87**: 6223-6227.
- Feng, D. F., and Doolittle, R. F. (1987). Progressive sequence alignment as a prerequisite to correct phylogenetic trees. *J. Mol. Evol.* **25**: 351-360.
- Godwin, A. K., Vanderveer, L., Schultz, D. C., Lynch, H. T., Altomare, D. A., Buetow, K. H., Daly, M., Getts, L. A., Masny, A., Rosenblum, N., Hogan, M., Ozols, R. F., and Hamilton, T. C.

- (1994). A common region of deletion on chromosome 17q in both sporadic and familial epithelial ovarian tumors distal to BRCA1. *Am. J. Hum. Genet.* **55**: 666-677.
- Iglewski, W. J. (1994). Cellular ADP-ribosylation of elongation factor 2. *Mol. Cell. Biochem.* **138**: 131-133.
- Mattheakis, H. C., Sor, F., and Collier, R. J. (1993). Diphthamide synthesis in *Saccharomyces cerevisiae*: Structure of the *DPH2* gene. *Gene* **132**: 149-154.
- Mattheakis, L. C., Shen, W. H., and Collier, R. J. (1992). *DPH5*, a methyltransferase gene required for diphthamide biosynthesis in *Saccharomyces cerevisiae*. *Mol. Cell. Biol.* **12**: 4026-4037.
- Mertens, F., Johansson, B., Hoglund, M., and Mitelman, F. (1997). Chromosomal imbalance maps of malignant solid tumors: A cytogenetic survey of 3185 neoplasms. *Cancer Res.* **57**: 2765-2780.
- Mertens, F., Rydholm, A., Bauer, H. F., Limon, J., Nedoszytko, B., Szadowska, A., Willen, H., Heim, S., Mitelman, F., and Mandahl, N. (1995). Cytogenetic findings in malignant peripheral nerve sheath tumors. *Int. J. Cancer* **61**: 793-798.
- Phillips, N. J., Ziegler, M. R., and Deaven, L. L. (1996). A cDNA from the ovarian cancer critical region of deletion on chromosome 17p13.3. *Cancer Lett.* **102**: 85-90.
- Schultz, D. C., Vanderveer, L., Berman, D. B., Hamilton, T. C., Wong, A. J., and Godwin, A. K. (1996). Identification of two candidate tumor suppressor genes on chromosome 17p13.3. *Cancer Res.* **56**: 1997-2002.
- Vargas, M. P., Zhuang, Z., Wang, C., Vortmeyer, A., Linehan, W. M., and Merino, M. J. (1997). Loss of heterozygosity on the short arm of chromosomes 1 and 3 in sporadic pheochromocytoma and extra-adrenal paraganglioma. *Hum. Pathol.* **28**: 411-415.
- Wilson, R., Ainscough, R., Andersen, K., Baynes, C., Berks, M., Bonfield, J., Burton, J., Connell, M., Copsey, T., Cooper, J., Coulson, A., Craxton, M., Dear, S., Du, Z., Durbin, R., Favello, A., Fulton, L., Gardner, A., Green, P., Hawkins, T., Hillier, L., Jier, M., Johnston, L., Jones, M., Kershaw, J., Kirsten, J., Laister, N., Latrielle, P., Lightning, J., Lloyd, C., McMurray, A., Mortimore, B., O'Callaghan, M., Parsons, J., Percy, C., Rifken, L., Roopra, A., Saunders, D., Shownkeen, R., Smaldon, N., Smith, A., Sonnhammer, E., Staden, R., Sulston, J., Thierry-Mieg, J., Thomas, K., Vaudin, M., Vaughan, K., Waterston, R., Watson, A., Weinstock, L., Wilkinson-Sproat, J., and Wohldman, P. (1994). 2.2 Mb of contiguous nucleotide sequence from chromosome III of *C. elegans*. *Nature* **368**: 32-38.

Mutation detection using a novel plant endonuclease

Catherine A. Oleykowski, Colleen R. Bronson Mullins, Andrew K. Godwin and Anthony T. Yeung*

Fox Chase Cancer Center, 7701 Burholme Avenue, Philadelphia, PA 19111, USA

Received July 8, 1998; Revised and Accepted August 25, 1998

ABSTRACT

We have discovered a useful new reagent for mutation detection, a novel nuclease CEL I from celery. It is specific for DNA distortions and mismatches from pH 6 to 9. Incision is on the 3'-side of the mismatch site in one of the two DNA strands in a heteroduplex. CEL I-like nucleases are found in many plants. We report here that a simple method of enzyme mutation detection using CEL I can efficiently identify mutations and polymorphisms. To illustrate the efficacy of this approach, the exons of the *BRCA1* gene were amplified by PCR using primers 5'-labeled with fluorescent dyes of two colors. The PCR products were annealed to form heteroduplexes and subjected to CEL I incision. In GeneScan analyses with a PE Applied Biosystems automated DNA sequencer, two independent incision events, one in each strand, produce truncated fragments of two colors that complement each other to confirm the position of the mismatch. CEL I can detect 100% of the sequence variants present, including deletions, insertions and missense alterations. Our results indicate that CEL I mutation detection is a highly sensitive method for detecting both polymorphisms and disease-causing mutations in DNA fragments as long as 1120 bp in length.

INTRODUCTION

Single-stranded nucleases such as S1 and mung bean nuclease nick DNA at single-stranded regions (1-3). However, the acid pH optima of these nucleases lead to DNA unwinding at A+T-rich regions and result in non-specific DNA degradation. For example, S1 nuclease was found not to cleave DNA at single base mismatches (4). The efficiency of mung bean nuclease at nicking supercoiled DNA is five orders of magnitude higher at pH 5 than at pH 8 (5). At neutral pH, a high concentration of mung bean nuclease is necessary to act on double-stranded DNA, mainly at A+T-rich regions (3). In this report, we show that celery and many plants possess novel endonucleases, characterized by neutral pH optima, that detect destabilized regions of DNA helices, such as at the site of a mismatch. The celery enzyme was named CEL I. The mismatch specificity of CEL I at neutral pH has enabled development of a highly effective and user-friendly mutation detection assay. We illustrate this CEL I method by detection of

mutations and polymorphisms of the *BRCA1* gene of a number of women affected with either breast and/or ovarian cancer and reporting a family history of these diseases.

MATERIALS AND METHODS

Preparation of plant extracts

Various plant tissues were homogenized in a Waring blender at 4°C and adjusted with a 10× solution to give the composition of buffer A [0.1 M Tris-HCl, pH 7.7, 10 μM phenylmethanesulfonyl fluoride (PMSF)]. The extracts were stored at -70°C. Equivalent data were obtained when the tissues were frozen in liquid nitrogen, ground to a powder with a mortar and pestle and then extracted with buffer A on ice.

Purification of CEL I

Celery stalks (7 kg) were extracted at 4°C with a juicer and adjusted with a 10× solution to give the composition of buffer A. The extract was concentrated with a 20-70% saturated ammonium sulfate precipitation step. The final pellet was dissolved in 250 ml buffer A and dialyzed against 0.5 M KCl in buffer A. The solution was incubated with 10 ml concanavalin A-Sepharose resin (Sigma) overnight at 4°C. The slurry was packed into a 2.5 cm diameter column and washed with 0.5 M KCl in buffer A. Bound CEL I was eluted with 90 ml 0.3 M α-D-mannose, 0.5 M KCl in buffer A at 65°C. CEL I was dialyzed against buffer B (25 mM potassium phosphate, 10 μM PMSF, pH 7.0) and applied to a 100 ml phosphocellulose P-11 column that had been equilibrated in buffer B. The bound enzyme was eluted with a linear gradient of KCl in buffer B. The peak of CEL I activity was next concentrated by dialysis against saturated ammonium sulfate. The enzyme precipitate was dialyzed against buffer C (50 mM Tris-HCl, pH 7.8, 0.2 M KCl, 10 μM PMSF, 1 mM ZnCl₂) and fractionated by size exclusion chromatography on a Superose 12 FPLC column in the same buffer. The center of the CEL I activity peak from this step was used as the purified CEL I in this study. Protein concentrations of the samples were determined by the Bicinchoninic acid protein assay (Pierce).

Preparation of mismatch-containing heteroduplexes

The oligonucleotides were synthesized on an Applied Biosystems DNA synthesizer in the Fannie E. Rippel Biotechnology Facility of our Institution and purified using a denaturing PAGE gel in the

*To whom correspondence should be addressed. Tel: +1 215 728 2488; Fax: +1 215 728 3647; Email: at_yeung@fccc.edu

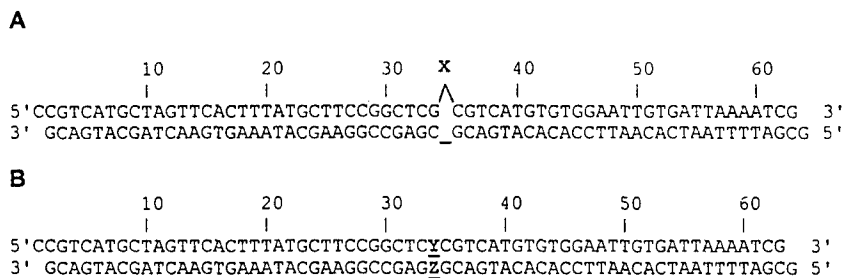


Figure 1. Design of the heteroduplexes containing base substitutions or DNA insertions. (A) Substrates with extrahelical DNA loop; (B) substrates with base substitution. Oligonucleotides containing variations of the nucleotides X, Y and Z were used to assemble all the permutations of mispaired substrates.

presence of 7 M urea at 50°C. DNA heteroduplex substrates of ~64 bp long containing mismatched base pairs or DNA loops (Fig. 1) were constructed by annealing partially complementary oligonucleotides. The single-stranded oligonucleotides were labeled at the 5'-termini with T4 polynucleotide kinase and [γ - 32 P]ATP prior to annealing with an unlabeled oligonucleotide. After annealing, all the substrates were made blunt-ended by the fill-in reaction of DNA polymerase I Klenow fragment using dCTP and dGTP and purified by non-denaturing PAGE as described (6) without exposure to UV light. DNA was eluted from the gel slices using an AMICON model 57005 electroeluter.

Mismatch endonuclease assay

5'- 32 P-labeled substrates (50–100 fmol) were incubated with CEL I preparation in buffer D (20 mM Tris-HCl, pH 7.4, 25 mM KCl, 10 mM MgCl₂) for 30 min at 37 or 45°C in 20 μ l reactions. Taq DNA polymerase (0.5–2.5 U) (Perkin Elmer) was added to each reaction where indicated. The presence of dNTP is not necessary for DNA polymerase to stimulate CEL I turnover. Ten micromolar dNTP was included only in the reactions of Figure 3A to illustrate a form of nick translation that may result when dNTP is present. The reaction was terminated by adding 10 μ l 1.5% SDS, 47 mM EDTA and 75% formamide plus tracking dyes, and analyzed on a denaturing 15% PAGE gel in 7 M urea run at 50°C. Autoradiography was used to visualize the radioactive bands. Chemical DNA sequencing ladders were included as size markers as previously described (6).

Sample ascertainment

As part of a Fox Chase Cancer Center (FCCC) Institutional Review Board approved protocol, peripheral blood samples were obtained from consenting affected high risk family members through the Margaret Dyson/Family Risk Assessment Program (FRAP). Individuals participating in FRAP have agreed to allow their samples to be used for a wide range of research purposes, including screening for mutations in candidate cancer predisposing genes, such as *BRCA1* (7). The participating individuals had previously been screened for *BRCA1* mutations by the Clinical Genetic Testing Laboratory at FCCC and were screened for sequence alterations by CEL I mutation detection in this study in a blind fashion.

DNA templates for *BRCA1* mutation analysis

Twenty five pairs of PCR primers specific for 22 coding exons in *BRCA1* were synthesized with 6-FAM dye (blue) at the 5'-end of each forward primer and with TET dye (green) at the 5'-end of each reverse primer. PCR was performed in a reaction volume of 20 μ l containing 100 ng genomic DNA as template, 10 mM Tris-HCl, pH 8.3, 50 mM KCl, 1.5 mM MgCl₂, 0.001% gelatin, 1 μ M both forward and reverse primer, 60 μ M each deoxyribonucleotide triphosphate, 5% dimethyl sulfoxide (DMSO) and 0.5 U Taq DNA polymerase. After an initial denaturation step at 94°C, the DNA was amplified through 20 cycles consisting of 5 s denaturation at 94°C, 1 min annealing at 65°C, decreasing by 0.5°C/cycle, and 1 min extension at 72°C. The samples were then subjected to an additional 30 cycles consisting of 5 s denaturation at 94°C, 1 min annealing at 55°C and 1 min extension at 72°C, with a final extension for 5 min at 72°C. The PCR reactions were purified using Wizard PCR Preps (Promega). The sizes of the DNA fragments generated by PCR ranged from 211 to 1120 bp.

CEL I mutation detection

Aliquots of 50–100 ng Wizard Prep processed DNA was heated to 94°C in buffer D and cooled to room temperature to form heteroduplexes. The heteroduplexes were incubated in 20 μ l buffer D with 0.1 μ l purified CEL I (0.01 μ g) and 0.5 U Taq DNA polymerase at 45°C for 30 min. No dNTP was added. The reactions were stopped with 1 mM *o*-phenanthroline and incubated for an additional 10 min at 45°C. The samples were processed through a Centriprep column (Princeton Separations) and dried in a SpeedVac. One microliter of ABI loading buffer (25 mM EDTA, pH 8.0, 50 mg/ml Blue Dextran), 4 μ l deionized formamide and 0.5 μ l TAMRA internal lane standard were added to the dried DNA pellet. The sample was heated at 90°C for 2 min, loaded onto a denaturing 34 cm well-to-read 4.25% polyacrylamide gel and analyzed on an ABI 373 Sequencer using GeneScan 672 Software (Perkin Elmer). Since the heteroduplexes were labeled with a different color on each strand, the mismatch-specific DNA nicking in each strand gave DNA fragments of two colors and different sizes that independently and complementarily pinpointed the mutation or polymorphism. All mutations and polymorphisms detected were confirmed by automated sequencing.

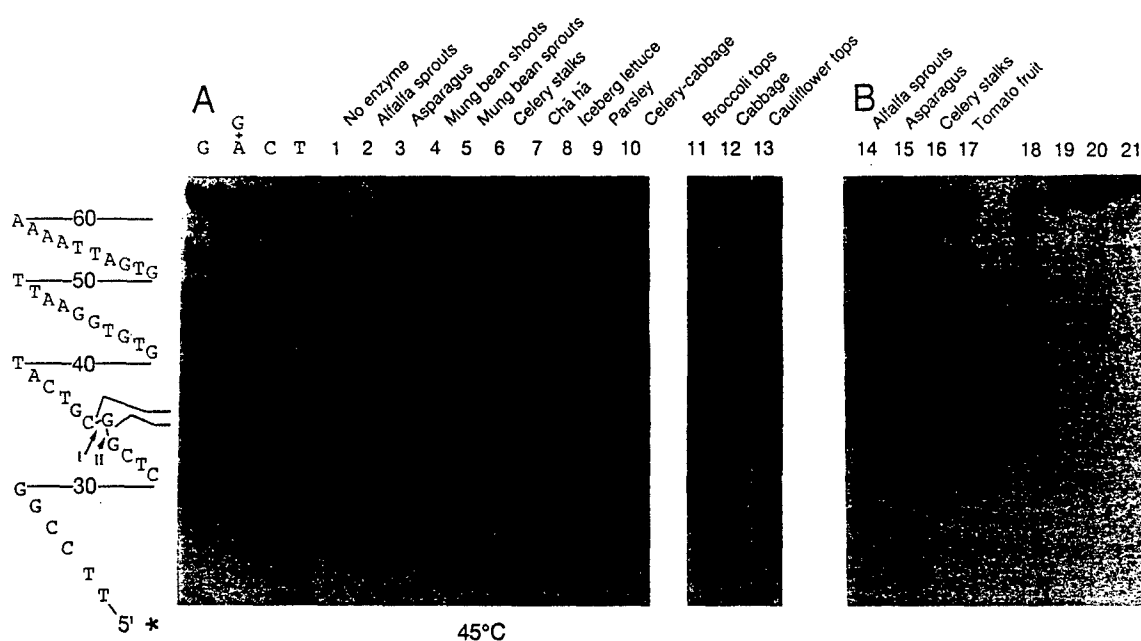


Figure 2. Conserved features of the CEL I-like mismatch endonucleases from different plants. (A) One microliter of plant extract was used in each incubation with a mismatch duplex containing an extrahelical G residue. The substrate was 5'-labeled in the top strand and incubation was at 45°C. (B) One milliliter of each of the crude extracts of the plants was applied to a 100 μ l column of concanavalin A-Sepharose resin (Sigma) in 20 mM HEPES, pH 7.0, 0.5 M KCl buffer, washed and eluted with 200 μ l 0.5 M α -D+-mannose in 0.5 M KCl, pH 7.0. One microliter of the eluted enzyme was used in the reactions in lanes 14–21. Lanes 18–21 were control reactions for lanes 14–17, respectively, using the perfectly base paired substrate.

RESULTS

Detection of CEL I-like activities in plant extracts

By incubating plant extracts with a mismatch-containing heteroduplex, we detected a novel mismatch endonuclease activity. This activity performs a single-strand cut on the 3'-side of a mismatch site (Fig. 2). The activity appears to be present in many common vegetables and in a variety of plant tissues: root, stem, leaf, flower and fruit. From each tissue, we have found a similar amount of mismatch endonuclease activity per gram of tissue (Fig. 2A, lanes 2–13). We named the prominent activity present in celery CEL I. The substrate initially used was a 5'-labeled duplex with an extrahelical G nucleotide mismatch that can alternate between two consecutive G residues, thereby giving two CEL I cut bands. These gel mobilities are consistent with the production of a 3'-OH group on the deoxyribose moiety (6). All the CEL I-like mismatch endonucleases cut the DNA at the same two alternate positions on the 3'-side of the mismatch. The mismatch endonucleases of alfalfa sprout, asparagus, celery and tomato were each found to bind to a concanavalin A-agarose column and were eluted by α -D+-mannose (Fig. 2B). Thus, CEL I-like activities appear to be mannosyl glycoproteins.

Purification of CEL I

Celery stalks were chosen to be a source of model enzyme because of the year-round availability of celery, a low amount of chloroplast proteins and pigments in the extracts and the high mismatch specificity of CEL I. The CEL I purification procedure started with celery juice, containing ~350 g protein, from 7 kg

celery stalk. The Superose 12 fraction contained 3 ml CEL I at 0.1 μ g/ μ l and is estimated to be ~10 000-fold purified with a recovery of 9%. SDS-PAGE followed by staining with Coomassie Blue R250 indicated that the purest CEL I contains more than one protein band of 34–39 kDa (data not shown). It is not clear yet whether these bands represent glycoforms of CEL I or whether proteins with unrelated properties are present.

Incision by CEL I at mismatches of single nucleotide DNA loops and nucleotide substitutions

The mismatch incision by purified CEL I in substrates containing a single extrahelical nucleotide is shown in Figure 3A (lanes 2–5). This analysis shows that CEL I has a preference for G > A > C > T in the extrahelical position. The activity of CEL I is stimulated by the presence of Taq DNA polymerase (Fig. 3A, lanes 6–10). This stimulation of CEL I does not require dNTP (data not shown). Taq DNA polymerase stimulation of incision at the weak extrahelical T substrate is ~30-fold (Fig. 3A, comparing lanes 5 and 10), as measured by densitometry of the autoradiogram bands (data not shown). The DNA polymerase stimulation is less for extrahelical G and A substrates (Fig. 3A, lanes 7 and 8, respectively) because these substrates are already efficiently cut by CEL I. Because of base pairing slippage in the extrahelical nucleotide G and C substrates (Fig. 3A, lanes 2 and 4), two incision bands were seen. At the extrahelical nucleotide that is closer to the 5'-terminus, in the presence of Taq DNA polymerase and dNTP in lanes 7 and 9 mismatch slippage allows nick translation to occur after CEL I incision. As a result, the lower

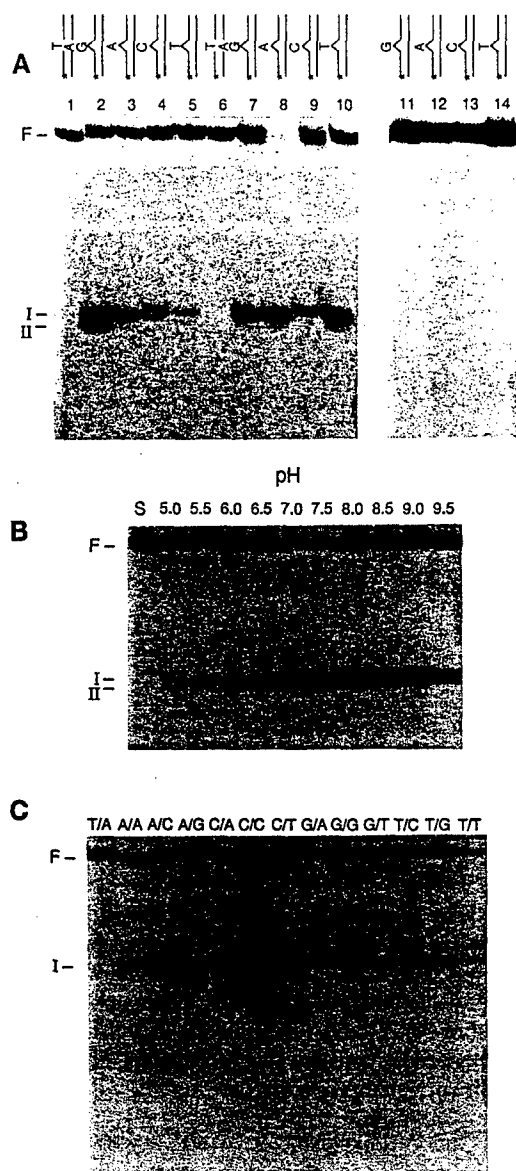


Figure 3. Mismatch incision of the purified CEL I nuclease at different mismatches. (A) Taq DNA polymerase stimulation of purified CEL I incision at DNA mismatches of a single extrahelical nucleotide. Autoradiograms of denaturing 15% polyacrylamide gels are shown. F, full-length substrate, 65 nt long, labeled at the 5'-terminus (*) of the top strand. Lanes 1-5 and 6-10, 50 fmol substrates, in the presence of 10 μ M dNTP, treated with 20 ng purified CEL I, without and with 0.5 U Taq DNA polymerase, respectively, for 30 min at 37°C; lanes 1 and 6, substrates containing no mismatch; lanes 11-14, substrates incubated with only Taq DNA polymerase in the presence of 10 μ M dNTP, with the autoradiogram exposure time extended 3 \times . The two cuts (I and II) in lanes 2 and 4 are due to mismatch slippage in alternative base pairing possibilities. One mismatched base at each cut site was repaired by DNA polymerase + dNTP in lanes 7 and 9. (B) pH profile of CEL I mismatch incision at a substrate with a single extrahelical G residue. S, substrate incubated without CEL I. Taq DNA polymerase and dNTP were not present in this study. If Taq DNA polymerase, but not dNTP, were included, the pH profile is similar, but the incision efficiency would be near completion in all lanes (data not shown). (C) CEL I incision at base substitutions. The top strands were 5'-labeled. Incubation with CEL I was for 30 min at 45°C in the presence of Taq DNA polymerase but no dNTP.

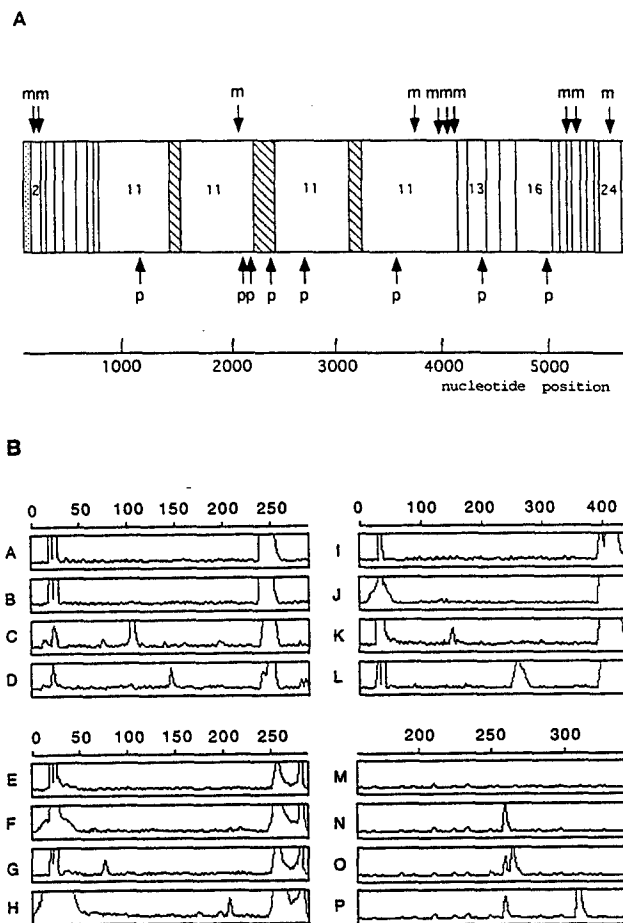


Figure 4. CEL I enzymatic mutation detection in the *BRCA1* gene. (A) Schematic presentation of the exons of the *BRCA1* gene and the polymorphisms and mutations detected in this report. The *BRCA1* gene is divided into 24 exons (22 coding exons). For CEL I mutation detection, each PCR usually covers one exon. Exon 11 is divided into four regions of ~1000 bp that overlap by at least 100 bp indicated by the diagonally shaded areas. All of exon 1, part of exon 2 and part of exon 24 are untranslated regions, as denoted by dotted areas. Exon 4 is not part of the mRNA (7). p, polymorphisms; m, mutations. (B) Electropherogram of CEL I mutation detection GeneScan analyses. Two color fluorescent heteroduplexes of the PCR products of the *BRCA1* gene were prepared as described in Materials and Methods. All lanes have CEL I treatment. Vertical axis, relative fluorescence units; horizontal axis, DNA length in nucleotides. (A-D) Deletion of A in exon 19. The CEL I mismatch-specific peaks seen at sizes 106 and 146 nt in (C) and (D) for the 6-FAM-labeled and the TET-labeled strand, respectively, were not present in the wild-type control for the FAM (A) and the TET (B) strands. Full-length PCR product was observed at 249 nt length and residual primers at 20-30 nt. The signal in the full-length position exceeded the linear range of the detector. (E-H) Detection of C \rightarrow T base substitution in exon 24. The PCR product was 286 bp. This C \rightarrow T base substitution was detected as blue at fragment sizes 76 and 77 nt in (G) and as green at fragment size 206 nt in (H) for the 6-FAM-labeled and the TET-labeled strand, respectively, but not in the wild-type control for the FAM (E) and the TET (F) strands. (I-L) Detection of a C insertion mutation in exon 20. The PCR product was 410 bp long. This insertion of a single C residue was detected at fragment sizes 151 and 259 nt for exon 20 in (K) and (L), respectively, for the 6-FAM-labeled and the TET-labeled strand, respectively. The mutation-specific CEL I cuts were not observed in the wild-type controls for the FAM (I) and the TET (J) strands. (M-P) Detection of mutations next to a polymorphism in exon 11. The PCR product was 1006 bp long. (M) Wild-type control treated with CEL I. (N) Polymorphism (2201 T \rightarrow C) identified by CEL I. (O) Two polymorphisms (2210 T \rightarrow C and 2196 G \rightarrow A) detected by CEL I. (P) Polymorphism (2210 T \rightarrow C) and mutation (K630ter; 2154A \rightarrow T) detected by CEL I. Only the data from the TET-labeled strands are presented in (M-P).


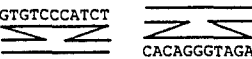
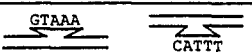

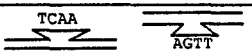
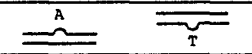
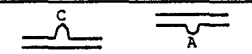
nt #	Exon #	p/m	DNA change	5' sequence	Heteroduplex formation	3' sequence
185	2	m	AG deletion	5' ATCTT		5' AGTGT
188	2	m	11 bp deletion	5' TTAGA		5' GGTA
1186	11	p	A → G	5' TAAGC	A/C G/T	5' GAAC
2154	11	m	A → T	5' GAGCC	A/A T/T	5' AGAAG
2196	11	p	G → A	5' GACAT	G/T A/C	5' ACAGC
2201	11	p	T → C	5' GACAG	T/G C/A	5' GATAC
2430	11	p	T → C	5' AGTAG	T/G C/A	5' AGTAT
2731	11	p	C → T	5' TGCTC	C/A T/G	5' GTTT
3667	11	p	A → G	5' CAGAA	A/C G/T	5' GGAGA
3819	11	m	5 bp deletion	5' GTAAA		5' CAATA
4153	11	m	A deletion	5' TGATG		5' AGAAA
4168	11	m	A → G	5' AACGG	A/C G/T	5' CTTGA
4184	11	m	4 bp deletion	5' AATAA		5' GAAGA
4427	13	p	T → C	5' GACTC	T/G C/A	5' TCTGC
4956	16	p	A → G	5' CCCAG	A/C G/T	5' GTCCA
Intron 18	19	m	A deletion	5' TCTTT		5' GGGGT
5382	20	m	C insertion	5' ATCCC		5' AGGAC
5622	24	m	C → T	5' TGACC	C/A T/G	5' GAGAG

Figure 5. Summary of mutations and polymorphisms detected in the *BRCA1* gene by CEL I in this study. m, mutation; p, polymorphism.

band of CEL I incision seen in lanes 2 and 4 was restored to full-length in lanes 7 and 9.

pH optimum of CEL I endonuclease

The pH optimum of CEL I appears to be in the neutral range although the enzyme is active from pH 5 to 9.5. The pH activity profile of CEL I cutting of the extrahelical G mismatch substrate without Taq DNA polymerase stimulation is shown in Figure 3B.

Incisions of CEL I at base substitutions

Base substitution mismatched substrates are also recognized by CEL I and cut on one of the two DNA strands for each mismatch duplex (Fig. 3C). Some of these substrates are less efficiently incised compared with those containing DNA loops. For the purpose of mutation detection *in vivo*, all base substitution mismatches can be detected by CEL I at 45°C in the presence of 0.5 U Taq DNA polymerase (Fig. 3C). Substrates with the 5'-terminus of the top strands labeled were used in this study. CEL I substrate preference shown here is C/C ≥ C/A ~ C/T ≥ G/G > A/C ~ A/A ~ T/C > T/G > G/T ~ G/A ~ A/G > T/T.

Detection of mutations and polymorphisms in the *BRCA1* gene

A CEL I-based assay was used to detect mutations and polymorphisms in various exons of the *BRCA1* gene (Fig. 4). Strong incision bands were observed for heteroduplex alleles but not for wild-type alleles (Fig. 4B). The CEL I assay is also capable of detecting multiple sequence variants within the same DNA strand (Fig. 4, panels M–P).

A summary of the mutations and polymorphisms in the *BRCA1* gene detected by CEL I in this study is shown in Figure 5. Sequence analyses of the coding regions and intron/exon boundaries confirmed that all known sequence variants were detected by CEL I. The DNA sequences flanking each mutation or polymorphism illustrate that CEL I detects mismatches in a variety of sequence contexts. Furthermore, no false positive or false negative conclusions were encountered.

DISCUSSION

Plants and fungi contain single-stranded specific nucleases that attack both DNA and RNA (8). S1 nuclease from *Aspergillus oryzae* (1), P1 nuclease from *Penicillium citrinum* (9) and mung bean nuclease from the sprouts of *Vigna radiata* (2–3) are Zn proteins active mainly near pH 5.0. CEL I is similar to these enzymes in that the most purified enzyme fraction shows some single-stranded DNase activity and endonuclease activity on supercoiled plasmids, relaxed double-stranded DNA, UV irradiated plasmids and Y-shaped DNA duplexes (data not shown). However, CEL I is most active on mismatch substrates. The neutral pH optimum, incision primarily at the phosphodiester bond immediately on the 3'-side of the mismatch and stimulation of activity by a DNA polymerase are properties that distinguish CEL I from the above nucleases. The mechanism for DNA polymerase stimulation of the CEL I activity is presently unknown. One possibility is that DNA polymerase has a high affinity for the 3'-OH group produced by CEL I incision at the mismatch and displaces CEL I simply by competition for the site. Such protein displacement will allow CEL I to recycle catalytically. For the purpose of mutation detection, DNA polymerases with 3'→5' exonuclease proofreading activity cannot be used. Such

DNA polymerases, of which the Klenow fragment of *E. coli* DNA polymerase I is an example, will excise the mismatch nucleotide after DNA polymerase displacement of CEL I at the site of mismatch incision. In the absence of dNTP, one will observe 3'→5' exonuclease degradation of the DNA fragment produced by CEL I mismatch incision. In the presence of dNTP, a highly efficient *in vitro* mismatch correction system will have been reconstituted (data not shown). It is necessary to test whether or not other proteins, such as DNA helicases, DNA ligases and DNA terminus-binding proteins, can also assist CEL I at mismatch incision *in vivo*.

In the CEL I detection scheme used in this paper, two alleles will form two alternate heteroduplex mispairs such that at least one mismatch in each pair should be a good substrate for CEL I. G/G is paired with C/C, A/G is paired with C/T, A/C is paired with G/T and T/T is recognized least well by CEL I, but an A/A mismatch will be present in such a heteroduplex preparation and will be detected by CEL I. As shown in Figure 5, flanking sequence context apparently does not adversely affect the ability of CEL I to identify a mutation. Even mismatches flanked by GC-rich regions (Fig. 1) are recognized. The four PCR products of *BRCA1* exon 11 are 889–1120 bp in length. Most of the time, mismatch incision will be observed as both colors in the electropherogram such that each independently confirms the position of the mutation/polymorphism. The sum of the two fragments is theoretically 1 nt more than the length of the PCR product. In the cases of mismatches that can wobble in alternative base pairings because of the sequence contexts and for large DNA loops the sum of the two fragments may deviate from the above rule.

The principle of mismatch recognition by CEL I appears to be different from T₄ endonuclease VII, which has also been used for enzyme mutation detection (11,12). The latter is a resolvase, which nicks one strand at the site of a mismatch and then in the other strand across from the DNA nick (12). Therefore, any nick can produce two corresponding fragments of the two colors. In the case of CEL I, the two fragments of the two colors represent two truly independent mutation detection events that complement each other to confirm the presence of the mutation. This distinction is because CEL I only nicks one strand of DNA in a mismatch heteroduplex at the site of the mismatch. There is no second cut in the opposite strand of the same DNA molecule after the first nick. Moreover, the CEL I mechanism allows the non-cut strand to be potentially useful as template for the removal of non-specific nicks, if any, by nick translation repair or ligation. Unlike resolvases, CEL I shows no tendency to nick duplex DNA at unique DNA sequences.

Other strengths of the CEL I mutation detection assay are its simplicity and its lack of preference for unique non-mismatch DNA sequences. Background non-specific DNA nicking is very low. The high signal-to-noise ratio of CEL I using fluorescent dye-labeled PCR products often allows mutations to be detected

by visual inspection of the GeneScan gel image. CEL I is a very stable enzyme, during both its purification, storage and assay.

CEL I mutation detection provides a mutation detection method based on different principles than DNA sequencing and single-strand conformation polymorphism (SSCP) (13). In genes such as *BRCA1*, mutations can occur in numerous positions, making it very difficult for most mutation detection methods to screen for mutations in this gene. To date, >520 individual sequence alterations are known in the *BRCA1* gene. The ability of CEL I to detect a mismatch at any one or more nucleotide positions without prior knowledge of the mutation provides promise of a very powerful method for screening mutations in cancer genes. Indeed, the ease of setting up and performing CEL I mutation detection should allow it to be established quickly in most laboratories.

ACKNOWLEDGEMENTS

This work was supported, in part, by grants NIH CA71426 and US Army DMAD17-97-1-7286 to A.T.Y., NIH CA70328 and US ARMY DAMD17-96-1-6088 to A.K.G., by institutional grants from the National Institutes of Health to the Fox Chase Cancer Center (CA06927, RR05539), an appropriation from the Commonwealth of Pennsylvania and a grant from the Glenmede Trust to the FCCC. The authors thank Dr Alfonso Bellacosa for critical reading of this manuscript.

REFERENCES

- Shank, T.E., Rhodes, C., Rigby, P.W.J. and Berg, P. (1975) *Proc. Natl Acad. Sci. USA*, **72**, 989–993.
- Kowalski, D., Kroeker, W.D. and Laskowski, M., Sr (1976) *Biochemistry*, **15**, 4457–4462.
- Sheflin, L.G. and Kowalski, D. (1984) *Nucleic Acids Res.*, **12**, 7087–7104.
- Loeb, L.A. and Silber, J.R. (1981) *Biochim. Biophys. Acta*, **656**, 256–264.
- Kowalski, D. and Sanford, J.P. (1982) *J. Biol. Chem.*, **257**, 7820–7825.
- Jones, B.K. and Yeung, A.T. (1988) *Proc. Natl Acad. Sci. USA*, **85**, 8410–8414.
- Miki, Y., Swenson, J., Shattuck-Eidens, D., Futreal, P.A., Harshman, K., Tavtigian, S., Liu, Q., Cochran, C., Nennett, L.M., Ding, W., Bell, R., Rosenthal, J., Hussey, C., Tran, T., McClure, M., Frye, C., Hattier, T., Phelps, R., Haugen-Strano, A., Katcher, H., Yakumo, K., Gholami, Z., Shaffer, D., Stone, S., Bayer, S., Wray, C., Bogden, R., Dayananth, P., Ward, J., Tonin, P., Narod, S., Bristow, P.K., Norris, F.H., Helvering, L., Morrison, P., Rosteck, P., Lai, M., Barrett, J.C., Lewis, C., Neuhausen, S., Cannon-Albright, L., Golgar, D., Wiseman, R., Kamb, A. and Skolnick, M.H. (1994) *Science*, **266**, 66–71.
- Linn, S.M., Lloyd, R.S. and Roberts, R.J. (eds) (1993) *Nucleases*, 2nd Edn. Cold Spring Harbor Laboratory Press, Cold Spring Harbor, NY.
- Maekawa, K., Tsunasawa, S., Dibo, G. and Sakiyama, F. (1991) *Eur. J. Biochem.*, **200**, 651–661.
- Youil, R., Kemper, B. and Cotton, R.G.H. (1996) *Genomics*, **32**, 431–435.
- Del Tito, B.J., Jr, Poff, H.E., Novotny, M.A., Cartledge, D.M., Walkwer, R.I., Earl, C.D. and Bailey, A.L. (1998) *Clin. Chem.*, **44**, 731–739.
- Solaro, P., Birkenkamp, K., Pfeiffer, P. and Kemper, B. (1993) *J. Mol. Biol.*, **230**, 868–877.
- Orita, M., Iwahana, H., Kanazawa, H., Hayashi, K. and Sekiya, T. (1989) *Proc. Natl Acad. Sci. USA*, **86**, 2766–2770.

Expression of OVCA1, a Candidate Tumor Suppressor, Is Reduced in Tumors and Inhibits Growth of Ovarian Cancer Cells¹

Wendy Bruening,² Amanda H. Prowse,² David C. Schultz,² Marina Holgado-Madruga, Albert Wong, and Andrew K. Godwin³

Department of Medical Oncology, Fox Chase Cancer Center, Philadelphia, Pennsylvania 19111 [W. B., A. H. P., D. C. S., A. K. G.]; Wistar Institute, Philadelphia, Pennsylvania 18014 [D. C. S.]; and Department of Microbiology and Immunology, Jefferson Cancer Institute, Thomas Jefferson University, Philadelphia, Pennsylvania 19107 [M. H.-M., A. W.]

ABSTRACT

Loss of all or part of one copy of chromosome 17p is very common in ovarian and breast tumors. *OVCA1* is a candidate tumor suppressor gene mapping to a highly conserved region on chromosome 17p13.3 that shows frequent loss of heterozygosity in breast and ovarian carcinomas. Western blot analysis of extracts prepared from breast and ovarian carcinomas revealed reduced expression of *OVCA1* compared with extracts from normal epithelial cells from these tissues. Subcellular localization studies indicate that *OVCA1* is localized to punctate bodies scattered throughout the cell but is primarily clustered around the nucleus. Attempts to create cell lines that stably expressed *OVCA1* from the cytomegalovirus promoter were generally unsuccessful in a variety of different cell lines. This reduction of colony formation was quantified in the ovarian cancer cell line A2780, where it was demonstrated that cells transfected with plasmids expressing *OVCA1* had a 50–60% reduction in colony number as compared with appropriate controls, and only a few of these clones expressed *OVCA1*, albeit at low levels. The clones that expressed exogenous *OVCA1* were found to have dramatically reduced rates of proliferation. Reduced growth rates correlated with an increased proportion of the cells in the G₁ fraction of the cell cycle compared with the parental cell line and decreased levels of cyclin D1. The low levels of cyclin D1 appeared to be caused by an accelerated rate of cyclin D1 degradation. Overexpression of cyclin D1 was able to override *OVCA1*'s suppression of clonal outgrowth. These results suggest that slight alterations in the level of *OVCA1*, such as would occur after reduction of chromosome 17p13.13 to hemizyosity, may result in cell cycle deregulation and promote tumorigenesis.

INTRODUCTION

Ovarian cancer is the leading cause of death from gynecological malignancy and the fourth leading cause of cancer death among American women, yet little is known about the molecular evolution of ovarian tumors. Only a few candidate tumor suppressor genes in sporadic ovarian cancer have thus far been identified. Although two familial breast/ovarian cancer genes, *BRCA1* and *BRCA2*, have been identified, mutations in sporadic ovarian cancers are rare in these genes. Other recently identified tumor suppressor genes that have been analyzed for mutations in ovarian tumors include *TSG101*, *PTEN*, *DPC4*, and *BARD1*. However, there has been little evidence reported suggesting that these genes are important in the pathogenesis of sporadic ovarian cancers (1–7). In addition, several interesting candidate tumor suppressor genes, *DOC2*, *NOEY2*, and *LOT1*, have recently been identified, and their roles in the development of ovarian cancer are currently being investigated (8–11). The *TP53* tumor

suppressor gene is, by far, the most frequently altered gene observed in ovarian cancer. In epithelial ovarian carcinomas, *TP53* mutations are present in ~50% of advanced-stage cancers. However, the low frequency of *TP53* mutations in cancers confined to the ovary and the near absence of mutations in benign and borderline ovarian neoplasms suggest that *TP53* alterations may be a relatively late event in the progression of ovarian cancer (12).

LOH⁴ for markers on the short arm of chromosome 17 is one of the most common genetic abnormalities in ovarian cancer. Two regions on 17p13, including *TP53* at 17p13.1 and a more telomeric region at 17p13.3 defined by markers D17S5/30 (equivalent to YNZ22.1) and D17S28 (equivalent to YNH37.3), have received the most attention (13). It has been reported that YNZ22.1 had a rate of LOH as high as 80%, and YNH37.3 showed >65% LOH in ovarian carcinomas. Loss at either D17S5/S30 or D17S28 was observed in 43% of low malignant potential tumors, 80% of carcinomas without metastases, and 90% of advanced-stage carcinomas. Interestingly, in the low malignant potential tumors, allelic losses at YNZ22.1 and YNH37.3 were not accompanied by LOH at *TP53*, suggesting the loss of a more distal tumor suppressor gene in early tumorigenesis (14, 15).

Alterations involving the NYH37.3/YNZ22.1 region on chromosome 17p13.3 are not limited to ovarian cancer. A recent study by the European Breast Cancer Linkage Consortium of 1280 breast tumors found that the frequency of LOH observed on the p arm of chromosome 17 was much higher than that observed on the q arm (16). Up to two-thirds of breast tumors show LOH at the YNZ22.1 locus (17–23), and this finding has been associated with markers of tumor aggression (16, 23–25). Breast tumors with LOH at YNZ22.1 have been associated with a higher risk of recurrence than those showing retention of this region (23, 25). This same region shows frequent LOH in small cell lung cancers (26–28), colon cancers (29), primitive neuroectodermal tumors (30–32), carcinoma of the cervix uteri (33–36), medulloblastoma (37–40), astrocytoma (41, 42), follicular thyroid carcinoma (43), malignant melanoma (44), hepatocellular carcinoma (45), and leukemia and lymphoma (46). In many of these studies, changes on chromosome 17p13.3 occur in the absence of alterations involving *TP53*, suggesting that a tumor suppressor gene(s) residing in this region on chromosome 17p13.3 may be involved in the development of many types of cancers.

We have previously reported the identification of a common region of allelic loss on 17p13.3 in ovarian cancer defined by the markers D17S28 and D17S5/S30 (47). These two loci span <20 kbp (47). By the use of positional cloning strategies, two candidate tumor suppressor genes, *OVCA1* and *OVCA2*, have been identified that map to the region that is most commonly lost in ovarian and breast tumors, chromosome 17p13.3 (47, 48). *OVCA1* demonstrates sequence similarity (20% identity) to one of the yeast enzymes in the diphthamide

Received 9/15/98; accepted 8/5/99.

The costs of publication of this article were defrayed in part by the payment of page charges. This article must therefore be hereby marked *advertisement* in accordance with 18 U.S.C. Section 1734 solely to indicate this fact.

¹ This work was supported in part by NIH Grant RO1 CA70328, the Susan G. Komen Foundation, the United States Army Medical Research and Materiel Command (Contract DAMD17-96-1-6088), the Hoxie Harrison Smith Foundation, the Butler Family Fund, and an appropriation from the Commonwealth of Pennsylvania. W. B. was supported by a fellowship from the NIH.

² The first three authors contributed equally to this work.

³ To whom requests for reprints should be addressed, at Department of Medical Oncology, Fox Chase Cancer Center, 7701 Burholme Avenue, Room W-304, Philadelphia, PA 19111. Phone: (215) 728-2756; Fax: (215) 728-2741; E-mail: a_godwin@fccc.edu.

⁴ The abbreviations used are: LOH, loss of heterozygosity; SSCP, single-strand conformation polymorphism; HA, hemagglutinin; GST, glutathione S-transferase; FACS, fluorescence-activated cell sorting; TUNEL, terminal deoxynucleotidyl transferase-mediated nick end labeling; VNTR, variable number of tandem repeats; CMV, cytomegalovirus; CD, Cowden disease; LDD, Lhermitte-Duclos disease; BZS, Bannayan-Zonena syndrome.

query page 2 - ok
11 - ok

synthetic pathway, DPH2, and to a number of proteins of unknown function from a variety of organisms, including yeasts, plants, insects, and mammals, indicating that this putative protein family is conserved throughout evolution. However, the amino acid sequence of OVCA1 does not demonstrate any conservation with the sequence of any known functional motif (47, 48). Northern blot analysis revealed that OVCA1 mRNA expression was lost or dramatically reduced in ovarian tumors and ovarian tumor cell lines (as compared with normal ovarian epithelial cells), indicating that loss or reduction of OVCA1 expression may contribute to ovarian tumorigenesis (47).

Studies in which genes are expressed in tumor cells have provided proof for the pivotal role of TP53, RB, CDKN2A/p16, and BRCA1 in reverting the transformed phenotype of tumor cells (49–55). Here, we report that OVCA1 can inhibit proliferation of ovarian tumor cells. In addition, we report the identification of genetic alterations of OVCA1 in ovarian tumor cell lines and in high-risk breast cancer families. These data strongly suggests that OVCA1 is a viable candidate for the breast and ovarian tumor suppressor gene at 17p13.3.

MATERIALS AND METHODS

Reagents and Cell Lines. Cell culture reagents were from Life Technologies, Inc., unless otherwise indicated, most other reagents were obtained from Sigma Chemical Co. (St. Louis, MO). Cell lines were obtained from American Type Culture Collection (Manassas, VA) or were derived in our laboratory (HOSE, human ovarian surface epithelial cell lines grown in primary culture; and HIO cell lines, SV40-immortalized human ovarian epithelial cells). A2780 cells were maintained in DMEM supplemented with 10% FCS and 0.2 IU/ml porcine insulin. COS-1, MCF-7, and MDA-MB8 cells were maintained in DMEM supplemented with 10% FCS. T47D cells were maintained in RPMI 1640 supplemented with 10% FCS and 0.2 IU/ml porcine insulin. SKBR3 cells were maintained in McCoy's 5a medium supplemented with 10% FCS. HOSE cells and HIO cell lines were maintained in a 1:1 mixture of medium 199 and MCDB-105 medium, supplemented with 5% FCS and 0.2 IU/ml porcine insulin. Unless otherwise stated, cells were transfected with Superfect (Qiagen, Chatsworth, CA), as described by the manufacturer. The A2780 clones that stably express OVCA1 were obtained after selection in G418 by standard methods and maintained in DMEM supplemented with 10% FCS and 0.5 mg/ml G418.

SSCP Analysis of OVCA1. PCR was carried out in a reaction volume of 10 μ l containing 100 ng of genomic DNA template, 10 mM Tris-HCl (pH 8.3), 50 mM KCl, 1.5 mM MgCl₂, 0.001% gelatin, 1 μ M forward and reverse primers, 60 μ M dNTPs, 0.1 μ Ci of [³²P]dATP (DuPont-NEN, Boston, MA), 5% DMSO, and 0.5 unit of AmpliTaq DNA polymerase (Perkin Elmer Corp., Foster City, CA). Following an initial denaturation step at 94°C for 4 min, DNA was amplified through 20 cycles consisting of 5 s of denaturing at 94°C, 1 min of annealing at 65°C (0.5°C/cycle), and 1 min of extension at 72°C. The samples were then subjected to an additional 25 cycles, consisting of 1 min of denaturation at 94°C, 1 min of annealing at 55°C, and 1 min of extension at 72°C and a final extension at 72°C for 5 min. PCR products were diluted 1:10 in 95% formamide, 10 mM NaOH, 0.25% bromophenol blue, and 0.25% xylene cyanol. Diluted products were denatured for 5 min at 95°C and flash-cooled on ice. Four μ l were loaded onto a 0.5 \times MDE gel (AT Biochem, Malvern, PA), prepared according to manufacturer's specifications, and electrophoresed at 6 W for 12–16 h at room temperature in 0.6 \times TBE [1 \times TBF, 0.09 M Tris, 0.09 M boric acid, and 0.002 M EDTA (pH 8.0)]. Following electrophoresis, the gel was dried and exposed to autoradiography film at -80°C for 4–24 h. Variant and normal SSCP bands were cut out from the gels after alignment with the autoradiograph, and the DNA was eluted in 100 μ l of distilled deionized H₂O at 37°C for 3 h. Two μ l of the eluted DNA were used as template for secondary PCRs, as described above, except that radiolabeled dATP was omitted. Following amplification, the DNA was collected on Wizard resin (Promega, Madison, WI) and eluted in 50 μ l of distilled deionized H₂O, and 50–100 fmol of purified PCR product were subjected to direct sequencing.

Plasmids. The eukaryotic expression vectors pcDNA3 and pcDNA3-LacZ were obtained from Invitrogen. The HA antibody tag (YPYDVPDYA) was added to the COOH or NH₂ terminus of the OVCA1 cDNA by standard PCR

technology, and the resulting tagged cDNAs were subcloned into pcDNA3 and are referred to as pcDNA3-HAOVCA1 or pcDNA3-OVCA1HA, depending on the location of the HA tag. The plasmid pGFP-C1, which expresses green fluorescent protein, was obtained from Clontech. The cDNA of OVCA1 was fused to the COOH terminus of the green fluorescent protein at the BglIII site to generate the plasmid pGFP-OVCA1. To prepare a GST fusion of OVCA1 in bacteria, we subcloned the OVCA1 cDNA, containing an NH₂-terminal HA tag, into pGEX-2T (Pharmacia).

Production of Anti-OVCA1 Antibodies. The 13-amino acid peptide RDGPGRGRAPRGC, corresponding to amino acids 20–31 of OVCA1 (where the terminal cysteine was added for conjugation purposes) was synthesized (Research Genetics, Huntsville, AL). Purity of the peptide was confirmed by high-performance liquid chromatography. The peptide was conjugated to maleimide activated keyhole limpet hemocyanin (Pierce, Rockford, IL) and used to immunize a New Zealand White rabbit (Cocalico, Reamstown, PA). Two mg of antigenic peptide were covalently linked to Aminolink agarose (Pierce) and used to purify anti-OVCA1 antibody from crude serum by affinity chromatography. The final antibody is referred to as TJ132. The antibody FC21 was produced by immunizing a New Zealand White rabbit (Cocalico) with a bacterially expressed carboxyl terminal portion of OVCA1 (amino acids 330–443). The resulting antiserum was immunoaffinity purified on Aminolink agarose covalently linked to bacterially expressed GST-OVCA1.

Purification of Bacterially Expressed OVCA1. BL21 bacteria were transformed with pGEX2T-OVCA1. Expression of the fusion protein was induced with 1 mM isopropyl- β -thio-galactopyranoside (Stratagene, La Jolla, CA). The bacteria were lysed by sonication, and GST-OVCA1 was purified from the soluble fraction by binding to glutathione-Sepharose 4B (Pharmacia). Pure OVCA1 was released by digesting with thrombin (Pharmacia), or the GST-OVCA1 fusion was eluted with excess glutathione. PET-OVCA1 (nucleotides 1011–1350) was expressed in BL21 bacteria and purified as an insoluble inclusion body by repeated washing of the insoluble fraction with 1% Triton X-100. The insoluble pellet was solubilized in 8 M urea-2% SDS. The protein (OVCA1 amino acids 330–443) was further purified by SDS-PAGE. The gel slice containing the protein was homogenized and used to immunize rabbits.

Preparation of Protein Extracts from Human Tumor Specimens. Normal human tissues were obtained from Clontech. Tumors were snap-frozen after surgical removal and stored in liquid nitrogen until use. One g of tumor tissue was rinsed twice with cold PBS and minced finely into small pieces. Tissue pieces were suspended in 1 ml of PBSTDS [0.137 M NaCl, 2.68 mM KCl, 10.6 mM Na₂HPO₄, 1.47 mM K₂H₂PO₄, 1% (v/v) Triton X-100, 0.5% (w/v) deoxycholate, 0.1% (v/v) SDS, 0.004% (w/v) NaF, 100 mg/ml phenylmethylsulfonyl fluoride, 1 mg/ml aprotinin, 1 mg/ml leupeptin, and 2 mM sodium orthovanadate, (pH 7.4)] and ground with a Polytron tissue grinder at 300–400 rpm for two 30-s intervals at 4°C. Tissue homogenates were clarified by centrifugation at 100,000 \times g for 1 hour at 4°C. Lipid layers were removed, and cytosolic extracts were aliquoted, snap-frozen in liquid nitrogen, and stored at -80°C. Quantitation of protein was achieved using a bicinchoninic acid/copper (II) sulfate assay (Sigma).

SDS-PAGE and Western Blot Analysis. Fifty μ g of total protein extract from tissues or 20 μ g of total protein from cell extracts, unless otherwise stated, were separated by standard SDS-PAGE and transferred to Immobilon-P (polyvinylidene difluoride; Millipore, Bedford, MA). The membranes were blocked with 3% BSA and probed with the anti-OVCA1 antibody TJ132, or blocked with 3% dried milk and probed with the indicated antibody. The signal was visualized using anti-rabbit antibodies coupled to HRP (Amersham) and developed using ECL reagents, as recommended by the manufacturer (Amersham).

Subcellular Fractionation. HOSE cells were homogenized in ice-cold hypotonic homogenization buffer [40 mM Tris (pH 7.4), 1 mM EDTA, 1 mM EGTA, 1 mM DTT, and 10% glycerol]. The nuclei were pelleted by centrifugation at 2500 rpm for 10 min. The supernatant was collected, and insoluble debris was pelleted at 180,000 \times g for 30 min to give the cytosol fraction. The nuclear pellet was washed twice with homogenization buffer containing 0.1 M KCl. The nuclear pellet was then extracted with homogenization buffer plus 0.45 M KCl for 1 h on ice, with frequent vortexing. Insoluble debris was pelleted at 180,000 \times g for 30 min to obtain the nuclear fraction.

Immunofluorescent Staining and Imaging. COS-1 cells were transfected with the indicated plasmids using Lipofectamine (Life Technologies, Inc.) or Superfect (Qiagen), as directed by the manufacturer. Forty-eight h after trans-

query page 8 - ok
query page 9 - ok
-0.5°C/cycle - is correct

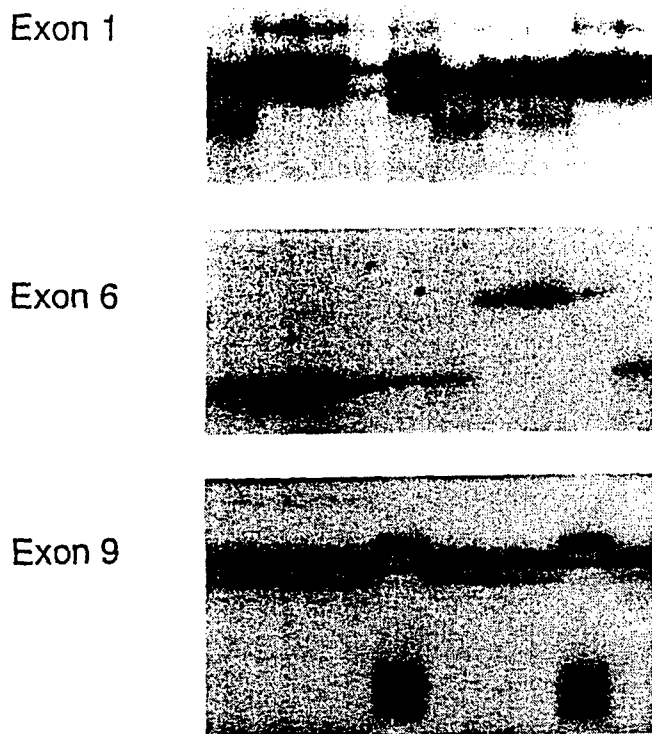


Fig. 1. Mutational analysis of OVCA1. Each exon and its surrounding intronic regions was amplified by PCR and analyzed for sequence variants by SSCP, as described in "Materials and Methods." Examples of the SSCP gel patterns are shown for 10 tumor samples for exons 1, 6, and 9. The exon 1 region has several sequence variants, shown in Lanes 1, 5, 6, 7, and 8 (left to right); exon 6 has one sequence variant, shown in Lanes 7, 8, and 9; and exon 9 has one sequence variant, shown in Lanes 5 and 9. All variants seen by SSCP were verified by directly sequencing a separate PCR.

fection, the cells were visualized. For green fluorescent proteins, the living cells were observed with a Nikon TE 800 upright microscope. For visualizing HA-tagged OVCA1 proteins, the cells were fixed for 20 min in 3.7% formaldehyde-PBS and then for 30 s in methanol. The cells were then stained with an anti-HA rabbit polyclonal antibody Y-11 (Santa Cruz Biotechnology, Santa Cruz, CA) in TBS [50 mM Tris (pH 8.0) and 140 mM NaCl] plus 0.03% Triton X-100 and 10% FCS. The staining was visualized with an antirabbit antibody coupled to Texas Red (Jackson ImmunoResearch Laboratory, Inc.). The stained cells were observed on a Biorad MRC 600 laser scanning confocal microscope, using COMOS Version 7.0.1 software. The images were rendered and pseudocolored with Voxel View 2.5.1 (Vital Images) software. Final prints were made using a codonics dye sublimation printer.

Stable Colony Formation Assay. A2780 cells (2.5×10^5 per 60-cm plate) were cotransfected with 5 μ g of pcDNA3-LacZ and 2.5 pmol of pcDNA3 control vector, pcDNA3-HAOVCA1, or p53 expression plasmid or the cyclin D1 expression plasmid. At 24 h posttransfection, G418 (Life Technologies, Inc.) was added to a final concentration of 0.5 mg/ml, or cells were stained for transient β -galactosidase activity. Antibiotic selection was continued for 10–14 days. Colonies were fixed with 0.2% formaldehyde and stained with 0.2% (w/v) crystal violet, and colonies containing >50 cells were scored.

Growth Curve Analysis. Cells were removed from the flask by trypsinization. The trypsin was inactivated by addition of complete medium to a final volume of 10 ml. One hundred μ l of cell suspension were diluted in 20 ml of Isoton solution (Coulter, Miami, FL), and the number of cells quantified on a Z1 Coulter counter (Coulter). Cells (200,000) were plated in triplicate in 35-mm tissue culture dishes and incubated at 37°C and 5.0% CO₂. Cells were counted in 24-h intervals by trypsinization and resuspension of cells in 10 ml of Isoton (Coulter) and counted on the Z1 Coulter counter (Coulter).

Pulse-Chase Labeling. Cells were seeded into 60-mm dishes and grown until they were 60% confluent. They were starved in minus-methionine medium (ICN) for 30 min, and then Trans35-Label (ICN) was added to 500

μ Ci/ml and the cells were labeled for 30 min. The radioactive medium was removed, and the cells were washed with large volumes of complete medium and then incubated in complete medium for the indicated times. The cells were then lysed in 100 μ l of PBSTDS. Insoluble debris was pelleted, and the lysates were diluted 10-fold into RIPA buffer [10 mM Tris (pH 8.0), 150 mM NaCl, 1% NP40, 0.1% SDS, and 0.5% deoxycholate]. Anti-cyclin D1 antibody (Santa Cruz Biotechnology) was added and the immunoprecipitates were collected on Protein A beads (Life Technologies, Inc.) and washed well with RIPA buffer. The immunoprecipitates were released by boiling in SDS-PAGE loading buffer and were separated by 12% SDS-PAGE. The amount of label incorporated into cyclin D1 was quantitated by Phosphorimager (Fuji).

FACS Analysis of Stable Transfectants. Cells (500,000) were seeded in 10 ml of complete medium supplemented with 0.5 mg/ml G418. Seventy-two h postseeding, cells were harvested and 1 million cells were prepared for FACS analysis by resuspending cell pellets in 1 ml of staining buffer [3.4 mM sodium citrate, 10 mM NaCl, 0.1% (v/v) NP40, and 75 mM ethidium bromide] and stored at 4°C for no more than 3 days. The cells were filtered through a 37- μ m nylon mesh and then analyzed by a flow cytometer (Becton Dickinson, San Jose, CA). Data for 20,000 events were gathered by CellQuest (Becton Dickinson, San Jose, CA) and analyzed by MacCycle (Phoenix Flow Systems, San Diego, CA).

TUNEL Staining. Cells were plated on coverslips and stained for TUNEL using an *in situ* cell death detection kit, as recommended by the manufacturer (Boehringer Mannheim).

RESULTS

Mutational Analysis of OVCA1 by SSCP. SSCP analysis was conducted on 50 ovarian tumors independent of LOH status for markers on 17p13.3 and on 20 breast tumors demonstrating allelic loss of OVCA1 and retention of TP53. Multiple sequence variants were identified throughout the gene (Fig. 1; Table 1). These sequence variants were deemed to be polymorphisms because these same alterations were either found in the corresponding germ line or resulted in either conservative or silent amino acid substitutions. The frequency of these putative polymorphisms was determined by SSCP analysis of 100 chromosomes from control individuals (Table 1). In addition, we identified two nonconservative amino acid substitutions: alanine 34 changed to an aspartic acid residue and serine 389 changed to an arginine residue. Each alteration was detected in the germ line of a woman with early-onset breast cancer who reported a family history of the disease. In both cases, the missense mutation/rare polymorphism was retained in the corresponding breast tumor DNA and showed reduction to homozygosity (data not shown). Evaluation of >100 control chromosomes has failed to detect these sequence variants. The individual carrying the A34D missense variant was diagnosed with breast cancer at age 37 and reported a history of one

Table 1 Nucleotide sequence variants observed in OVCA1 in tumors^a

Exon	Codon	Base	Change	Result	Frequency ^b
1	7	2	C→T	Ala→Val	0.39
2	34	2	C→A	Ala→Asp	0.00
2	72	3	C→T	Ala→Ala	ND
4	104	3	G→A	Val→Val	ND
4	138	3	G→T	Leu→Leu	ND
5	188	3	G→A	Ser→Ser	0.20
9	335	1	C→G	Leu→Val	0.09
9	337	3	C→T	Pro→Pro	0.18
11	389	3	C→A	Ser→Arg	0.00
12	432	3	C→T	Ser→Ser	0.01
13	NC		C→G		ND

^a The variants shown are those that were detected in the coding and 3' untranslated region regions. Sequence variants that were detected in the promoter and in introns 5, 6, 11, and 12 are not listed. Codon refers to the amino acid affected by the nucleotide change. Base indicates the nucleotide position of the codon affected. Change describes the nature of the nucleotide alteration. Result describes the affect the nucleotide alteration has on the amino acid. ND, not determined; NC, noncoding sequence.

^b Allele frequency in control population was determined by examination of 100 chromosomes from unaffected individuals.

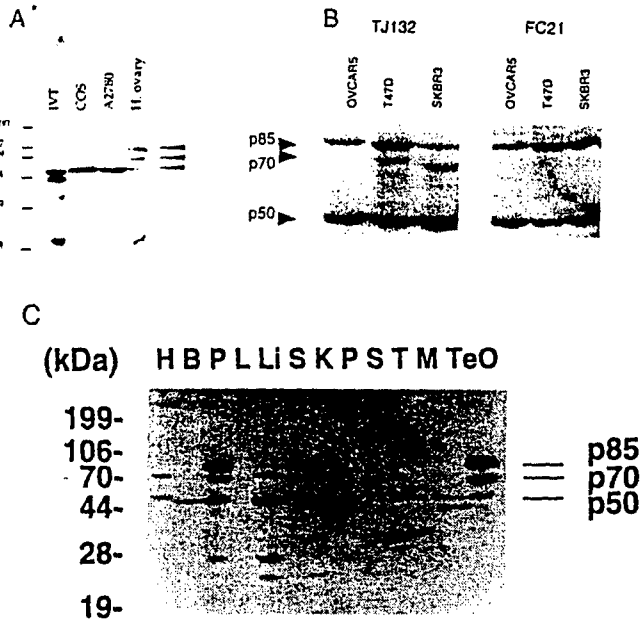


Fig. 2. Characterization of OVCA1 expression. A, extracts from the indicated tissues and cell lines were separated by 10% SDS-PAGE and transferred to Immobilon-P, as described in "Materials and Methods." The blot was then probed with the anti-OVCA1 antibody TJ132, as described in "Materials and Methods." Lane IVT, *in vitro* translated pcDNA3-HAOVCA1; Lane COS, extract of COS-1 cells that had been transfected with pcDNA3-HAOVCA1; Lane A2780, extract of the ovarian tumor cell line A2780; Lane H. ovary, extract of whole human ovary. Arrowheads, three different polypeptides that TJ132 recognizes (p50, p70, and p85). B, 20 μ g of each indicated cell line extract were separated in duplicate by 10% PAGE, transferred to Immobilon-P, and probed with the indicated antibodies, as described in "Materials and Methods." One of the duplicate blots was probed with the anti-OVCA1 antibody TJ132, and the other was probed in parallel with the anti-OVCA1 antibody FC21. OVCA5 is a cell line derived from an ovarian tumor, whereas T47D and SKBR3 are cell lines derived from breast tumors. C, 50 μ g of extracts from various human tissues (Clontech) were separated by 12% SDS-PAGE and processed for Western blotting, as described in "Materials and Methods." The blot was probed with the anti-OVCA1 antibody TJ132. Lane H, heart; Lane B, brain; Lane P, placenta; Lane L, lung; Lane Li, liver; Lane S, skeletal muscle; Lane K, kidney; Second Lane P, pancreas; Second Lane S, spleen; Lane T, thymus; Lane M, mammary gland; Lane Te, testis; Lane O, ovary.

first-degree relative and two second-degree relatives with the disease (ages of onset unknown). The individual carrying the S389R missense variant was diagnosed with breast cancer at age 49. She reported that her mother was affected with breast cancer at age 55 and that two maternal aunts were diagnosed with the disease at 61 and 65 years of age. The functional significance of these mutations is not yet clear; preliminary experiments exploring their effect on the OVCA1 protein are presented below.

Southern Blot Analysis of OVCA1. To assess deletions or rearrangements within the OVCA1 gene, we performed Southern blotting of 60 normal/ovarian tumor DNA pairs using the full-length OVCA1 cDNA as the probe. The vast majority of the tumors had lost one copy of the OVCA1 gene. No rearrangements or large interstitial deletions were detected in the remaining copy. However, a 7-kbp *EcoRI* fragment was observed to be variable in length due to changes in the VNTR, *i.e.*, YNH37.3, which is intragenic to OVCA1 (data not shown). We did not observe any correlation between the length of the VNTR fragment and an increased risk of developing ovarian cancer.

Western Blot Analysis of OVCA1. Conceptual translation of OVCA1 predicts a 443-amino acid protein with M_r ~50,000. An antibody that recognizes 11 amino acids at the NH₂ terminus of OVCA1 was prepared by immunizing rabbits with a peptide. The antiserum was affinity-purified and was designated TJ132. Another antibody that recognizes the COOH terminus of OVCA1 (amino acids 330-443) was prepared by immunoaffinity purification following immunization of rabbits with a bacterially expressed polypeptide and

was designated FC21. Both antibodies were able to recognize bacterially expressed OVCA1 by Western blotting (data not shown). In addition, these antibodies were able to recognize a protein of M_r ~50,000 in extracts prepared from COS-1 cells that had been transiently transfected with pcDNA3-HAOVCA1 and in whole-cell lysates from the ovarian tumor cell line A2780 (Fig. 2A). Recognition of this M_r 50,000 protein could be completed with a molar excess of the antigenic peptide, indicating that the antibodies recognize the authentic OVCA1 protein (data not shown). In addition to the M_r 50,000 protein, both antibodies detected proteins of M_r ~85,000, as observed in extracts prepared from a variety of sources, including normal human tissues, primary cultures of HOSE cells and a number of cell lines (Figs. 2 and 3; data not shown). The NH₂-terminal antibody TJ132 also recognized proteins of M_r ~70,000, but these species were variable in amount and presence and were not recognized by antibodies directed against the COOH terminus of the protein. The secondary antibody alone did not recognize any of the three proteins (M_r 50,000, 70,000, and 85,000; data not shown). The identity of the M_r 70,000 and M_r 85,000 proteins is unknown, as are their relationships with the M_r 50,000 OVCA1 protein; however, the available evidence suggests that the M_r 85,000 form is an alternatively spliced or posttranslationally modified form of OVCA1 and that the p70 form is either unrelated to OVCA1 or is a breakdown product of the p85 form. Alternatively, the p85/p70 forms could be unrelated, cross-reacting proteins. However, this is unlikely because completely different anti-OVCA1 antibodies recognize the p85 protein, and recognition of the M_r 85,000 protein by TJ132 can be competed with a molar excess of

ⓐ
X
completed
ⓑ

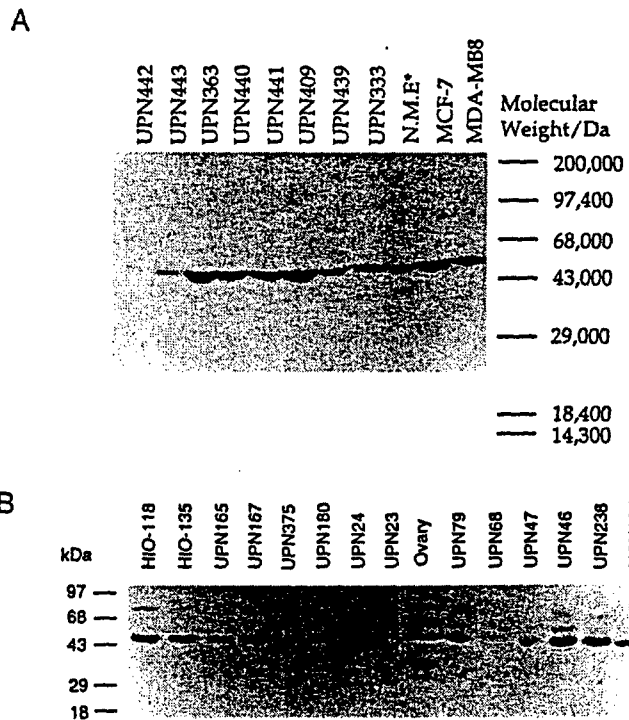


Fig. 3. Expression of OVCA1 in tumors. A, 50 μ g of each sample were separated by 12% SDS-PAGE and transferred to Immobilon-P, as described in "Materials and Methods." The blot was probed with the anti-OVCA1 antibody TJ132. UPN, extracts from primary tumors; MCF-7 and MDA-MB8, extracts from cell lines derived from breast tumors; N.M.E., extract from normal breast epithelial cells grown in short-term primary tissue culture. Equal loading of the blots was confirmed by staining with Coomassie Blue for total protein after probing. B, protein extracts (50 μ g) from primary ovarian tumors (UPN), normal human ovarian surface epithelial cell lines (HIO), and a normal ovary (Ovary) were separated by 12% SDS-PAGE and transferred to Immobilon-P, as described in "Materials and Methods." The blot was probed with the anti-OVCA1 antibody TJ132. Equal loading of the blots was confirmed by staining the blots for total protein with Coomassie Blue after probing.

change completed to competed!

4/C

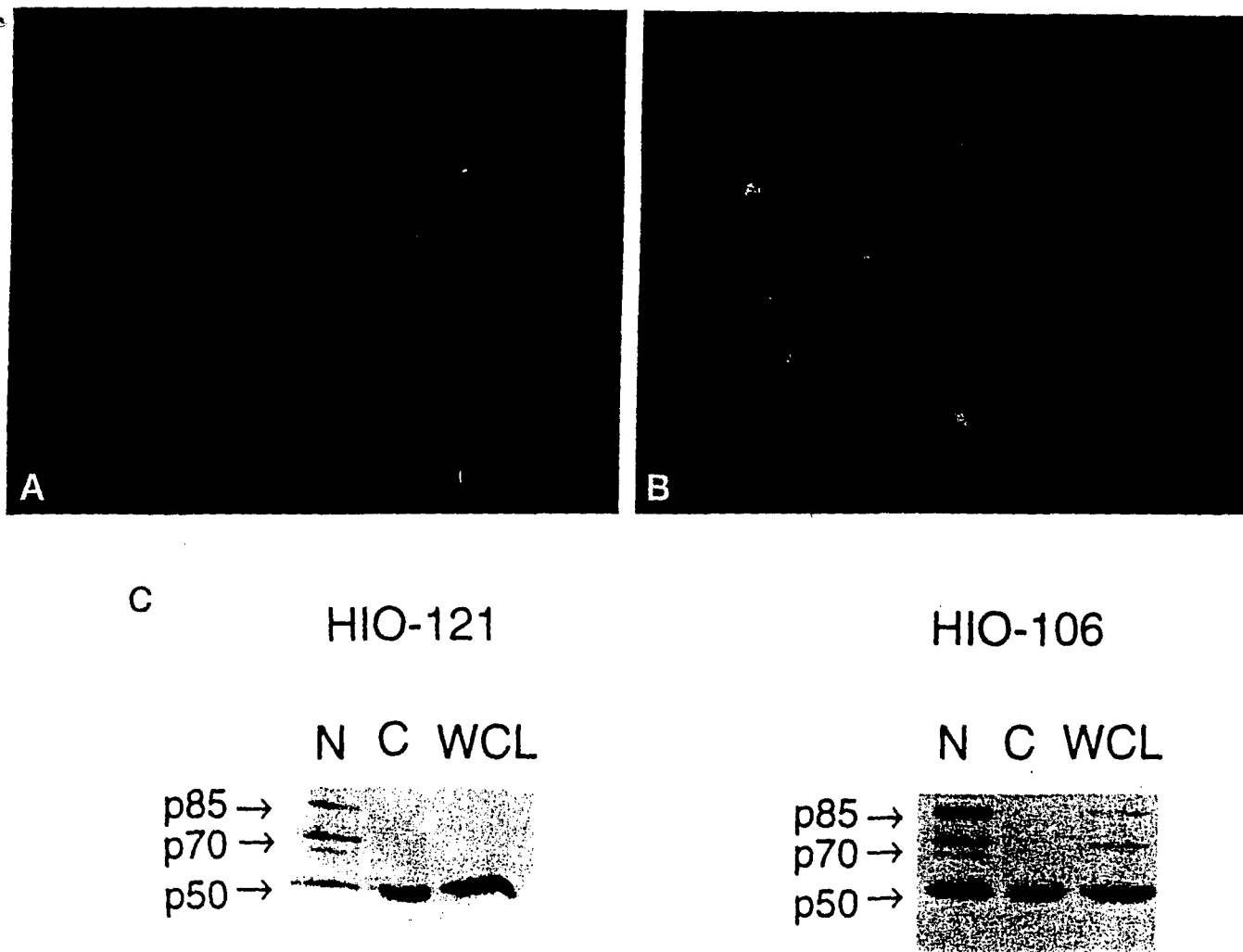


Fig. 4. Subcellular localization of OVCA1. COS-1 cells were transiently transfected with pcDNA3 or with pcDNA3-OVCA1HA. Forty-eight h after transfection, the cells were fixed and stained with an anti-HA tag antibody (Y-11; Santa Cruz Biotechnology), as described in "Materials and Methods." A, cells transfected with pcDNA3; B, cells transfected with pcDNA3-OVCA1HA. At the level of sensitivity needed to obtain high resolution of the OVCA1HA staining, the mock-transfected cells are not visible. C, subcellular fractionation of SV40-immortalized human ovarian surface epithelial cell lines (HIO). Cell lines were fractionated as described in "Materials and Methods," and 50 μ g of the corresponding extracts were separated by 12% SDS-PAGE and transferred to Immobilon-P. The Western blot shown was probed with the anti-OVCA1 antibody TJ132. Lane WCL, whole-cell extract; Lane C, cytoplasmic fraction; Lane N, nuclear fraction.

the antigenic peptide. Because FC21 and TJ132 gave almost identical patterns by Western blotting (Fig. 2B), most of the data shown used only the antibody TJ132.

OVCA1 was found to be expressed in many different tissues (Fig. 2C). In some cases, the M_r 70,000 and M_r 85,000 proteins were very prominent, whereas the M_r 50,000 protein was less so (notably the ovary and placenta) and, in other tissues, the p50 form was predominant (liver and thymus). Note that, although extracts from total breast tissue appeared to express little or no OVCA1 (Fig. 2C), breast epithelial cells did express the p50 OVCA1 protein (Fig. 3A, N.M.E.*). We explain this apparent discrepancy as being due to epithelial cells making up only a low percentage of the total breast. Analysis of breast and ovarian tumor extracts demonstrated variable expression levels of p50 and an almost complete absence of the p70/p85 species (Fig. 3). Expression levels of p50 were reduced as compared to normal epithelial cells in 21 of 59 ovarian (37%) and 18 of 46 breast (39%) carcinomas. p85 and p70 were not detected in the majority of tumors analyzed (100% of breast tumors and 85% of ovarian tumors) (Fig. 3). No correlation was evident between reduced expression and clinical prognostic factors.

Subcellular Localization of OVCA1. To aid in understanding the function of OVCA1, we determined its subcellular localization.

COS-1 cells were transfected with either an empty vector pcDNA3 or with pcDNA3-OVCA1HA, which expresses OVCA1 fused to a COOH-terminal HA tag. Immunostaining of transfected cells with an anti-HA antibody (Y-11; Santa Cruz Biotechnology) indicates that OVCA1 is located throughout the cell. A widespread diffuse staining was seen, in addition to strongly staining punctate bodies (Fig. 4A and B). These bodies were scattered throughout the cell and were heavily clustered around the nucleus. A similar pattern was obtained in immortalized HOSE cells transfected with pcDNA3-OVCA1HA and when the cells were immunostained with the specific anti-OVCA1 antibody, TJ132 (data not shown). To further confirm the localization, we fused OVCA1 to the COOH terminus of the green fluorescent protein. COS-1 cells expressing the green fluorescent protein-OVCA1 fusion again demonstrated a punctate, primarily perinuclear localization of the protein set against a weaker, diffuse staining throughout the cell (data not shown).

Fractionation studies confirmed that the M_r 50,000 OVCA1 protein is located throughout the cell (Fig. 4C). However, the M_r 70,000 and M_r 85,000 species appeared to be exclusively located within the nucleus (Fig. 4C).

Suppression of Clonal Outgrowth. Attempts to generate cell lines that stably expressed OVCA1 were unsuccessful. Very few clones

F4

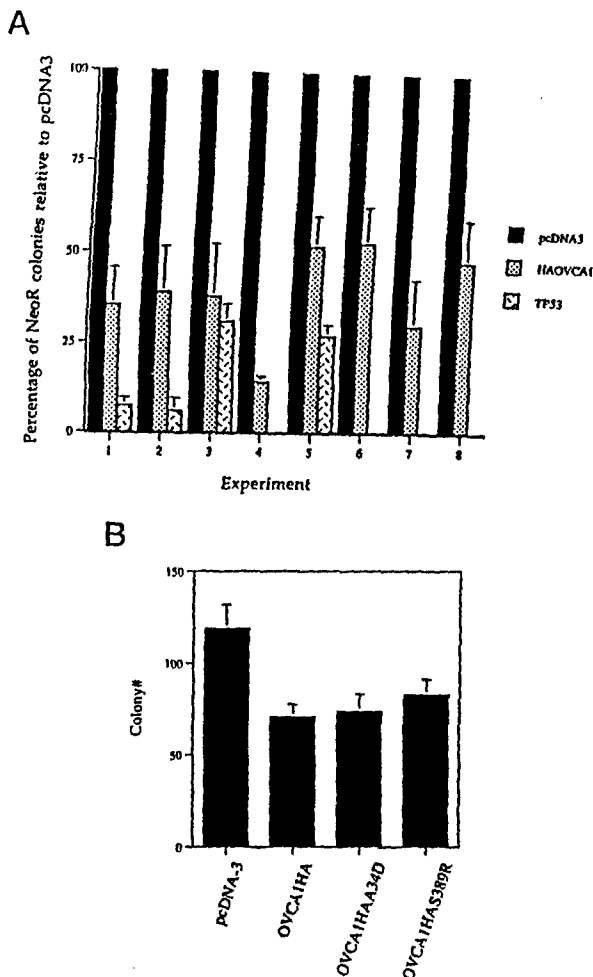


Fig. 5. Suppression of clonal outgrowth by OVCA1 in A2780 ovarian cancer cells. A2780 cells were transfected with the indicated plasmids and selected for resistance to G418, as described in "Materials and Methods." Ten to 14 days posttransfection, the colonies were stained and counted. A, the percentage of G418 (Neo^R) colonies that formed relative to the number formed after transfection with pcDNA3 (defined as 100% in each experiment) along the ordinate. Abscissa, data from eight independent transfection experiments. A wild-type TP53 expression vector was included in some experiments as a positive control for colony suppression. B, the total number of colonies obtained after transfection with the indicated plasmids and selection with G418. pcDNA3 is the parent vector; OVCA1HA expresses the wild-type OVCA1 plus a COOH-terminal HA tag; and A34D and S389R refer to the point mutations, discussed in the text, that were introduced into the wild-type OVCA1HA construct using standard PCR technology. Columns, means of three independently repeated experiments; bars, SD.

were found to express OVCA1, and those that did expressed only low levels of the protein. This phenomenon was consistently observed in a number of different cell types (RAT-1, U2OS, MCF-7, HIO118, and T47D cells; data not shown). To quantitate this effect, we transfected equimolar amounts of a mammalian expression vector containing the NH₂-terminal HA-tagged OVCA1 open reading frame (pcDNA3-HAOVCA1) and an empty expression vector (pcDNA3) into the ovarian cancer cell line A2780. A2780 cells were chosen for further analysis because they are well-characterized ovarian tumor cells that normally express fairly low levels of OVCA1 p50 and almost no p85/p70 OVCA1 (Fig. 2). As a positive control for growth suppression, an expression vector that expresses wild-type p53 protein was included in some of the colony number experiments. Evaluation of colony formation in the presence of geneticin (G418) consistently resulted in a 50–60% reduction in colony number in cells transfected

with the OVCA1 expression construct compared with controls (Fig. 5 A). This effect was reproducibly observed in more than four independent transfection experiments. Suppression of clonal outgrowth was independent of plasmid DNA purity because (we tested three different preparations of plasmid DNA) and ~~also~~ whether equivalent molar amounts or microgram amounts of plasmid were transfected. Furthermore, experiments in which an expression vector containing the gene encoding for the β -galactosidase protein were cotransfected with OVCA1 indicate that the reduction in clonal outgrowth is not an artifact due to differences in transfection efficiency (data not shown).

The A34D and S389R alterations described above, detected in the germ line of women with breast cancer and with a strong family history of the disease, were rebuilt into the pcDNA3-OVCA1HA expression plasmid using standard PCR technology. Both altered proteins were expressed well in transient transfection assays (data not shown). However, both alterations were found to suppress colony formation 50–60%, as compared with controls, similar to wild-type OVCA1 (Fig. 5B).

Growth Kinetics of Stable Transfectants. To verify that the suppression effect was due to exogenous OVCA1 expression, individual colonies were clonally expanded after G418 selection. A total of seven colonies from pcDNA3 vector control transfected cells and 15 colonies from pcDNA3-HAOVCA1 transfected cells were amplified following selection in G418 for 10 days. All colonies selected from pcDNA3 vector control plates expanded and formed stable cultures. In contrast, only 9 of 15 colonies selected from pcDNA3-HAOVCA1 transfected cells expanded to form a stable culture. Because an in-frame HA epitope was fused to the open reading frame of OVCA1 at the NH₂ terminus, the level of exogenous protein produced in these clones could be monitored. Western blot analysis revealed that there was approximately equimolar expression of exogenous and endogenous OVCA1 in only four of nine stable pcDNA3-HAOVCA1 clones (OV-5, OV-6, OV-9, and OV-13; Fig. 6).

Of the HAOVCA1 transfectants with exogenous expression, no major differences in morphological features were observed when compared to parental A2780 cells (data not shown). Cells were plated at limited dilutions and monitored for growth kinetics. Two independent clones, OV-5 and OV-13, displayed ~8- and 10-fold reductions in total cell number compared with expression vector controls and parental A2780 cells, respectively. A third clonal line, OV-9, demon-

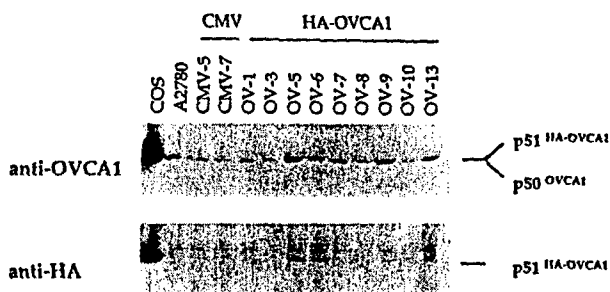


Fig. 6. Maintenance of exogenous OVCA1 expression in stable transfectants of A2780 ovarian cancer cells. A2780 cells were transfected with an HAOVCA1 expression vector and then selected for resistance to G418, as described in "Materials and Methods." Clones were chosen at random and amplified. After amplification, extracts were prepared from the cells, as described in "Materials and Methods." Ten μ g of each extract were separated by duplicate 10% SDS-PAGE. The gels were transferred to Immobilon-P and probed with the indicated antibodies, as described in "Materials and Methods." Top, total OVCA1 antigen was detected with the anti-OVCA1 antibody T1132. Bottom, exogenous OVCA1 antigen was detected with the anti-HA mAb 16B12 (BabCo, Richmond, CA). Lane COS, protein extract prepared from COS cells transiently transfected with an HAOVCA1 expression vector; Lanes A2780, protein extract prepared from the parental cell line; Lanes CMV, cell lines derived from pcDNA3 transfected cells; Lanes OV, cell lines derived from HAOVCA1-transfected cells.

Query page 13
change sentence #2.
- remove "because"
"also"
(we tested three... DNA)

No sure what
 this query is for
 this page

AUTHOR: SEE QUERY
 ON MANUSCRIPT
 PAGE 18

OVCA1 IS REDUCED IN TUMORS AND INHIBITS GROWTH

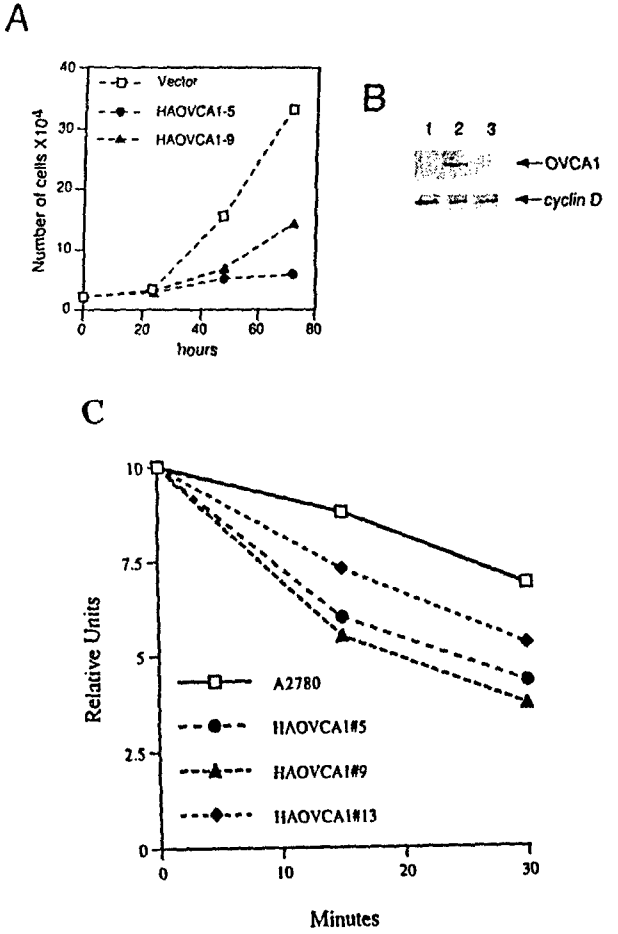


Fig. 7. Suppression of growth rate by OVCA1. A, the proliferation of A2780 clonal lines was monitored over time, as described in "Materials and Methods." Vector (□; CMV-5) is A2780 cells that have stably integrated the plasmid pcDNA3; HAOVCA1-5 (●; OV-5) and HAOVCA1-9 (▲; OV-9) are two lines that stably express OVCA1. The parental cell line, A2780, gave results that were virtually identical to those of the CMV-5 cell line (data not shown), and the stably expressing OVCA1 clone OV-13 gave results similar to that of OV-5 (data not shown). The graph represents the growth rates for the cell lines over the indicated time period and is representative of a number of independent experiments. Ordinate, number of cells (10⁴); abscissa, days in 24-h time points. B, OVCA1 expression (Western blot probed with the anti-HA tag antibody Y-11; Santa Cruz Biotechnology) and cyclin D1 expression (the Western blot showing OVCA1 expression was reprobed with an anti-cyclin D1 antibody; Santa Cruz Biotechnology) in the indicated cell lines: Lane 1, CMV-5; Lane 2, OV-5; Lane 3, OV-9. The parental cell line, A2780, gave results that were virtually identical to those of the CMV-5 cell line (data not shown), and the stably expressing OVCA1 clone OV-13 gave results that were similar to those of OV-5 (data not shown). C, the stability of cyclin D1 was monitored by pulse-chase (³⁵S)methionine labeling of the indicated cells followed by immunoprecipitation of the labeled cyclin D1. The immunoprecipitates were separated on SDS-PAGE and quantitated by Phosphorimager (Fuji). Abscissa, minutes after initiation of the chase; ordinate, relative units of labeling incorporated into cyclin D1. The graph is representative of a number of independent experiments.

F7

strated a 4-fold reduction in total cell number over the same time interval compared with controls (Fig. 7A). On the basis of these growth curves, the cell doubling times between parental A2780 and OVCA1-expressing stable clones were found to be considerably different. A2780 cells doubled 2–2.5 times during a 24-h period, whereas OV-5, OV-9, and OV-13 doubled ~1–1.5 times during the same time interval. Consistent with the reduced growth rate, the clones stably expressing OVCA1 had a dramatic reduction in cyclin D1 levels (Fig. 7B). The reduction of steady-state cyclin D1 levels appeared to be primarily due to an increased rate of degradation of cyclin D1 in cells expressing HAOVCA1 compared with the parental cell line (Fig. 7C).

FACS Analysis of Stable Transfectants. Two main mechanisms, apoptosis and cell cycle arrest, may account for the growth suppression observed in stable clones expressing exogenous OVCA1. To investigate the mechanism of growth suppression, we seeded parental A2780 cells and each of the stable transfectants at an equal number of cells. Seventy-two h postseeding, the cells were harvested, nuclei were stained with ethidium bromide, and cell cycle distribution was measured by FACS analysis. As illustrated in Fig. 8, a 10–20% increase in the number of cells in the G₁ fraction was observed in clones OV-5, OV-9, and OV-13 compared with parental A2780 cells and stable vector control cells, CMV-5. No subdiploid cell peaks suggestive of apoptosis were observed. To further investigate the possibility of apoptosis playing a role in reduced cell number, we subjected clones OV-5 and OV-9 to TUNEL staining and compared them with the vector control cells. There were no TUNEL-positive cells on the vector control cell slides. A total of 1.2% of the OV-9 cells were TUNEL-positive, and 4% of the OV-5 cells were TUNEL-positive, suggesting that, although rates of apoptosis are slightly elevated in A2780 cells stably expressing OVCA1, apoptosis does not fully account for the drastic reduction in growth rates (data not shown).

F8

Cyclin D1 Overexpression Can Partially Overcome OVCA1's Suppression of Clonal Outgrowth. Reduction of cyclin D1 levels by OVCA1 may be the primary cause of OVCA1's growth-suppressive

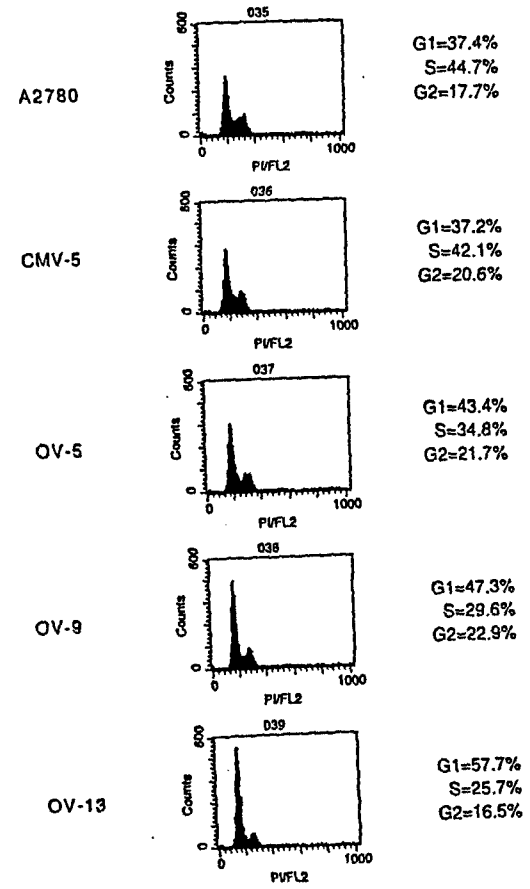


Fig. 8. FACS analysis of stable transfectants. Cell cycle distributions were determined 72 h postseeding by flow cytometry, as described in "Materials and Methods." DNA profiles represent cell number (counts) along the ordinate and DNA content (PI/FL2) along the abscissa. Percentage of cells in each phase of the cell cycle is listed on the right. G₁, both the G₀ and G₁ populations of cells; S, the population of cells in DNA synthesis; G₂, both the G₂ and M populations of cells.

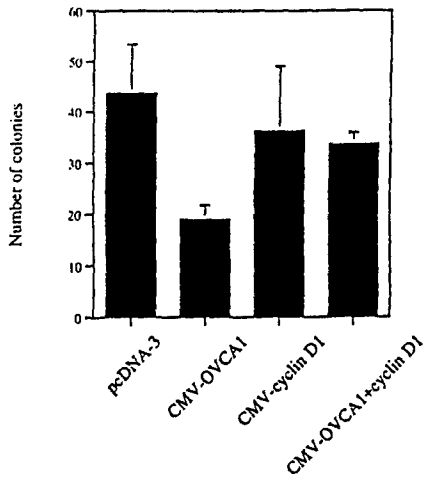


Fig. 9. Overexpression of cyclin D1 can override OVCA1's suppression of clonal outgrowth. A2780 cells were transfected with the indicated plasmids, as described in "Materials and Methods." Resistant colonies were selected in G418 for 14 days and then they were fixed and stained. Colonies with >50 cells were counted. The experiment was repeated three times. *pcDNA-3*, transfected with 1 μ g of *pcDNA3* and 1 μ g of *pskII*; *CMV-OVCA1*, transfected with 1 μ g of *pcDNA3-OVCA1HA* and 1 μ g of *pskII*; *CMV-cyclin D1*, transfected with 1 μ g of *CMV-cyclin D1* (carries no selectable marker) and 1 μ g of *pcDNA3*; *CMV-OVCA1+cyclin D1* was transfected with 1 μ g of *pcDNA3-OVCA1HA* and 1 μ g of *CMV-cyclin D1*.

effect. To test this theory, we cotransfected A2780 cells with *pcDNA3-OVCA1HA* and *CMV-cyclin D1*. The cells were transfected with *pcDNA3* alone, *pcDNA3-OVCA1HA* alone, *CMV-cyclin D1* alone, or both *pcDNA3-OVCA1HA* and *CMV-cyclin D1*. *pcDNA3* and *pskII* were added as necessary to equalize the amount of selectable marker and plasmid DNA in each transfection. After selection for 14 days in G418, the colonies were fixed, stained, and counted. As noted previously, cells transfected with the *OVCA1* expression construct formed ~50% fewer colonies than did cells transfected with *pcDNA3* (Fig. 9). Cells transfected with the cyclin D1 expression vector formed almost as many colonies as did cells transfected with *pcDNA3*. Cells cotransfected with *pcDNA3-OVCA1HA* and *CMV-cyclin D1* formed ~75% fewer colonies than did cells transfected with *pcDNA3* and almost the same number of colonies formed by cells transfected with *CMV-cyclin D1* alone, suggesting that overexpression of cyclin D1 can compensate for overexpression of *OVCA1*.

DISCUSSION

Molecular studies of human neoplasms suggest that a tumor suppressor locus exists on chromosome 17p13.3 near the VNTR markers YNH37.3 and YNZ22.2 (14-18, 20-25). To date, only two genes have been reported that map within the critical region of allelic loss on chromosome 17p13.3: *OVCA1* and *OVCA2* (47, 48). We have found that *OVCA2* cannot suppress tumor cell proliferation.⁵ The amino acid sequence of *OVCA1* contains little information with regard to its biological function. The only portion of the protein that is similar to previously identified proteins is a region in the NH₂ terminus that is similar to a domain found in a number of proteins isolated from a variety of species (47, 48). Unfortunately, the function of this domain is unclear. The only member of this putative gene family to which a function has been assigned is the yeast protein DPH2, which is known to play a role in the synthesis of diphthamide (56). It is unlikely that *OVCA1* is the human homologue of the yeast *dph2* because at least one other human gene, *DPH2L2*, is more similar to the yeast *dph2* than is *OVCA1* (57).

⁵ T. White and A. Prowse, unpublished observations.

Screening of a panel of primary breast ($n = 20$) and ovarian ($n = 50$) tumors for alterations of *OVCA1* revealed two distinct missense changes and multiple polymorphisms in both the coding and noncoding regions. Both missense changes were detected in breast tumors, and each alteration was present in the germ line of a woman with a strong family history of this disease. In both cases, the missense mutation/rare polymorphism was retained in the corresponding breast tumor DNA and showed reduction to homozygosity. Evaluation of >100 control chromosomes failed to detect these sequence variants. The probands do not have unusual ancestries, indicating that the sequence alterations are unlikely to be related to a specific ethnic group. Unfortunately, the probands are deceased, and we do not have informed consent to contact other members of their respective families. Both of these probands have tested negative for germ-line mutations in *BRCA1* and *BRCA2*.⁶ However, neither amino acid substitution alters *OVCA1*'s ability to suppress colony formation, suggesting that either these alterations are nonfunctional polymorphisms or that they affect some as yet undefined function of *OVCA1* or perhaps alter the function of the p85 form of *OVCA1*. Our observation is of particular significance because, in a recent European Consortium study, an association between LOH at the *OVCA1* locus and a positive family history of breast cancer was observed (16).

We also assessed ovarian tumors for large alterations involving the *OVCA1* gene by Southern blotting; however, no rearrangements or large interstitial deletions were detected. One previous study has reported a homozygous deletion in an ovarian carcinoma that involved both D17S28 and D17S30 but not any other flanking markers (15). Overall, no somatic mutations were detected within the coding region of *OVCA1* at the DNA level in either primary breast or ovarian tumors.

Because *OVCA1* does not appear to be commonly mutated in tumors and tumor cell lines, we sought to determine whether changes in its protein levels are more frequent in breast and ovarian cancer. Western blot analysis of extracts from breast and ovarian tumors suggest that expression of p50 *OVCA1* is reduced in at least one-third of the tumor specimens evaluated. The larger putative forms of *OVCA1* (p70/p85) are absent or highly reduced in almost 100% of the tumor specimens evaluated. The mechanism whereby the p70/p85 forms of *OVCA1* are generated is as yet unclear. Several different antibodies raised against different regions of *OVCA1* recognize the larger isoforms, confirming that they are closely related to the p50 *OVCA1*. Most likely, the p85 form is the product of an as yet undefined alternatively spliced exon or posttranslational modification. The p70 form is not recognized by antibodies directed against the COOH terminus of *OVCA1*, suggesting that it is either a degradation product of the p85 form or an unrelated, cross-reacting protein. If reduction of *OVCA1* levels is important in tumorigenesis, then reintroduction of *OVCA1* into tumor cell lines should revert, at least partially, the transformed phenotype. Because the p85/p70 isoforms are most consistently lost from tumors, reintroduction of these forms would be most informative. However, because they have not yet been completely defined, our experiments were confined to reintroduction of the p50 isoform. Attempts to stably express *OVCA1* from the CMV promoter in a variety of cell lines were unsuccessful. This phenomenon crossed species lines, being apparent in cells derived from both rodents and primates; was independent of p53 status; and was evident in both immortalized and transformed cells, suggesting that overexpression of *OVCA1* either blocks growth or is toxic to the cells.

Overexpression of *OVCA1* in the ovarian cancer cell line A2780 provided some clues about the function of *OVCA1*. It was possible to

⁶ A. K. Godwin, unpublished observations.

isolate a few clones that expressed exogenous OVCA1. In all cases, the level of exogenous expression was not high and was, at most, equivalent to the amount of OVCA1 normally seen in A2780 cells. Cells expressing exogenous OVCA1 were found to have a 4-fold (OV-9) to 10-fold (OV-13) reduction in growth compared with parental A2780 cells. The cellular mechanisms by which OVCA1 suppresses growth could fall into three categories: apoptosis, replicative senescence, or cell cycle arrest. On the basis of the amino acid sequence of OVCA1, it is unclear which, if any, of these pathways OVCA1 may affect. It is unlikely that OVCA1 promotes cell death to any great extent. TUNEL labeling and FACS analysis suggest that, although the OVCA1 stably expressing clones have a slightly elevated rate of apoptosis, it is not significant enough to account for the dramatic reduction in proliferation rates. It is also unlikely that exogenous OVCA1 restores replicative senescence because stable overexpression of OVCA1 did not affect rates of colony outgrowth (data not shown).

Cell cycle analysis of the OVCA1 stably expressing clones suggests that decelerated growth was associated with an increased percentage of the population in the G₀-G₁ phase of the cell cycle. We observed a reduction of cyclin D1 levels caused by destabilizing the protein, and this may be the direct cause of the slowed proliferation rates. In support of this hypothesis, cotransfection of cyclin D1 was able to override OVCA1's suppression of clonal outgrowth. Cyclin D levels are primarily regulated at the transcriptional level in response to extracellular mitogenic stimulation; however, in the absence of such stimulation, cyclin D is rapidly degraded by calpain proteases (Ref. 58; reviewed in Ref. 59). It is not yet clear as to how increased levels of OVCA1 leads to destabilization of cyclin D1. Deregulation of cyclin D1 has been implicated in the generation of many types of tumors. In some tumors, overexpression of cyclin D1 is achieved by amplification of the *cyclin D1* gene (reviewed in Ref. 60). However, in other tumors, including ovarian tumors, overexpression of cyclin D1 is not associated with genetic alterations, suggesting that some other mechanism, perhaps an increase in stability, is the cause of the abnormality (61, 62).

Analyses of ovarian and other tumors clearly indicate that allelic loss of chromosome 17p13.13 is one of the more frequently observed molecular alterations; >70% of ovarian tumors, at least two-thirds of breast tumors, and many other types of tumors have lost part or all of one copy of chromosome 17 (see "Introduction"). It was previously thought that both alleles of a tumor suppressor gene must be inactivated, as addressed by the "two-hit" hypothesis for tumorigenesis of Knudson (63). However, it has recently been shown that genes such as the murine gene *p27/kip1* and the *PTEN* gene are haploinsufficient for tumor suppression (64, 65). Abnormally low levels of the p27 protein are frequently found in human carcinomas (66-70). However, it had never been possible to establish a causal link between p27 and tumor suppression because only rare instances of homozygous inactivating mutations of the *p27* gene were found in human tumors (71-74). However, it was shown that both *p27* nullizygous and *p27* heterozygous mice were predisposed to tumors in multiple tissues when challenged with γ -irradiation or a chemical carcinogen (64). Molecular analyses of tumors in *p27* heterozygous mice showed that the remaining wild-type allele was neither mutated nor silenced (64). The *PTEN* gene encodes a dual-specificity phosphatase mutated in a variety of human cancers (75-77). *PTEN* germ-line mutations are found in three related human autosomal dominant disorders, CD, LDD, and BZS, characterized by tumor susceptibility and developmental defects (78-80). It was recently reported that *PTEN*^{+/-} mice and chimeric mice derived from *PTEN*^{+/-} embryonic stem cells showed hyperplastic/dysplastic changes in the prostate, skin and colon, which are characteristic of CD, LDD, and BZS, respectively

(65). They also spontaneously developed germ cell, gonadostromal, thyroid, and colon tumors, suggesting that *PTEN* haploinsufficiency plays a causal role in CD, LDD, and BZS (65). These studies, therefore, suggest that there is another class of tumor suppressor genes, in which genes that exhibit haploinsufficiency, leading to reduced levels of the protein, are important for tumorigenesis.

The data presented here and elsewhere, *i.e.*, high rate of allelic loss observed for chromosome 17p13.3 in ovarian tumors, the reduced expression of OVCA1 in ovarian tumors, and the observation that an equimolar level of exogenous p50 OVCA1 suppresses the growth rate of tumor cells up to 10-fold, suggest that a slight reduction in the level of expression of OVCA1 is sufficient for loss of growth regulation. The high rate of loss of one copy of chromosome 17p in breast and ovarian tumors may contribute to carcinogenesis by reducing *OVCA1* to hemizyosity. Future efforts aimed at clarifying the biochemical function of OVCA1 will aid in confirming the role that this gene has in tumorigenesis as well as its normal cellular function.

ACKNOWLEDGMENTS

We thank John Boyd for his help with the microscopy and Lisa Vanderveer for her technical assistance.

REFERENCES

1. Thai, T. H., Du, F., Tsan, J. T., Jin, Y., Phung, A., Spillman, M. A., Massa, H. F., Muller, C. Y., Ashfaq, R., Mathis, J. M., Miller, D. S., Trask, B. J., Baer, R., and Bowcock, A. M. Mutations in the BRCA1-associated RING domain (*BARD1*) gene in primary breast, ovarian, and uterine cancers. *Hum. Mol. Genet.*, 7: 195-202, 1998.
2. Carney, M. E., Maxwell, G. L., Lancaster, J. M., Gumbs, C., Marks, J., Berchuck, A., and Futreal, P. A. Aberrant splicing of the *TSG101* tumor suppressor gene in human breast and ovarian cancers. *J. Soc. Gynecol. Invest.*, 5: 281-285, 1998.
3. Gayther, S. A., Barski, P., Batley, S. J., Li, L., de Foy, K. A., Cohen, S. N., Ponder, B. A., and Caldas, C. Aberrant splicing of the *TSG101* and *FHIT* genes occurs frequently in multiple malignancies and in normal tissues and mimics alterations previously described in tumors. *Oncogene*, 15: 2119-2126, 1997.
4. Obata, K., Morland, S. J., Watson, R. H., Hitchcock, A., Chenevix-Trench, G., Thomas, E. J., and Campbell, I. G. Frequent *PTEN/MMAC1* mutations in endometrioid but not serous or mucinous epithelial ovarian tumors. *Cancer Res.*, 58: 2095-2097, 1998.
5. Maxwell, G. L., Risinger, J. I., Tong, B., Shaw, H., Barrett, J. C., Berchuck, A., and Futreal, P. A. Mutation of the *PTEN* tumor suppressor gene is not a feature of ovarian cancers. *Gynecol. Oncol.*, 70: 13-16, 1998.
6. Yokomizo, A., Tindall, D. J., Hartmann, L., Jenkins, R. B., Smith, D. I., and Liu, W. Mutation analysis of the putative tumor suppressor *PTEN/MMAC1* in human ovarian cancer. *Int. J. Oncol.*, 13: 101-105, 1998.
7. Schutte, M., Hruban, R. H., Hedrick, L., Cho, K. R., Nadasdy, G. M., Weinstein, C. L., Bova, G. S., Isaacs, W. B., Cairns, P., Nawroz, H., Sidransky, D., Casero, R. A. J., Meltzer, P. S., Hahn, S. A., and Kern, S. E. *DPC4* gene in various tumor types. *Cancer Res.*, 56: 2527-2530, 1996.
8. Yin Hua, Y., Fengji, X., Peng, H., Fang, X., Zhao, S., Li, Y., Cuevas, B., Kuo, W. L., Gray, J. W., Siciliano, M., Mills, G. B., and Bast, R. C. NOEY2 (*ARHI*), an imprinted putative tumor suppressor gene in ovarian and breast carcinomas. *Proc. Natl. Acad. Sci. USA*, 96: 214-219, 1999.
9. Mok, S. C., Chan, W. Y., Wong, K. K., Cheung, K. K., Lau, C. C., Ng, S. W., Baldini, A., Colitti, C. V., Rock, C. O., and RS, B. *DOC-2*, a candidate tumor suppressor gene in human epithelial ovarian cancer. *Oncogene*, 16: 2381-2387, 1998.
10. Abdollahi, A., Godwin, A., Miller, P., Getts, L., Schultz, D., Taguchi, T., Testa, J., and Hamilton, T. Identification of a gene containing zinc-finger motifs based on lost expression in malignantly transformed rat ovarian surface epithelial cells. *Cancer Res.*, 57: 2029-2034, 1997.
11. Abdollahi, A., Roberts, D., Godwin, A., Schultz, D., Sonoda, G., Testa, J., and Hamilton, T. Identification of a zinc-finger gene at 6q25: a chromosomal region implicated in the development of many solid tumors. *Oncogene*, 14: 1973-1979, 1997.
12. Godwin, A., Schultz, D., Hamilton, T., and Knudson, A. Oncogenes and tumor suppressor genes. In: W. Hoskins, C. Perez, and R. Young (eds.). Principles and Practice of Gynecological Oncology, pp. 107-148. Philadelphia: J. B. Lippincott Co., 1997.
13. Lynch, H. T., Casey, M. J., Lynch, J., White, T. E. K., and Godwin, A. K. Genetics and ovarian carcinoma. *Semin. Oncol.*, 25: 265-280, 1998.
14. Phillips, N., Ziegler, M. R., SaHa, B., and Xynos, F. Allelic loss on chromosome 17 in human ovarian cancer. *Int. J. Cancer*, 54: 85-91, 1993.
15. Phillips, N., Ziegler, M., Radford, D., Fair, K., Steinbrueck, T., Xynos, F., and Donis-Keller, H. Allelic deletion on chromosome 17p13.3 in early ovarian cancer. *Cancer Res.*, 56: 606-611, 1996.

garry page 25 - ok
garry page 27 -

16. Phelan, C., Borg, A., Cuny, M., Crichton, D., Balderson, T., Andersen, T., Caligo, M., Lidereau, R., Lindblom, A., Seitz, S., Kelsell, D., Hamann, U., Rio, P., Thorlacius, S., Papp, J., Olah, E., Ponder, B., Bignon, Y.-J., Scherneck, S., Barkardottir, R., Borresen-Dale, A.-L., Eyfjord, J., Theillet, C., Thompson, A., Devilee, P., and Larsson, C. Consortium study on 1280 breast carcinomas: allelic loss on chromosome 17 targets subregions associated with family history and clinical parameters. *Cancer Res.*, 58: 1004-1012, 1998.
17. Mackay, J., Elder, P., Steel, C., Forrest, A., and Evans, H. Allele loss on short arm of chromosome 17 in breast cancers. *Lancet*, 17: 1384-1385, 1988.
18. Devilee, P., Pearson, P., and Cornelisse, C. Allele losses in breast cancer. *Lancet*, 1: 1544-1545, 1989.
19. Singh, S., Simon, M., Meybohm, I., Jantke, I., Jonat, W., Maass, H., and Goedde, H. Human breast cancer: frequent p53 allele loss and protein overexpression. *Hum. Genet.*, 90: 635-640, 1993.
20. Cornelis, R., van Vliet, M., Vos, C., Cleton-Jansen, A.-M., van de Vijver, M., Peterse, J., Khan, P., Borresen, A.-L., Cornelisse, C., and Devilee, P. Evidence for a gene on 17p13.3, distal to TP53, as a target for allelic loss in breast tumors without p53 mutations. *Cancer Res.*, 54: 4200-4206, 1994.
21. Harada, Y., Katagiri, T., Ito, I., Akiyama, F., Sakamoto, G., Kasumi, F., Nakamura, Y., and Emi, M. Genetic studies of 457 breast cancers. *Cancer (Phila.)*, 74: 2281-2286, 1994.
22. Stack, M., Jones, D., White, G., Liscia, D., Venesio, T., Casey, G., Crichton, D., Varley, J., Mitchell, E., Heighway, J., and Santibanez-Koref, M. Detailed mapping and loss of heterozygosity analysis suggests a suppressor locus involved in sporadic breast cancer within a distal region of chromosome band 17p13.3. *Hum. Mol. Genet.*, 4: 2047-2055, 1995.
23. Thompson, A., Crichton, D., Elton, R., Clay, M., Chetty, U., and Steel, C. Allelic imbalance at chromosome 17p13.3 (Ynz22) in breast cancer is independent of p53 mutation or p53 overexpression and is associated with poor prognosis at medium-term follow-up. *Br. J. Cancer*, 77: 797-800, 1998.
24. Ito, I., Yoshimoto, M., Iwase, T., Watanabe, S., Katagiri, T., Harada, Y., Kasumi, F., Yasuda, S., Mitomi, T., Emi, M., and Nakamura, Y. Association of genetic alterations on chromosome 17 and loss of hormone receptors in breast cancer. *Br. J. Cancer*, 71: 438-441, 1995.
25. Nagai, M. A., Medeiros, A., Brentani, M. M., Marques, L. A., Mazoyer, S., and Mulligan, L. M. Five distinct deleted regions on chromosome 17 defining different subsets of human primary breast tumor. *Oncogene*, 52: 448-453, 1995.
26. Marchetti, A., Buttitta, F., Merlo, G., Diella, F., Pellegrini, S., Pepe, S., Macchiarini, P., Chella, A., Angeletti, A., Callahan, R., Bistocchi, M., and Squartini, F. p53 alterations in non-small cell lung cancers correlate with metastatic involvement of hilar and mediastinal lymph nodes. *Cancer Res.*, 53: 2846-2851, 1993.
27. Takahashi, T., Nau, M. M., Chiba, I., *et al.* p53: a frequent target for genetic abnormalities in lung cancer. *Science (Washington DC)*, 246: 491-494, 1989.
28. Konishi, H., Takahashi, T., Kozaki, K., Yatabe, Y., Mitsudomi, T., Fujii, Y., Sugiura, T., Matsuda, H., Takahashi, T., and Takahashi, T. Detailed deletion mapping suggests the involvement of a tumor suppressor gene at 17p13.3, distal to p53, in the pathogenesis of lung cancers. *Oncogene*, 17: 2095-2100, 1998.
29. Baker, S., Fearon, E., Nigro, J., Hamilton, S., Preisinger, A., Jessup, J., van Tuinen, P., Ledbetter, D., Barker, D., Nakamura, Y., White, R., and Vogelstein, B. Chromosome 17 deletions and p53 gene mutations in colorectal carcinomas. *Science (Washington DC)*, 244: 217-221, 1989.
30. Haataja, L., Raffel, C., Ledbetter, D., Tanigami, A., Petersen, D., Heisterkamp, N., and Groffen, J. Deletion within the *D17S34* locus in a primitive neuroectodermal tumor. *Cancer Res.*, 57: 32-34, 1997.
31. Biegel, J., Rorke, L., Janss, A., Sutton, L., and Parmiter, A. Isochromosome 17q demonstrated by interphase fluorescence *in situ* hybridization in primitive neuroectodermal tumors of the central nervous system. *Genes Chromosomes Cancer*, 14: 85-96, 1995.
32. Biegel, J., Burk, C., Barr, F., and Emanuel, B. Evidence for a 17p tumor related locus distinct from p53 in pediatric primitive neuroectodermal tumors. *Cancer Res.*, 52: 3391-3395, 1992.
33. Park, S.-Y., Kang, Y.-S., Kim, B.-G., Lee, S.-H., Lee, E.-D., Lee, K.-H., Park, K.-B., and Lee, J.-H. Loss of heterozygosity on the short arm of chromosome 17 in uterine cervical carcinomas. *Cancer Genet. Cytogenet.*, 79: 74-78, 1995.
34. Kersemaekers, A.-M., Kenter, G., Hermans, J., Fleuren, G., and van de Vijver, M. Allelic loss and prognosis in carcinoma of the uterine cervix. *Int. J. Cancer*, 79: 411-417, 1998.
35. Kersemaekers, A., Hermans, J., Fleuren, G., and van de Vijver, M. Loss of heterozygosity for defined regions on chromosomes 3, 11 and 17 in carcinomas of the uterine cervix. *Br. J. Cancer*, 77: 192-200, 1998.
36. Atkin, N. B., and Baker, M. C. Chromosome 17p loss in carcinoma of the cervix uteri. *Cancer Genet. Cytogenet.*, 37: 229-233, 1989.
37. Saylors, R., Sidransky, D., Friedman, H. S., Bigner, S. H., Bigner, D. D., Vogelstein, B., and Brodeur, G. M. Infrequent p53 gene mutations in medulloblastomas. *Cancer Res.*, 51: 4721-4723, 1991.
38. McDonald, J., Daneshvar, L., Willert, J., Matsumura, K., Waldman, F., and Cogen, P. Physical mapping of chromosome 17p13.3 in the region of a putative tumor suppressor gene important in medulloblastoma. *Genomics*, 23: 229-232, 1994.
39. Scheurten, W., Krauss, J., and Kuhl, J. No preferential loss of one parental allele of chromosome 17p13.3 in childhood medulloblastoma. *Int. J. Cancer*, 63: 372-374, 1995.
40. Cogen, P., Daneshvar, L., Metzger, A., Duyk, G., Edwards, M., and Sheffield, V. Involvement of multiple chromosome 17p loci in medulloblastoma tumorigenesis. *Am. J. Hum. Genet.*, 50: 584-589, 1992.
41. Chattopadhyay, P., Rathore, A., Mathur, M., Sarkar, C., Mahapatra, S., and Sinha, S. Loss of heterozygosity of a locus on 17p13.3, independent of p53, is associated with higher grades of astrocytic tumours. *Oncogene*, 15: 871-875, 1997.
42. Saxena, A., Clark, W., Robertson, J., Ikejiri, B., Oldfield, E., and Ali, I. Evidence for the involvement of a potential second tumor suppressor gene on chromosome 17 distinct from p53 in malignant astrocytomas. *Cancer Res.*, 52: 6716-6721, 1992.
43. Grebe, S., McIver, B., Hay, I., Wu, P., Maciel, L., Drabkin, H., Goellner, J., Grant, C., Jenkins, R., and Eberhardt, N. Frequent loss of heterozygosity on chromosomes 3p and 17p without VHL or p53 mutations suggests involvement of unidentified tumor suppressor genes in follicular hybrid carcinoma. *Clin. Endocrinol. Metab.*, 82: 3684-3691, 1997.
44. Tomlinson, I., Gammack, A., Stickland, J., Mann, G., MacKie, R., Kefferd, R., and McGee, J. D. Loss of heterozygosity in malignant melanoma at loci on chromosomes 11 and 17 implicated in the pathogenesis of other cancers. *Genes Chromosomes Cancer*, 7: 169-172, 1993.
45. Nishida, N., Fukuda, Y., Kokuryu, H., Toguchida, J., Yandell, D., Ikenaga, M., Imura, H., and Ishizaki, K. Role and mutational heterogeneity of the p53 gene in hepatocellular carcinoma. *Cancer Res.*, 53: 368-372, 1993.
46. Sankar, M., Tanaka, K., Kumaravel, T., Anif, M., Shintani, T., Yagi, S., Kyo, T., Dohy, H., and Kamada, N. Identification of a commonly deleted region at 17p13.3 in leukemia and lymphoma associated with 17p abnormality. *Leukemia (Baltimore)*, 12: 510-516, 1998.
47. Schultz, D. C., Vanderveer, L., Berman, D. B., Hamilton, T. C., Wong, A. J., and Godwin, A. K. Identification of two candidate tumor suppressor genes on chromosome 17p13.3. *Cancer Res.*, 56: 1997-2002, 1996.
48. Phillips, N. J., Ziegler, M. R., and Deaven, L. L. A cDNA from the ovarian cancer critical region of deletion on chromosome 17p13.3. *Cancer Lett.*, 102: 85-90, 1996.
49. Baker, S. J., Markowitz, S., Fearon, E. R., Willson, J. K., and Vogelstein, B. Suppression of human colorectal carcinoma cell growth by wild-type p53. *Science (Washington DC)*, 249: 912-915, 1990.
50. Bookstein, R., Shew, J. Y., Chen, P. L., Scully, P., and Lee, W. H. Suppression of tumorigenicity of human prostate carcinoma cells by replacing a mutated RB gene. *Science (Washington DC)*, 247: 712-715, 1990.
51. Eliyahu, D., Michalovitz, D., Eliyahu, S., Pinhasi-Kimhi, O., and Oren, M. Wild-type p53 can inhibit oncogene-mediated focus formation. *Proc. Natl. Acad. Sci. USA*, 86: 8763-8767, 1989.
52. Finlay, C. A., Hinds, P. W., and Levine, A. The p53 proto-oncogene can act as a suppressor of transformation. *Cell*, 57: 1083-1093, 1989.
53. Holt, J. T., Thompson, M. E., Szabo, C., Robinson-Benion, C., Arteaga, C. L., King, M. C., and Jensen, R. A. Growth retardation and tumour inhibition by BRCA1. *Nat. Genet.*, 12: 298-302, 1996.
54. Huang, H. J. S., Yee, J. K., Shew, J. Y., Chen, P. L., Bookstein, R., Friedmann, T., Lee, E. Y. H., *et al.* Suppression of the neoplastic phenotype by replacement of the RB gene in human cancer cells. *Science (Washington DC)*, 242: 1563-1566, 1988.
55. Liggett, W. H. J., Dewell, D. A., Rocco, J., Ahrendt, S. A., Koch, W., and Sidransky, D. p16 and p16^{ink4} are potent growth suppressors of head and neck squamous carcinoma cells *in vitro*. *Cancer Res.*, 56: 4119-4123, 1996.
56. Mattheakis, L. C., Sor, F., and Collier, R. J. Diphthamide synthesis in *Saccharomyces cerevisiae*: structure of the *DPH2* gene. *Gene*, 132: 149-154, 1993.
57. Schultz, D. C., Balasara, B. R., Testa, J. R., and Godwin, A. K. Cloning and localization of the human diphthamide biosynthesis protein-2 gene, hDPH2. *Genomics*, 52: 186-191, 1998.
58. Choi, Y. H., Lee, S. J., Nguyen, P. M., Jang, J. S., Lee, J., Wu, M. L., Takano, E., Maki, M., Henkart, P. A., and Trepel, J. B. Regulation of cyclin D1 by calpain protease. *J. Biol. Chem.*, 272: 28479-28484, 1997.
59. Sherr, C. J. D-type cyclins. *Trends Biochem. Sci.*, 20: 187-190, 1995.
60. Motokura, T., and Arnold, A. Cyclin D and oncogenesis. *Curr. Opin. Genet. Dev.*, 3: 5-10, 1993.
61. Masciullo, V., Scambia, G., Marone, M., Giannitelli, C., Ferrandina, G., Bellacosa, A., Benedetti, P., and Mancuso, S. Altered expression of cyclin D1 and CDK4 genes in ovarian carcinomas. *Int. J. Cancer*, 74: 390-395, 1997.
62. Welker, M., Lukas, J., Strauss, M., and Bartek, J. Enhanced protein stability: a novel mechanism of D-type cyclin over-abundance identified in human sarcoma cells. *Oncogene*, 13: 419-425, 1996.
63. Knudson, A. G. Mutation and cancer: statistical study of retinoblastoma. *Proc. Natl. Acad. Sci. USA*, 68: 820-823, 1971.
64. Ferro, M. L., Randel, E., Gurley, K. E., Roberts, J. M., and Kemp, C. J. The murine gene p27 Kip1 is haplo-insufficient for tumour suppression. *Nature (Lond.)*, 396: 177-180, 1998.
65. Di Cristofano, A., Pesce, B., Cordon-Cardo, C., Pandolfi, P. P. Pten is essential for embryonic development and tumour suppression. *Nat. Genet.*, 19: 348-355, 1998.
66. Yang, R. M., Naitoh, J., Murphy, M., Wang, H. J., Phillipson, J., deKernion, J. B., Loda, M., and Reiter, R. E. Low p27 expression predicts poor disease-free survival in patients with prostate cancer. *J. Urol.*, 159: 941-945, 1998.
67. Yasui, W., Kudo, Y., Semba, S., Yokozaki, H., and Tahara, E. Reduced expression of cyclin-dependent kinase inhibitor p27Kip1 is associated with advanced stage and invasiveness of gastric carcinomas. *Jpn. J. Cancer Res.*, 88: 625-629, 1997.
68. Esposito, V., Baldi, A., De Luca, A., Groger, A. M., Loda, M., Giordano, G. G., Caputi, M., Baldi, F., Pagano, M., and Giordano, A. Prognostic role of the cyclin-dependent kinase inhibitor p27 in non-small cell lung cancer. *Cancer Res.*, 57: 3381-3385, 1997.
69. Loda, M., Cukor, B., Tam, S. W., Lavin, P., Fiorentino, M., Draetta, G. F., Jessup, J. M., and Pagano, M. Increased proteasome-dependent degradation of the cyclin-dependent kinase inhibitor p27 in aggressive colorectal carcinomas. *Nat. Med.*, 3: 231-234, 1997.

Query page 28 - 1 page reference (#18)
 attached authors (#27)
 (#54)

AUTHOR: SEE QUERY
ON MANUSCRIPT
PAGE 33, 34

1

OVCA1 IS REDUCED IN TUMORS AND INHIBITS GROWTH

- X
70. Porter, P. L., Malone, K. E., Heagerty, P. J., Alexander, G. M., Gatti, L. A., Firpo, E. J., Daling, J. R., and Roberts, J. M. Expression of cell-cycle regulators p27Kip1 and cyclin E, alone and in combination, correlate with survival in young breast cancer patients. *Nat. Med.*, **3**: 222-225, 1997.
71. Spirin, K. S., Simpson, J. F., Takeuchi, S., Kawamata, N., Miller, C. W., and Koeffler, H. P. p27/Kip1 mutation found in breast cancer. *Cancer Res.*, **56**: 2400-2404, 1996.
72. Kawamata, N., Morosetti, R., Miller, C. W., Park, D., Spirin, K. S., Nakamaki, T., Takeuchi, S., Hatta, Y., Simpson, J., Wilczynski, S., *et al.* Molecular analysis of the cyclin-dependent kinase inhibitor gene p27/Kip1 in human malignancies. *Cancer Res.*, **55**: 2266-2269, 1995.
73. Morosetti, R., Kawamata, N., Gombart, A. F., Miller, C. W., Hatta, Y., Hiramata, T., Said, J. W., Tomonaga, M., and Koeffler, H. P. Alterations of the p27KIP1 gene in non-Hodgkin's lymphomas and adult T-cell leukemia/lymphoma. *Blood*, **86**: 1924-1930, 1995.
- X 74. Pietenpol, J. A., Bohlander, S. K., Sato, Y., Papadopoulos, N., ~~Li, D.~~ Friedman, C., Trask, B. J., Roberts, J. M., Kinzler, K. W., Rowley, J. D., *et al.* Assignment of the human p27Kip1 gene to 12p13 and its analysis in leukemias. *Cancer Res.*, **55**: 1206-1210, 1995.
75. Li, J., Yen, C., Liaw, D., Podsypanina, K., Bose, S., Wang, S. I., Puc, J., Miliareis, C., Rodgers, L., McCombie, R., Bigner, S. H., Giovanella, B. C., Ittmann, M., Tycko, B., Hibshoosh, H., Wigler, M. H., and Parsons, R. PTEN, a putative protein tyrosine phosphatase gene mutated in human brain, breast, and prostate cancer. *Science* (Washington DC), **275**: 1943-1947, 1997.
76. Steck, P. A., Pershouse, M. A., Jasser, S. A., Yung, W. K., Lin, H., Ligon, A. H., Langford, L. A., Baumgard, M. L., Hattier, T., Davis, T., Frye, C., Hu, R., Swedlund, B., Teng, D. H., and Tavtigian, S. V. Identification of a candidate tumour suppressor gene, *MMAC1*, at chromosome 10q23.3 that is mutated in multiple advanced cancers. *Nat. Genet.*, **15**: 356-362, 1997.
77. Guldberg, P., Thor Straten, P., Birck, A., Ahrenkiel, V., Kirkin, A. F., and Zeuthen, J. Disruption of the *MMAC1/PTEN* gene by deletion or mutation is a frequent event in malignant melanoma. *Cancer Res.*, **57**: 3660-3663, 1997.
78. Liaw, D., Marsh, D. J., Li, J., Dahia, P. L., Wang, S. I., Zheng, Z., Bose, S., Call, K. M., Tsou, H. C., Peacocke, M., Eng, C., and Parsons, R. Germline mutations of the *PTEN* gene in Cowden disease, an inherited breast and thyroid cancer syndrome. *Nat. Genet.*, **16**: 64-67, 1997.
79. Marsh, D. J., Coulon, V., Lunetta, K. L., Rocca-Serra, P., Dahia, P. L., Zheng, Z., Liaw, D., Caron, S., Duboue, B., Lin, A. Y., Richardson, A. L., Bonnetblanc, J. M., Bressieux, J. M., Cabarrot-Moreau, A., Chompret, A., Demange, L., Eeles, R. A., Yahanda, A. M., Fearon, E. R., Frycker, J. P., Gorlin, R. J., Hodgson, S. V., Huson, S., Lacombe, D., Eng, C., *et al.* Mutation spectrum and genotype-phenotype analyses in Cowden disease and ~~Bannayan-Zonana~~ Bannayan-Zonana syndrome, two hamartoma syndromes with germline *PTEN* mutation. *Hum. Mol. Genet.*, **7**: 507-515, 1998.
- X 80. Nelen, M. R., van Staveren, W. C., Peeters, E. A., Hassel, M. B., Gorlin, R. J., Hamm, H., Lindboe, C. F., Fryns, J. P., Sijmons, R. H., Woods, D. G., Mariman, E. C., Padberg, G. W., and Kremer, H. Germline mutations in the *PTEN/MMAC1* gene in patients with Cowden disease. *Hum. Mol. Genet.*, **6**: 1383-1387, 1997.

Query #33 - effected additional authors (#74)
Query #34 - " " " (#79)

Identification and Structural Analysis of Human RBM8A and RBM8B: Two Highly Conserved RNA-Binding Motif Proteins That Interact with OVCA1, a Candidate Tumor Suppressor

Ana M. Salicioni,* Mingrong Xi,† Lisa A. Vanderveer,* Binaifer Balsara,‡ Joseph R. Testa,‡ Roland L. Dunbrack, Jr.,§ and Andrew K. Godwin*^{†,1}

*Department of Medical Oncology, †Human Genetics Program, and §Basic Science Division, Fox Chase Cancer Center, Philadelphia, Pennsylvania 19111; and ‡West China University of Medical Sciences, Chengdu, Sichuan Province, P.R. China

Received April 6, 2000; accepted June 22, 2000

The *OVCA1* gene is a candidate for the breast and ovarian tumor suppressor gene at chromosome 17p13.3. To help determine the function(s) of *OVCA1*, we used a yeast two-hybrid screening approach to identify *OVCA1*-associating proteins. One such protein, which we initially referred to as BOV-1 (binder of *OVCA1*-1) is 173 or 174 amino acids in length and appears to be a new member of a highly conserved RNA-binding motif (RBM) protein family that is highly conserved evolutionarily. Northern blot analysis revealed that *BOV-1* is ubiquitously expressed and that three distinct messenger RNA species are expressed, 1-, 3.2-, and 5.8-kb transcripts. The 1-kb transcript is the most abundant and is expressed at high levels in the testis, heart, placenta, spleen, thymus, and lymphocytes. Using fluorescence *in situ* hybridization and the 5.8-kb complementary DNA probe, we determined that *BOV-1* maps to both chromosome 5q13–q14 and chromosome 14q22–q23. Further sequence analysis determined that the gene coding the 1- and the 3.2-kb transcripts (HGMW-approved gene symbol *RBM8A*) maps to 14q22–q23, whereas a second highly related gene coding for the 5.8-kb transcript resides at chromosome 5q13–q14 (HGMW-approved gene symbol *RBM8B*). The predicted proteins encoded by *RBM8A* and *RBM8B* are identical except that *RBM8B* is 16 amino acids shorter at its N-terminus. Molecular modeling of the RNA-binding domain of *RBM8A* and *RBM8B*, based on homology to the sex-lethal protein of *Drosophila*, identifies conserved residues in the RBM8 protein family that are likely to contact RNA in a protein–RNA complex. The conservation of sequence and structure through such an evolutionarily divergent group of organisms suggests an important function for the RBM8 family of proteins. © 2000 Academic Press

INTRODUCTION

Analyses of ovarian, breast, and other human tumors indicate that allelic loss of chromosome 17p13.3 is one of the most frequently observed molecular alterations. Recent data from our laboratory suggest that the ovarian cancer 1 gene (*OVCA1*)² gene is a strong candidate for the breast and ovarian tumor suppressor gene at chromosome 17p13.3, yet the biochemical function is unknown (Bruening *et al.*, 1999; Schultz *et al.*, 1996). To help determine the function(s) of *OVCA1*, we used a yeast two-hybrid screening approach to identify *OVCA1*-associating proteins. Several proteins were identified; however, the most common was a protein containing an RNA-binding motif.

RNA-binding proteins (RBPs) play key roles in the posttranscriptional regulation of gene expression in eukaryotic cells. Once produced in the nucleus, messenger RNAs (mRNAs) are transported to the cytoplasm where the protein synthesis machinery is located, and there is an array of posttranscriptional mechanisms that control mRNA stability, localization, and translation (St Johnston, 1995). Many of these processes are mediated by RBPs and by small RNAs as stable ribonucleoprotein (RNP) complexes. Characterization of these proteins has led to the identification of several conserved RNA-binding motifs (Birney *et al.*, 1993; Burd and Dreyfuss, 1994a). The most notable feature of many of these proteins is the presence of one or more RNA-recognition motifs (RRMs). The RRM is a 90-amino-acid protein domain that binds single-stranded RNA. In contrast to the RRM, much less is known about the structure and function of other RNA-binding motifs, including the arginine/serine-rich (RS) and arginine/glycine-rich (RG) regions. We report here the initial characterization and structural analysis of *RBM8A* and a closely related member of this highly conserved RNA-binding motif protein family referred

Sequence data from this article have been deposited with the EMBL/GenBank Data Libraries under Accession Nos. AF231511 and AF231512.

¹ To whom correspondence should be addressed at Department of Medical Oncology, Room W304, Fox Chase Cancer Center, 7701 Burholme Avenue, Philadelphia, PA 19111. Telephone: (215) 728-2756. Fax: (215) 728-2741. E-mail: A.Godwin@fccc.edu.

² Abbreviations used: *OVCA1*, ovarian cancer 1 gene; *BOV-1*, binder of *OVCA1*-1 gene; RBM, RNA-binding motif; ORF, open reading frame; cDNA, complementary deoxyribonucleic acid; UTR, untranslated region; FISH, fluorescence *in situ* hybridization.

to as RBM8B, which interact with a candidate tumor suppressor.

MATERIALS AND METHODS

Yeast two-hybrid interaction trap analysis. The two-hybrid screening of protein interaction was performed by standard protocols (Golemis and Serebriiskii, 1998) using a human fetal brain yeast expression library in the vector pJG4-5 kindly donated by Dr. Erica Golemis (Fox Chase Cancer Center), pMW103 as the LacZ reporter, and an N-terminal or a C-terminal bait, corresponding to amino acids 2 to 161 or 225 to 443 of OVCA1 (i.e., LexA-OVCA1a.a.2-161 or LexA-OVCA1a.a.225-443), respectively.

Cloning of binder of OVCA1-1 (BOV-1). The entire coding regions of *BOV-1a*, *b*, and *c* were obtained by using an *EcoRI/XhoI* 724-bp complementary DNA (cDNA) fragment, to probe directly a human fetal brain Uni-ZAP XR cDNA library (Stratagene, La Jolla, CA) by standard approaches. DNA from selected phage clones was sequenced.

Northern analysis. The expression of *BOV-1* mRNA in various human tissues was determined by hybridization of an ~800-bp *BOV-1* cDNA fragment to multiple tissue Northern blots, according to protocols previously described (Schultz *et al.*, 1996).

Fluorescence in situ hybridization analysis of *BOV-1* cDNA. Fluorescence *in situ* hybridization (FISH) and detection of immunofluorescence were carried out as previously described (Bell *et al.*, 1995). A 5.8-kb cDNA clone corresponding to *BOV-1c* was biotinylated by standard nick-translation methods. Probes were denatured and hybridized to metaphase spreads overnight at 37°C. Hybridized probe was detected with fluorescein-labeled avidin and amplified by addition of anti-avidin antibody (Oncor) and a second layer of fluorescein-labeled avidin. The chromosome preparations were counterstained with DAPI and observed with a Zeiss Axiophot epifluorescence microscope equipped with a cooled charge-coupled device camera (Photometrics, Tucson, AZ) operated by a Macintosh computer workstation. Digitized images of DAPI staining and FITC signals were captured, pseudocolored, and merged using Oncor version 1.6 software.

Mammalian cell culture and transfection procedures. The African green monkey kidney cell line COS-1 (American Type Culture Collection, Manassas, VA) was maintained in Dulbecco's modified Eagle's medium (DMEM) supplemented with 10% fetal calf serum. The entire coding region of *BOV-1a/b* was PCR-amplified by using oligonucleotides containing both T7 epitope-tag coding sequences and *KpnI/NotI* overhangs and directionally cloned into the *KpnI/NotI* sites of the pCDNA3 expression vector (Invitrogen, Carlsbad, CA), creating a full-length in-frame T7-*BOV-1* fusion protein. COS-1 cells were transiently transfected with the indicated plasmid using FuGene (Roche), as directed by the manufacturer, and used for immunofluorescence studies.

Immunofluorescence microscopy. COS-1 cells were seeded onto coverslips in 100-mm dishes and grown to 50% confluence. Forty-eight hours after transfection, cells were fixed in 3% paraformaldehyde and then permeabilized with 2% Triton X in PBS. After incubation with monoclonal antibodies against the T7 tag (Novagen, Madison, WI), cells were washed and then incubated with a FITC-conjugated anti-mouse antibody (Jackson ImmunoResearch Laboratories Inc., West Grove, PA). Slides were visualized with a Nikon Eclipse E800 epifluorescence microscope, and immunofluorescence images were taken with a Nikon camera.

Sequence comparison analysis. Nucleic acid and amino acid homology searches were conducted by using the NetBLAST and FastA programs of the GCG sequence analysis package (Madison, WI) by searching the complete combined GenBank/EMBL and GenBank CDS translations + SwissProt + PDB + SPupdate + PIR databases, respectively. The expressed sequence tag database at NCBI was searched with the BLAST program.

Homology modeling of the RNA recognition motif domain of *BOV-1/RBM8*. We used methods described previously to build a model of the RBM8 RRM domain (Dunbrack, 1999). Briefly, PSI-BLAST was used to build a sequence profile of the RBM8 family by iteratively searching the nonredundant protein sequence database available from NCBI (Altschul and Koonin, 1998). We used four iterations of PSI-BLAST, and only sequences with expectation values better than 0.0001 were included in the sequence profile matrix. Upon completion, this matrix was used to search a database of protein sequences in the Protein Data Bank (Berman *et al.*, 2000) of experimentally determined protein structures. This resulted in a list of proteins that could be used as a template for modeling of RBM8A/B. Models of RBM8A/B were built from two of these structures using the side-chain conformation prediction program SCWRL (Bower *et al.*, 1997). SCWRL builds side chains on a template backbone by first placing residues according to a backbone-dependent rotamer library (Dunbrack and Cohen, 1997), followed by a combinatorial search to remove steric overlaps.

RESULTS

Isolation of *BOV-1* cDNA

We used a yeast two-hybrid screen to identify cDNAs from a human fetal brain library encoding proteins that were able to interact with OVCA1. A C-terminal bait of OVCA1, corresponding to amino acids 225 to 443, yielded the only protein interactors. A total of 3.5×10^5 primary transformants were screened, resulting in the identification of 28 redundant clones coding for 4 OVCA1 interactor candidates. The most redundant clone, initially referred to as *BOV-1* (binder of OVCA1-1), accounted alone for 54% of the total cDNA isolated. It represented 15 independent isolates of a cDNA of 700 bp in length, encoding a 173-amino-acid protein. The three additional candidate OVCA1 binders were BIP/GRP78 and two previously uncharacterized proteins (data not included).

Northern Analysis of *BOV-1*

The expression pattern of *BOV-1* mRNA was evaluated by multiple tissue Northern blotting. Three major mRNA species were detected, *BOV-1a*, *1b*, and *1c*, of ~1, ~3.2, and ~5.8 kb, respectively. While these species were expressed in all tissues to varying degrees, the 1-kb transcript was most abundant in testis, heart, placenta, spleen, thymus, and lymphocytes (Fig. 1). The three mRNA species, *BOV-1a*, *1b*, and *1c*, could also be detected in mammalian cell lines to varying degrees (data not shown).

Cloning of *BOV-1* cDNA

To aid in the characterization of *BOV-1*, we isolated 30 cDNA clones from a human fetal brain library using a random-primed 700-bp cDNA probe and sequenced 14 of them to determine the nucleotide sequence and predicted amino acid sequence of *BOV-1a*, *1b*, and *1c*. Our results indicate that *BOV-1a* (the abundant ~1-kb transcript) represents the entire coding region identified through the yeast two-hybrid screen and that *BOV-1b* results from the use of an alternative polyadenylation signal (Accession No. AF231511). Based on initial sequence analysis, it appears that *BOV-1c* may

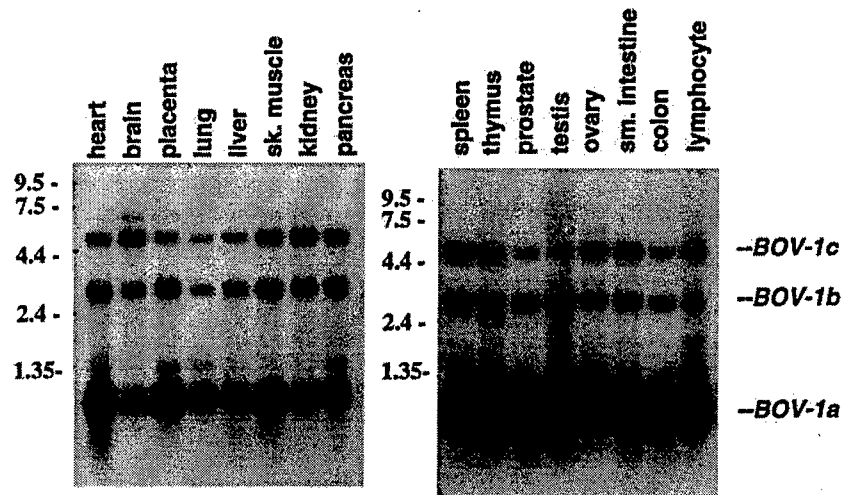


FIG. 1. Tissue expression pattern of BOV-1 mRNA. Blots containing 5 μ g of poly(A)⁺ selected mRNA from each of the indicated human tissues were hybridized with an ~800-bp BOV-1a/b cDNA clone. Size standards are in kilobases.

be the product of alternative exon splicing and the use of the alternative polyadenylation signal (Accession No. AF231512).

The cDNA encoding *BOV-1a* consists of 700 bp including 20 bp of 5'-untranslated region (UTR), an AUG leading into an open reading frame (ORF) of 173 amino acids, and a 3'-UTR of 161 bp. The cDNA for *BOV-1b* differs from *BOV-1a* in that the 3'-UTR is substantially longer, 2236 bp versus 161 bp, respectively. The cDNA encoding *BOV-1c* consists of 5786 bp including 3074 bp of 5'-UTR, an ORF of 158 amino acids, and a 3'-UTR of 2238 bp. At the nucleotide level, *BOV-1b* and *BOV-1c*

cDNAs are identical except for the 5'-UTRs (compare sequences for Accession Nos. AF231511 and AF231512).

The predicted protein encoded by *BOV-1c* differs from *BOV-1a/b* in that the protein is predicted to be 15 amino acids shorter (see Fig. 2; translation of protein encoded by *BOV-1c* is predicted to start at the second methionine, but includes an additional amino acid at codon 27); otherwise the proteins are identical. The predicted molecular masses for the BOV-1a/b and BOV-1c proteins are 20 and 18 kDa, and their isoelectric points occur at pH 5.78 and pH 7.62, respectively.

A

```

1   MADVLDLHEAGGEDFAMDEEDGDESIHKLKEKAKKRKGRGFGSEGSRRMR
51  EDYDSVEQDGDPEPGPQRSVEGWILFVTGVHEEATEEDIHDKFAEYGEIKN
101 IHLNLDRRRTGYLKGTYLVEYETYKEAQAAMEGLNGQDLMGQPISVDWCFV
151  RGPPKGGKRRGRRRSRSPDRRRR
  
```

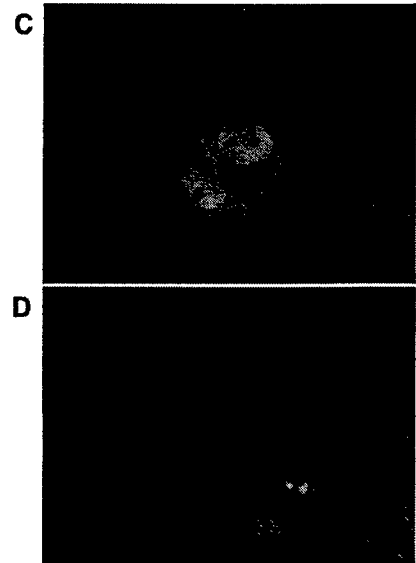
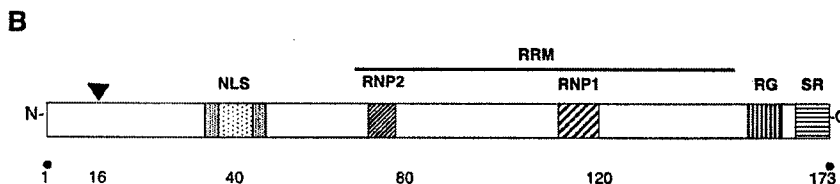


FIG. 2. RBM8A structural (A and B). (A) The predicted primary sequence of the protein encoded by *BOV-1a/b* cDNA is shown, and the RNA-recognition motif (RRM) is underlined. The arrow indicates the methionine where protein encoded by *BOV-1c* is predicted to start. (B) A schematic diagram highlighting structural domains of *BOV-1a/b* is presented in the lower panel. The RRM and both RNP1 (residues 113–120) and RNP2 (residues 74–79) consensus sequences are indicated. A putative bipartite nuclear localization signal (NLS) is predicted to be present at the N-terminus of *BOV-1a/b*. The diagram also shows the arginine/glycine-rich (RG) box (residues 151–162) and a serine/arginine-rich (SR) domain (residues 163–173) identified in the C-terminus of *BOV-1a/b*. The protein encoded by *BOV-1c* is predicted to be either 15 or 16 amino acids shorter than *BOV-1a/b*. The arrow indicates the methionine where protein encoded by *RBM8B* is predicted to start. (C and D) Immunolocalization of *BOV-1a/b* in COS-1 cells. COS-1 cells were transiently transfected with pcDNA3/T7-*BOV-1*. Forty-eight hours after transfection, cells were fixed and stained with a mouse monoclonal anti-T7 tag antibody (Novagen), followed by staining with FITC-conjugated anti-mouse antibody (Jackson Immunochemicals) (C) and counterstaining with DAPI (Sigma) (D).

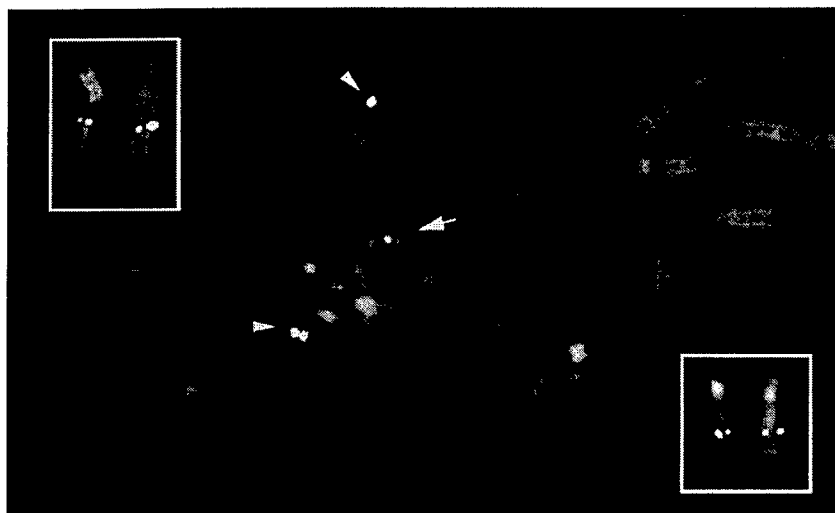


FIG. 3. Chromosomal localization of *BOV-1a/b* and *BOV-1c* by FISH. Partial metaphase spread showing specific hybridization signals at chromosome 5q13–q14 (arrowheads). Arrow indicates specific hybridization signals at chromosome 14q22–q23. (Left inset) *BOV-1c*-specific hybridization at 5q13–q14 to individual chromosomes from other metaphases. (Right inset) *BOV-1c*-specific hybridization at 14q22–q23 to individual chromosomes from other metaphases.

Comparison of 12 of the 14 *BOV-1* cDNA clones identified a sequence variant involving codon 43 (GAA) of *BOV-1a/b* (or codon 27 of *BOV-1c*). In 66.7% (8/12) of the clones, this additional codon was present. These transcripts would be predicted to encode a protein of 174 amino acids (*BOV-1a/b*). In comparison, this polymorphism was not detected in any of the *BOV-1c* cDNA clones.

Chromosomal Mapping of *BOV-1* cDNA

We mapped the chromosomal location of *BOV-1* by FISH using the 5.8-kb cDNA probe, corresponding to the *BOV-1c* transcript. Of the 51 signals observed, 24 (47%) hybridized specifically at 5q13–q14 in 19 of the 20 metaphase spreads scored. In 11 of 20 (55%) metaphase spreads, signals were also detected on chromosome 14, specifically at 14q22–q23. Sixteen (31%) of the 51 signals observed mapped to 14q22–q23, indicating that two closely related genes may exist at these two sites (Fig. 3). Finally, we should note that six metaphases showed weak hybridization (single signals) in the 1qh region, possibly suggesting the presence of a pseudogene (Zhao *et al.*, 2000).

Nucleotide Sequence Analysis of *BOV-1* cDNAs

Comparison analysis of *BOV-1a/b* using the BLASTN program demonstrated 99% nucleotide homology (score = 898; *E* value 0.0) to a human EST from a colon carcinoma (HCC) cell line cDNA library (Accession No. AA30779). Comparison of the 5'-UTR of the *BOV-1c* cDNA with the GenBank databases demonstrated 99.4% nucleotide homology over 314 nt (in the reverse orientation) to human integrin-binding protein Del-1 (Del1) mRNA (1712–1399 nt of Del1 and 2668–2981 nt of *BOV-1c*) (Accession Nos. U70312 and AF231512). The 3'-UTR for both *BOV-1b* and *BOV-1c* also shared nucleotide identity with a human cDNA

(Accession No. AL049219) (score = 496; *E* = 1.0×10^{-137}) identified in fetal brain.

Based on comparison of the cDNA sequence for *BOV-1a/b* and available genomic sequence (Accession No. AF231511), the *BOV-1a/b* gene appears to lack introns, whereas *BOV-1c* contains at least one intron (Accession No. AF231512; and data not shown). The genomic sequencing matching the *BOV-1a/b* cDNA sequence was placed on chromosome 14, further indicating that *BOV-1a/b* (Accession No. AF231511) and *BOV-1c* (Accession No. AF231512) are distinct genes that reside on different chromosomes. Based on our mapping and sequence data, approved names for *BOV-1a/b* and *BOV-1c* have recently been assigned by the Human Gene Nomenclature Committee (<http://www.gene.ucl.ac.uk/nomenclature>) and are *RBM8A* and *RBM8B*, respectively.

Protein Sequence Analysis and Subcellular Localization of *BOV-1/RBM8*

The deduced primary amino acid sequence of *RBM8A* and *RBM8B* indicates the presence of one copy of an RNA-binding domain (RBD) in the central region (amino acid residues 71–148 or 55–132, respectively), also known as an RRM (Figs. 2A and 2B). This RRM contains one set of the two consensus nucleic acid-binding motifs, RNP-1 (aa 113–120 for *RBM8A* and aa 97–104 for *RBM8B*) and RNP-2 (aa 74–79 for *RBM8A* and aa 58–63 for *RBM8B*), which are characteristic of the heterogeneous nuclear ribonucleoprotein (hnRNP) family of proteins. The *RBM8A* and *RBM8B* amino acid sequence also contains a putative bipartite nuclear localization signal (Robbins *et al.*, 1991) at the N-terminus (aa 33–51 for *RBM8A* and aa 17–35 for *RBM8B*) and a stretch rich in glycine residues (not shown). Interestingly, the C-terminus of the *RBM8A* and *RBM8B* proteins (residues 151–173 and 136–158,

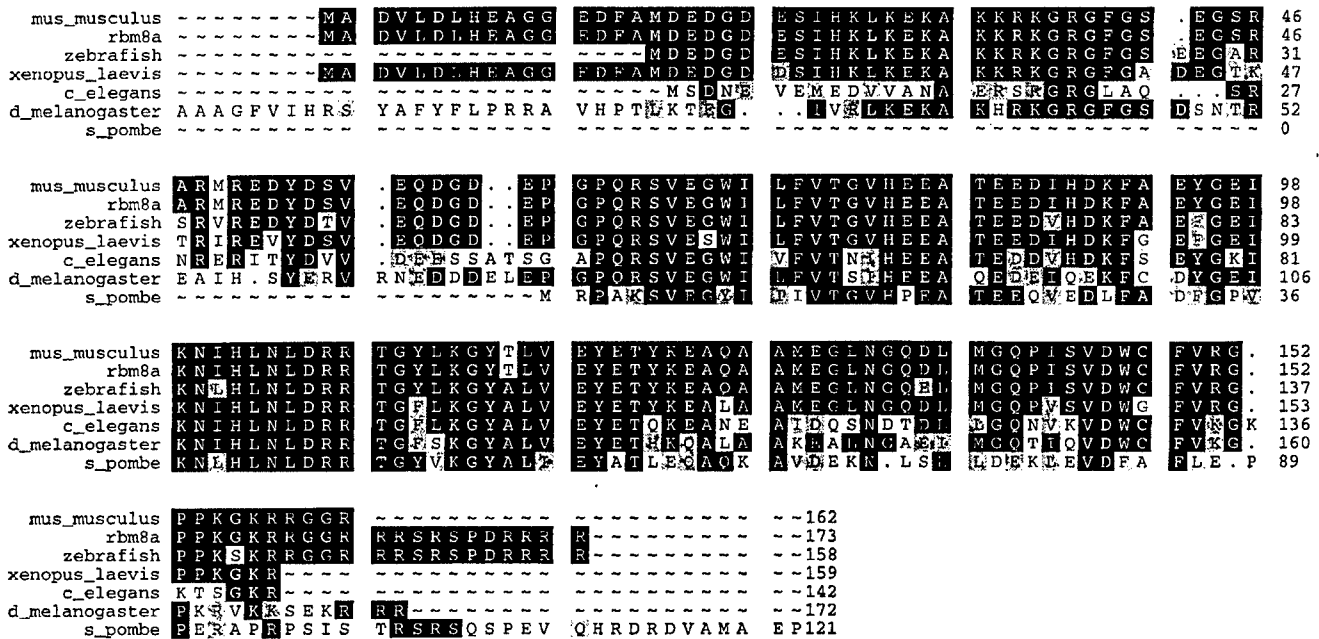


FIG. 4. RBM8A protein sequence alignment with hypothetical proteins identified in *M. musculus* (100% identity), zebrafish (93.7%/98.7%), *X. laevis* (91.2%/95.6%), *D. melanogaster* (63%/76%), *C. elegans* (60.5%/75.3%), and *S. pombe* (48.8%/64.5%), using the UWGCG PileUp program. Percentages of identity/similarity relative to RBM8A are indicated in parentheses. GenBank Accession Nos. AL0022712, AI943400, AW200013, AC006074, CAA83626, and AL021813, respectively. White letters in black boxes indicate identical residues. Shading indicates conserved residues.

respectively) shows significant homology to the serine/arginine-rich (SR) domain of the splicing factor SC35 (Fu and Maniatis, 1992), as well as a domain rich in glycine and arginine (residues 151–162 for RBM8A and residues 135–146 for RBM8B), reminiscent of the RG box described in human nucleolin (Nigg, 1997). In addition, we analyzed the intracellular distribution of RBM8A by immunofluorescence analysis. Immunolocalization experiments using COS-1 cells transfected with a T7-tagged RBM8A expression vector indicate that full-length RBM8A is localized mostly in the cell nucleus and is finely diffused throughout the cytoplasm (Figs. 2C and 2D).

RBM8 proteins appear to be highly conserved evolutionarily. Sequence analysis of the predicted RBM8A and RBM8B coding sequence using both FastA and TBLASTN algorithms revealed that *Mus musculus*, zebrafish, *Xenopus laevis*, *Drosophila melanogaster*, *Caenorhabditis elegans*, and *Schizosaccharomyces pombe* encode hypothetical proteins remarkably similar to RBM8A and RBM8B at the amino acid level (Fig. 4; and data not shown). The percentages of amino acid identity and similarity relative to RBM8A are indicated in the legend to Fig. 4. *M. musculus* hypothetical protein (AL0022712) is 11 amino acids shorter than RBM8A and 100% identical to RBM8A, while zebrafish and *X. laevis*, for example, encode hypothetical proteins with 93.7 and 91.2% identity to RBM8A, respectively. The sequence similarity is spread throughout the entire amino acid sequence and is most pronounced in the RRM region, extending from amino acid residues 70 to 150 of the RBM8A sequence.

RBM8 Protein Model

To gain more information on the RNA-binding properties of RBM8A, we built a three-dimensional model of the RRM domain of RBM8A. Sequence analysis using PSI-BLAST (see Materials and Methods) indicated that there were 18 possible template structures in six families in the Protein Data Bank that could be used to build the RRM domain of RBM8. We chose two of these, the sex-lethal protein from *Drosophila* (Sxl, PDB entry 1b7f) (Handa *et al.*, 1999) and the poly(A)-binding protein (PABP, PDB entry 1cvj) (Deo *et al.*, 1999), since both of these sequences could be aligned with RBM8A without insertions or deletions. The resulting sequence alignment is shown in Fig. 5A. In addition, both structures contained RNA so that interactions between RBM8A and RNA could also be modeled.

We built models of RBM8A from both of these structures using the side-chain conformation prediction program SCWRL (Bower *et al.*, 1997). A superposition of the backbones of these two models is shown in Fig. 5B. The root-mean-square (RMS) deviation of the backbones is 0.82 Å. The sequence identity between Sxl and PABP is 31%, while the sequence identity between RBM8 and Sxl is 24% and that between RBM8A and PABP is 27%. Since these sequence identities are similar, we expect that the model of the RRM of RBM8A is quite accurate, with an RMS comparable to the Sxl-PABP RMS of 0.82 Å.

In Fig. 5C, we show the model of RBM8A based on Sxl. Residues that bind to RNA are indicated in Fig. 5C. These include F75, T77, H102, R107, F111, Y115, L117, and P142. Some of these residues are identical or

A

BOV-1	67	RSVEGWILFVTGVHEEATEEDIHDKFAEYGEIKNIHLNLDRRTCGLKGYTLVEYETYKEA
PABP	6	PSYPMASLVYGDLPDVTGANLYEKFSAPGPILEIRVCRDMI TRRSLGYAYVNFQQPADA
SXL	1	--ASNTNLIYNYLPQDMTDRRLYALFRAIGPINTCRIMRDYKTCYSYGYAEVDETSSEMD
BOV-1	127	QAAMEGLNGQDLMGQPIISVDWC
PABP	66	ERALDTNDFVTKGKPVRIWWS
SXL	59	QRAIKVLNGITVYRNKRLKVSVA

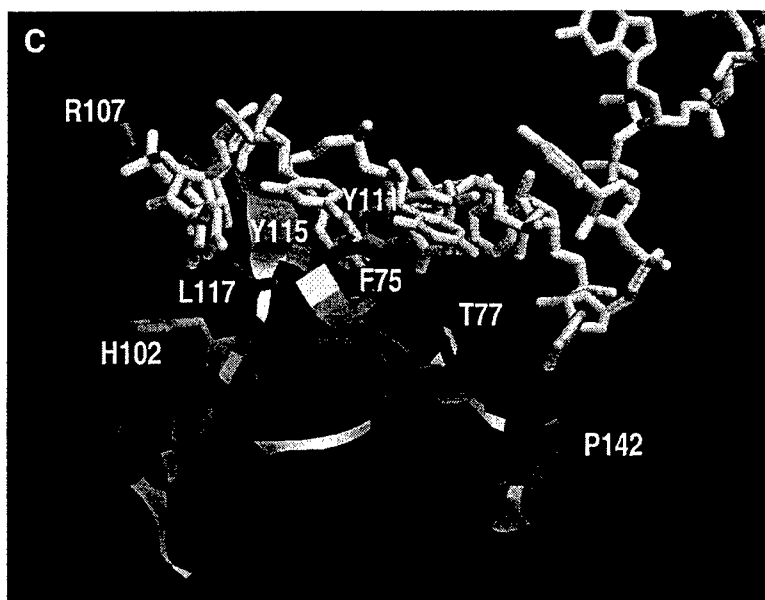
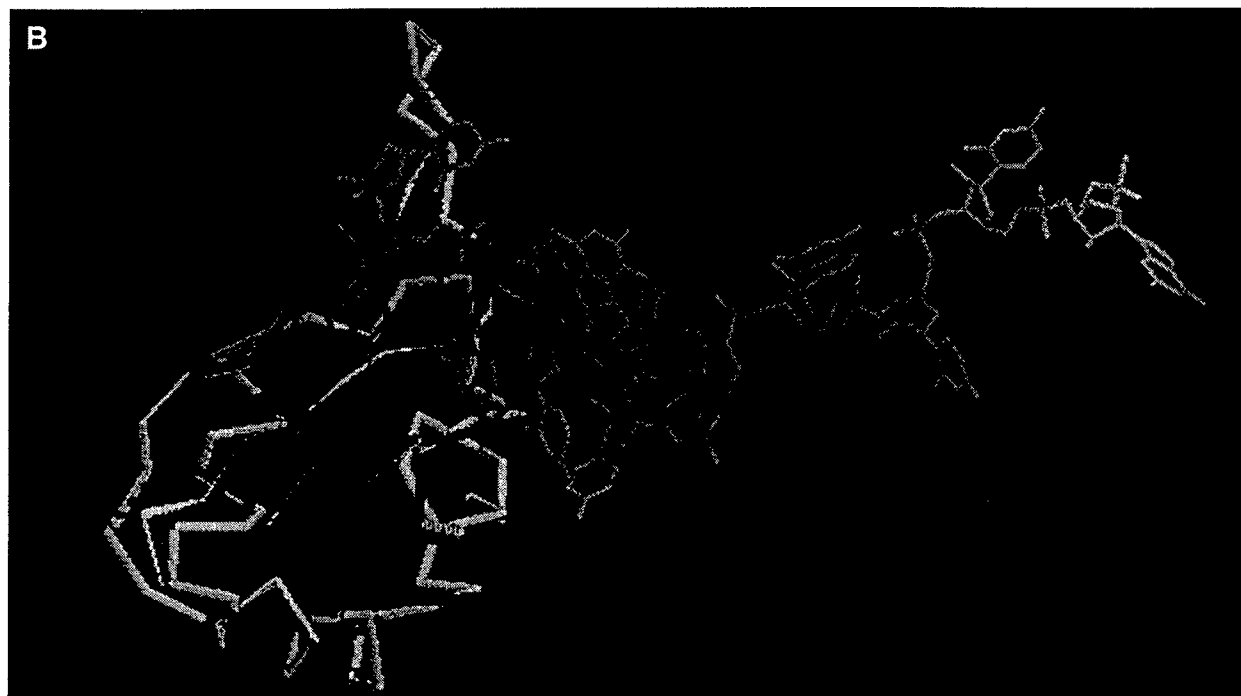


FIG. 5. Homology modeling of the RNA recognition motif domain of RBM8A. (A) Sequence alignment of RBM8A RNA-binding domain with PABP and Sxl from PDB entries 1CVJ and 1B7F, respectively. (B) Superposition of models of BOV-1/RBM8A based on the structures of Sxl (protein in purple and RNA in green) and PABP (protein in yellow and RNA in red). The root-mean-square deviation of the protein backbone C α coordinates is 0.82 Å. (C) Model of RBM8A based on Sxl in a complex with single-stranded RNA with sequence GUUUUUUUU. Residues that contact the RNA in either the Sxl or the PABP models are indicated.

similar in Sxl and/or PABP, which may indicate similar interactions between these side chains and RNA. For example, RBM8A F75 is a tyrosine in PABP and forms an aromatic ring-stacking interaction with an

adenine in the RNA. In Sxl this residue is an isoleucine, making a hydrophobic interaction with a uracil base. RBM8A Y115 is a tyrosine in both Sxl and PABP, making a ring-stacking interaction with an adenine in

PABP and a hydrogen bond to a uracil ring carbonyl in Sxl. RBM8A Y111 is also a tyrosine in Sxl, which makes a hydrogen bond with a uracil carbonyl in Sxl. While it is not possible to predict the RNA-binding sequence for RBM8A from the model, it is clear that many of the residues typical of RNA-protein interactions in this family of proteins are contained in the RNA-binding site of RBM8A. Since many of these interactions make contact with RNA bases, mutations of these residues are likely to alter the binding affinity of RBM8A for its natural RNA ligand.

DISCUSSION

Understanding the biological function of the ovarian tumor suppressor OVCA1 may provide new insights into how breast and ovarian cancers develop. To discover important clues into the function of OVCA1, we used a yeast two-hybrid interaction trap method to identify proteins that interact with OVCA1. We identified several candidates (Salicioni *et al.*, unpublished results), including a novel protein that contains a highly conserved RNA-binding motif, initially referred to as BOV-1. In this paper, we demonstrate that *BOV-1a/b* (renamed *RBM8A*) maps to chromosome 14q22-q23 and that the closely related novel gene *BOV-1c* (renamed *RBM8B*) maps to chromosome 5q13-q14. Furthermore, the protein encoded by *RBM8B* is identical to RBM8A except that it is 16 amino acids shorter at the N-terminus and thus appears to be a new member of a highly conserved RBM protein family. Since both RNA transcripts are ubiquitously expressed in human tissues and are predicted to encode a protein, it is unlikely that either gene that we identified is a pseudogene. Two sequences related to RBM8A, (Accession Nos. AF127761 and AF161463) were released in the GenBank database while this article was in preparation. Our results are further supported by the knowledge that genes coding for RNA-binding proteins have diversified by duplication of genes and intragenic domains (Bandzulis *et al.*, 1989; Birney *et al.*, 1993). A three-dimensional model of the RRM domain of RBM8A/B indicates that these RBM8 sequences will fold properly into an RNA-binding domain, forming a hydrophobic core between a β -sheet and two α -helices.

In eukaryotic cells, different classes of RNA are synthesized in the nucleus, including mRNA, ribosomal RNA, transfer RNA (tRNA), and small nuclear RNA, and must be actively exported to the cytoplasm. After the transcription of tRNA genes, the resulting RNAs undergo numerous changes before a mature translation-competent species is produced. These changes have been found to include terminal processing, intron splicing, editing, deamination, and addition on the nucleotide level (see review by Ibba and Soll (1999)), many of which are mediated by RBPs and by small RNAs as stable RNP complexes. The most notable feature of the RBPs is the presence of one or more copies of the RRM, the most widely found and best-characterized RNA-binding motif (Birney *et al.*, 1993; Burd and

Dreyfuss, 1994a). We have determined that both RBM8A and RBM8B have only one copy of this RRM with one set of the two consensus nucleic acid-binding motifs, RNP-1 and RNP-2, which are characteristic of the hnRNP family of proteins.

The RRM is the only RNA-binding motif for which detailed structural information is available. The structures of several RRM proteins have been determined, and all consist of the same basic protein fold. These include the NH₂-terminal RBD of U1 snRNP A (Tang and Rosbash, 1996), the U1 domain of hnRNP A1 (Xu *et al.*, 1997), the single RBD of hnRNP C (Gorlach *et al.*, 1994), the tandem RRMs of the sex-lethal protein (SXL) (Crowder *et al.*, 1999), and the poly(A)-binding protein (PABP) (Deo *et al.*, 1999). On one hand, SXL governs sexual differentiation and dosage compensation in *D. melanogaster* by binding specific RNA transcripts, while it is known that the mRNA poly(A) tail is an important contributor to both translation initiation and mRNA stabilization/degradation (Sachs and Wahle, 1993). We have built models of RBM8A based on the Sxl and PABP structures. These models identify residues on the surface of the sheet that are likely to bind single-stranded RNA and share identity in other RNA-binding domains with the same protein fold. Since many of these interactions make contact with RNA bases, mutations of these residues are likely to alter the binding affinity of RBM8A and RBM8B for its natural RNA ligand.

In contrast to the RRM, much less is known about the structure and function of the RS and RG motifs or other auxiliary domains found in the RBPs. In considering the possible essential function of RBM8 proteins, sequence analysis of RBM8A and RBM8B allowed us to predict the presence of clusters of arginine/serine-rich and arginine/glycine-rich regions. Furthermore, RBM8A and RBM8B have significant homology to the RG and SR domains described for other human members of the RRM superfamily, i.e., nucleolin, the EWS proto-oncogene, and splicing factors, with important roles in mRNA biogenesis and rRNA synthesis and in the Ewing sarcoma translocation (Burd and Dreyfuss, 1994b; Delattre *et al.*, 1992).

An increasing number of proteins appear to be multifunctional, participating in transcriptional and post-transcriptional events. The tumor suppressor WT1, initially considered to be a typical transcription factor (Hastie, 1994), may also be involved in splicing (Lamond, 1995). Interestingly, the N-terminus of WT1 may also contain a cryptic RRM, discovered through molecular modeling (Kennedy *et al.*, 1996). Furthermore, recent evidence shows that WT1 colocalizes and is physically associated with splice factors and suggests that deregulation of splicing may be a crucial factor in the tumorigenesis of the genitourinary system (Davies *et al.*, 1999). Aberrant splicing has been linked to the early and intermediate stages of mammary tumor formation (Stickeler *et al.*, 1999), and a deregulated expression balance between hnRNPs and SR factors has

been reported for human colon tumor formation and metastasis (Ghigna *et al.*, 1998).

The importance of our findings is reflected in the recent discoveries that several human and other vertebrate genetic disorders (Buckanovich and Darnell, 1997; Dropcho and King, 1994; Nishiyama *et al.*, 1998) are caused by aberrant expression of RNA-binding proteins. Furthermore, recent genetic linkage studies suggest that both 5q13-q14 and 14q22-q23 loci may be implicated in the etiology of human cancers and other diseases (Black *et al.*, 1999; Knuutila *et al.*, 1999; Zech *et al.*, 1999). The conservation of RBM8A and RBM8B sequences through such an evolutionarily divergent group of organisms, from yeast to mice and human, points toward an important function for the RBM8 family of proteins. Our work also provides a starting point for further structural, biochemical, and genetic studies of the RBM8 protein family and the biological relevance of its interaction with OVCA1 in the context of normal and abnormal cell growth.

ACKNOWLEDGMENTS

We thank Dr. Erica Golemis for providing us with the human fetal brain cDNA expression library and Dr. Dominique Broccoli for her advice on the immunofluorescence analysis. This work was supported in part by National Institutes of Health Grant RO1 CA-70328 (to A.K.G.), by United States Army Medical Research Grant DAMD17-96-1-6088 (A.K.G.), by a grant from the American Cancer Society (R.L.D.), and by an appropriation from the Commonwealth of Pennsylvania.

REFERENCES

- Altschul, S. F., and Koonin, E. V. (1998). Iterated profile searches with PSI-BLAST—A tool for discovery in protein databases. *Trends Biochem. Sci.* **23**: 444–447.
- Bandziulis, R. J., Swanson, M. S., and Dreyfuss, G. (1989). RNA-binding proteins as developmental regulators. *Genes Dev.* **3**: 431–437.
- Bell, D. W., Taguchi, T., Jenkins, N. A., Gilbert, D. J., Copeland, N. G., Gilks, C. B., Zweidler-McKay, P., Grimes, H. L., Tschlis, P. N., and Testa, J. R. (1995). Chromosomal localization of a gene, GF1, encoding a novel zinc finger protein reveals a new syntenic region between man and rodents. *Cytogenet. Cell Genet.* **70**: 263–267.
- Berman, H. M., Westbrook, J., Feng, Z., Gilliland, G., Bhat, T. N., Weissig, H., Shindyalov, I. N., and Bourne, P. E. (2000). The Protein Data Bank. *Nucleic Acids Res.* **28**: 235–242.
- Birney, E., Kumar, S., and Krainer, A. R. (1993). Analysis of the RNA-recognition motif and RS and RGG domains: Conservation in metazoan pre-mRNA splicing factors. *Nucleic Acids Res.* **21**: 5803–5816.
- Black, G. C., Perveen, R., Wiszniewski, W., Dodd, C. L., Donnai, D., and McLeod, D. (1999). A novel hereditary developmental vitreo-retinopathy with multiple ocular abnormalities localizing to a 5-cM region of chromosome 5q13–q14. *Ophthalmology* **106**: 2074–2081.
- Bower, M. J., Cohen, F. E., and Dunbrack, R. L., Jr. (1997). Prediction of protein side-chain rotamers from a backbone-dependent rotamer library: A new homology modeling tool. *J. Mol. Biol.* **267**: 1268–1282.
- Bruening, W., Prowse, A. H., Schultz, D. C., Holgado-Madruga, M., Wong, A., and Godwin, A. K. (1999). Expression of OVCA1, a candidate tumor suppressor, is reduced in tumors and inhibits growth of ovarian cancer cells. *Cancer Res.* **59**: 4973–4983.
- Buckanovich, R. J., and Darnell, R. B. (1997). The neuronal RNA binding protein Nova-1 recognizes specific RNA targets in vitro and in vivo. *Mol. Cell. Biol.* **17**: 3194–3201.
- Burd, C. G., and Dreyfuss, G. (1994a). Conserved structures and diversity of functions of RNA-binding proteins. *Science* **265**: 615–621.
- Burd, C. G., and Dreyfuss, G. (1994b). RNA binding specificity of hnRNP A1: Significance of hnRNP A1 high-affinity binding sites in pre-mRNA splicing. *EMBO J.* **13**: 1197–1204.
- Crowder, S. M., Kanaar, R., Rio, D. C., and Alber, T. (1999). Absence of interdomain contacts in the crystal structure of the RNA recognition motifs of Sex-lethal. *Proc. Natl. Acad. Sci. USA* **96**: 4892–4897.
- Davies, R., Moore, A., Schedl, A., Bratt, E., Miyahawa, K., Ladomery, M., Miles, C., Menke, A., van Heyningen, V., and Hastie, N. (1999). Multiple roles for the Wilms' tumor suppressor, WT1. *Cancer Res.* **59**: 1747s–1750s; discussion 1751s.
- Delattre, O., Zucman, J., Plougastel, B., Desmaze, C., Melot, T., Peter, M., Kovar, H., Joubert, I., de Jong, P., Rouleau, G., *et al.* (1992). Gene fusion with an ETS DNA-binding domain caused by chromosome translocation in human tumours. *Nature* **359**: 162–165.
- Deo, R. C., Bonanno, J. B., Sonenberg, N., and Burley, S. K. (1999). Recognition of polyadenylate RNA by the poly(A)-binding protein. *Cell* **98**: 835–845.
- Dropcho, E., and King, P. (1994). Autoantibodies against the Hel-N1 RNA-binding protein among patients with lung carcinoma: An association with type I anti-neuronal nuclear antibodies. *Ann. Neurol.* **36**: 200–205.
- Dunbrack, R. L., Jr. (1999). Comparative modeling of CASP3 targets using PSI-BLAST and SCWRL. *Proteins, Suppl.* **3**: 81–87.
- Dunbrack, R. L., Jr., and Cohen, F. E. (1997). Bayesian statistical analysis of protein side-chain rotamer preferences. *Protein Sci.* **6**: 1661–1681.
- Fu, X. D., and Maniatis, T. (1992). Isolation of a complementary DNA that encodes the mammalian splicing factor SC35. *Science* **256**: 535–538.
- Ghigna, C., Moroni, M., Porta, C., Riva, S., and Biamonti, G. (1998). Altered expression of heterogenous nuclear ribonucleoproteins and SR factors in human colon adenocarcinomas. *Cancer Res.* **58**: 5818–5824.
- Golemis, E., and Serebriiskii, I. (1998). Two-hybrid system/interaction trap. In "Cells: A Laboratory Manual" (D. Spector, R. Goldman, and L. Leinwand, Eds.), pp. 69.61–69.40, Cold Spring Harbor Laboratory Press, Cold Spring Harbor, NY.
- Gorlach, M., Burd, C. G., and Dreyfuss, G. (1994). The determinants of RNA-binding specificity of the heterogeneous nuclear ribonucleoprotein C proteins. *J. Biol. Chem.* **269**: 23074–23078.
- Handa, N., Nureki, O., Kurimoto, K., Kim, I., Sakamoto, H., Shimura, Y., Muto, Y., and Yokoyama, S. (1999). Structural basis for recognition of the tra mRNA precursor by the Sex-lethal protein. *Nature* **398**: 579–585.
- Hastie, N. D. (1994). The genetics of Wilms' tumor—A case of disrupted development. *Annu. Rev. Genet.* **28**: 523–558.
- Ibba, M., and Soll, D. (1999). Quality control mechanisms during translation. *Science* **286**: 1893–1897.
- Kennedy, D., Ramsdale, T., Mattick, J., and Little, M. (1996). An RNA recognition motif in Wilms' tumour protein (WT1) revealed by structural modelling. *Nat. Genet.* **12**: 329–331.
- Knuutila, S., Aalto, Y., Autio, K., Bjorkqvist, A. M., El-Rifai, W., Hemmer, S., Huhta, T., Kettunen, E., Kiuru-Kuhlefelt, S., Larramendy, M. L., Lushnikova, T., Monni, O., Pere, H., Tapper, J., Tarkkanen, M., Varis, A., Wasenius, V. M., Wolf, M., and Zhu, Y. (1999). DNA copy number losses in human neoplasms. *Am. J. Pathol.* **155**: 683–694.

- Ladomery, M. (1997). Multifunctional proteins suggest connections between transcriptional and post-transcriptional processes. *BioEssays* **19**: 903-909.
- Lamond, A. I. (1995). RNA processing. Wilms' tumour—The splicing connection? *Curr. Biol.* **5**: 862-865.
- Nigg, E. (1997). Nucleocytoplasmic transport: Signals, mechanisms and regulation. *Nature* **386**: 779.
- Nishiyama, H., Danno, S., Kaneko, Y., Itih, K., Yokoi, H., Fukumoto, M., Okuno, M., Millan, J., Matsuda, T., Yoshida, O., and Fujita, J. (1998). Decreased expression of cold-inducible RNA-binding protein (CIRP) in male germ cells at elevated temperature. *Am. J. Pathol.* **152**: 289-296.
- Robbins, J., Dilworth, S. M., Laskey, R. A., and Dingwall, C. (1991). Two interdependent basic domains in nucleoplasmin nuclear targeting sequence: Identification of a class of bipartite nuclear targeting sequence. *Cell* **64**: 615-623.
- Sachs, A., and Wahle, E. (1993). Poly(A) tails metabolism and function in eucaryotes. *J. Biol. Chem.* **268**: 22955-22958.
- Schultz, D. C., Vanderveer, L., Berman, D. B., Hamilton, T. C., Wong, A. J., and Godwin, A. K. (1996). Identification of two candidate tumor suppressor genes on chromosome 17p13.3. *Cancer Res.* **56**: 1997-2002.
- St Johnston, D. (1995). The intracellular localization of messenger RNAs. *Cell* **81**: 161-170.
- Stickeler, E., Kittrell, F., Medina, D., and Berget, S. M. (1999). Stage-specific changes in SR splicing factors and alternative splicing in mammary tumorigenesis. *Oncogene* **18**: 3574-3582.
- Tang, J., and Rosbash, M. (1996). Characterization of yeast U1 snRNP A protein: Identification of the N-terminal RNA binding domain site and evidence that the C-terminal RBD functions in splicing. *RNA* **2**: 1058-1070.
- Xu, R., Jokhan, L., Cheng, X., Mayeda, A., and Krainer, A. (1997). Crystal structure of human UP1, the domain of hnRNP A1 that contains two RNA-recognition motifs. *Structure* **5**: 559-570.
- Zech, J. C., Morle, L., Vincent, P., Alloisio, N., Bozon, M., Gonnet, C., Milazzo, S., Grange, J. D., Trepsat, C., Godet, J., and Plauchu, H. (1999). Wagner vitreoretinal degeneration with genetic linkage refinement on chromosome 5q13-q14. *Graefes Arch. Clin. Exp. Ophthalmol.* **237**: 387-393.
- Zhao, X-F., Nowak, N. J., Shows, T. B., and Aplan, P. D. (2000). MAGOH interacts with a novel RNA-binding protein. *Genomics* **63**: 145-148.

OVCA2, not OVCA1/DPH2L is down-regulated during retinoid-induced differentiation and apoptosis

Amanda H. Prowse ^{(1) §}, Lisa Vanderveer⁽¹⁾, Simon W.F. Milling⁽³⁾, Roland L. Dunbrack, Jr⁽⁴⁾
Xiang-Xi Xu ⁽¹⁾ and Andrew K. Godwin ^(1,2)

⁽¹⁾ Department of Medical Oncology, Fox Chase Cancer Center

⁽²⁾ Human Genetics Program, Fox Chase Cancer Center

⁽³⁾ Department of Cell and Developmental Biology, Fox Chase Cancer Center

⁽⁴⁾ Basic Science Division, Fox Chase Cancer Center

^(§) To whom correspondence should be addressed: Amanda H. Prowse, Department of Medical Oncology, Room w322, Fox Chase Cancer Center, 7701 Burholme Ave, Philadelphia, PA 19111.

E-mail: AH_Prowse@fccc.edu

Telephone: (215) 728-2756. Fax: (215) 728-2741

Keywords: OVCA1, OVCA2, All-trans Retinoic Acid, RA, N-(4-hydroxyphenyl)retinamide, 4HPR.

Journal Category: Cancer Cell Biology.

ABSTRACT

Retinoids, the natural and synthetic derivatives of Vitamin A have been shown to regulate the growth and differentiation of a wide variety of cell types and consequently have enormous potential as chemotherapeutic agents. We have previously identified two genes, referred to as *OVCA1* and *OVCA2*, which are located in a small region showing a high frequency of allelic loss in breast and ovarian tumors. We have analyzed the expression of *OVCA1* and *OVCA2* in cells in response to treatment with All-trans Retinoic Acid (RA) and N-(4-hydroxyphenyl)retinamide (4HPR), or under conditions of low serum and confluence in order to further determine the roles of *OVCA1* and *OVCA2* in cell growth, apoptosis and differentiation. We show that *OVCA2* is ubiquitously expressed and that it is downregulated in the lung cancer cell line Calu-6 and the promyelocytic leukemia cell line HL-60 following treatment with RA and 4HPR. In contrast, expression of the candidate tumor suppressor, *OVCA1*, is unaffected by these treatments. Furthermore, we demonstrate that *OVCA2* is evolutionarily conserved and shows regional homology with dihydrofolate reductases (DHFRs), specifically with hydrolase folds found in alpha-beta hydrolases. *OVCA2* may therefore have an important role in growth regulation and its downregulation may be involved in the anti-proliferative effects mediated by RA and 4HPR.

INTRODUCTION

Retinoids, the natural and synthetic derivatives of Vitamin A have been shown to regulate the growth and differentiation of a wide variety of cell types and consequently have enormous potential as chemotherapeutic agents (Evans et al., 1999; Hansen et al., 2000). The diverse effects of retinoids are mediated by binding to at least six retinoid receptors which fall into two subfamilies: retinoic acid receptors (RARs) α , β and γ , and the retinoid X receptors (RXRs) α , β and γ (Chambon et al., 1994). The RARs and RXRs act as transcription factors, binding as homo- and heterodimers to retinoid response elements in the promoter regions of target genes and thus enhancing or

repressing transcription. In addition RARs and RXRs can inhibit the expression of AP1-dependent genes by antagonizing AP1 activity (DiSepio et al., 1999; Nagpal et al., 1995; Salbert et al., 1993). However, many of the downstream targets that lead to retinoid induced growth arrest, differentiation and/or apoptosis remain to be identified. In addition, synthetic retinoids, such as 4HPR, which have been developed as chemoprevention agents with an acceptable toxicity profile, may well differ in their mechanism of action (Clifford et al., 1999; Kitareewan et al., 1999; Sun et al., 1999).

We, and others have previously defined a minimum region of allelic loss (MRAL) on chromosome 17p13.3 in genomic DNA from ovarian tumors (Phillips et al., 1996; Schultz et al., 1996). Positional cloning and sequencing techniques revealed at least two candidate tumor suppressor genes in the ~ 20kb MRAL, referred to as *OVCA1* and *OVCA2*. The *OVCA1* and *OVCA2* genes overlap one another in the MRAL, and have one exon in common (Schultz et al., 1996). Since translation of *OVCA1* does not proceed into the shared exon (exon 13 in *OVCA1* and exon 2 in *OVCA2*), the genes encode for completely distinct *OVCA1* and *OVCA2* proteins. We have previously shown that *OVCA1* is a strong candidate for a tumor suppressor gene: it is downregulated in a proportion of breast and ovarian tumors and overexpression of *OVCA1* reproducibly inhibits colony formation in a variety of tumor cell lines (Bruening et al., 1999). However, recent studies have suggested that *OVCA1* may be downregulated following differentiation or growth arrest induced by RA, contrary to a role as a tumor suppressor (Liu et al., 2000). Therefore, we have analyzed both *OVCA1* and *OVCA2* protein levels in a variety of cell lines treated with All-trans Retinoic Acid (RA) and N-(4-hydroxyphenyl)retinamide (4HPR), or under conditions of low serum and confluence in order to further determine the roles of *OVCA1* and *OVCA2* in cell growth, apoptosis and differentiation. We show that *OVCA2* is downregulated in the lung cancer cell line Calu-6 and the promyelocytic leukemia cell line HL-60 treated with RA and 4HPR, but that *OVCA1* is unaffected. *OVCA2* may therefore have an important role in growth regulation and its downregulation may be involved in the anti-proliferative effects mediated by RA and 4HPR. In addition, we present a further characterization of *OVCA2* and show that it is a highly

conserved gene that is related to a variety of alpha-beta hydrolases including esterases, lipases and other enzymes.

MATERIALS AND METHODS

Northern Blot Analysis. Multiple tissue Northern blots containing 5 μ g of poly(A)⁺-selected mRNA from various human tissues were purchased from Clontech. Blots were hybridized with a ~830 bp cDNA probe corresponding to exon 13 of *OVCA1* and exon 2 of *OVCA2* or a ~200 bp cDNA probe corresponding to exon 1 of *OVCA2*.

Antibodies. Anti- β -actin was purchased from Sigma. The anti-*OVCA1* antibodies TJ132 and FC22 have been described previously (Bruening et al., 1999). For the production of anti-*OVCA2* antibodies a peptide corresponding to amino acids 27 to 41 of *OVCA2* was synthesized (Research Genetics, Huntsville, AL). Purity of the peptide was confirmed by high performance liquid chromatography. The peptide was conjugated to maleimide activated keyhole limpet hemocyanin (Pierce, Rockford, IL) and was used to immunize a New Zealand White rabbit (Cocalico Biologicals, Reamstown, PA). Two mg of antigenic peptide were covalently linked to Aminolink agarose (Pierce) and was used to purify anti-*OVCA2* antibody according to the manufacturer's instructions. The final antibody was referred to as TJ143.

Cell lines. Cos-1, MCF-7, SKOV-3, HeLa, A2780, Calu-6 and F9 cells were maintained in DMEM supplemented with 10% FCS, glutamine and insulin. F9 cells were grown on gelatin coated flasks. A549 cells were maintained in Kaighn's modification of Ham's F12 medium supplemented with 10% FCS and glutamine. HL-60 cells were maintained in RPMI1640 supplemented with 20% FCS and glutamine. Human ovarian surface epithelial cell lines expressing SV-40 large T-antigen (HIO cells) have been previously described (Schultz et al., 1995).

cDNA Cloning and Cell Transfections. Cloning of the full-length *OVCA2* cDNA and genomic DNA was previously described (Schultz et al., 1996). Genomic *OVCA2* DNA was subcloned into the mammalian expression vector pcDNA3 (Invitrogen) by PCR-amplifying a DNA fragment using gene specific primers containing BamHI (5') or EcoRI (3') restriction endonuclease sites, digesting the fragment, and cloning it into the multiple cloning sequence of pcDNA3. To produce an N-terminal hemagglutinin (HA) tagged *OVCA2* expression vector, *OVCA2* cDNA was first cloned into the HA containing mammalian expression vector, J3H then the HA-*OVCA2* cDNA was subcloned into pcDNA3. Cell lines were transfected during the log phase of growth with 5µg of vector using the Superfect reagent (QIAGEN), according to manufacturer's instructions.

Preparation of Protein Extracts. Whole cell extracts were made by incubating cells in PBSTDS (10mM Na₂HPO₄, 150mM NaCl, 1% triton X-100, 0.5% deoxycholic acid, 0.1% SDS, 0.2% NaN₃, 1mM EDTA, 5mM NaF, 100µg/ml PMSF, 1µg/ml leupeptin, 0.7 µg/ml pepstatin, pH 7.25) as described previously (Bruening et al., 1999). Quantitation of protein was determined using a bicinchoninic acid/copper (II) sulfate assay (Sigma). Extracts from normal human tissues were purchased from Clontech.

SDS-PAGE and Western Blot Analysis. Fifty µg of total protein extract from tissues or 30µg of total protein from cell extracts, unless otherwise stated, were separated by standard SDS-PAGE and transferred to Immobilon-P (Millipore). The membranes were blocked either in 3% BSA and probed with anti-*OVCA1* antibody TJ132 or in 5% dried milk and probed with the anti-*OVCA2* antibody TJ143, the anti-*OVCA1* antibody FC22 or the anti-β-actin antibody (Sigma).

Cell Culture Treatments. All-trans Retinoic Acid (RA) (Sigma) and N-(4-hydroxyphenyl)retinamide (4HPR) (NIH) were dissolved in ethanol at a stock concentration of 10mM. Cells were treated for a period of 4 days and culture media with or without drugs was replaced every 48 hours. F9 cells were treated with 10⁻⁷M RA and 1µM 4HPR. Calu-6 and A549

cells were treated with 10 μ M RA and 4HPR and HL-60 cells were treated with 1 μ M RA and 3 μ M 4HPR. A549 cells were cultured in 1% FCS for 1 week or were cultured for 3 days after confluence.

Sequence Analysis. GenBank/EMBL and SwissProt. sequences showing homology to OVCA2 were identified using the basic local alignment search tool (BLAST, NCBI). DNA and amino acid sequence comparisons and motif analyses were performed with the Wisconsin Package versions 8 and 9.1 (Genetics Computer Group, GCG).

Homology Modeling of OVCA2. We used methods described previously to build a model of OVCA2 (Dunbrack, 1999; Salicioni et al., 2000). Briefly, PSI-BLAST was used to build a sequence profile of OVCA2 by iteratively searching the non-redundant protein sequence database available from NCBI (Altschul and Koonin, 1998). Only sequences with expectation values better than 0.0001 were included in the sequence profile matrix. Upon completion, this matrix was used to search a database of protein sequences in the Protein Data Bank (Berman et al., 2000) of experimentally determined protein structures. A model of OVCA2 was built using the side-chain conformation prediction program SCRWL (Bower et al., 1997), which works by building sidechains on a template backbone by first placing residues according to a backbone-dependent rotamer library (Dunbrack and Cohen, 1997), followed by a combinatorial search to remove steric overlaps.

RESULTS

***OVCA1* and *OVCA2* are distinct genes.**

We and others have previously defined a minimum region of allelic loss (MRAL) on chromosome 17p13.3 in genomic DNA from ovarian tumors (Phillips et al., 1996; Schultz et al., 1996). Positional cloning and sequencing techniques revealed two genes in the MRAL, referred to as *OVCA1/DPH2L* and *OVCA2* which overlap one another in the MRAL, and have one exon in

common (Phillips et al., 1996; Schultz et al., 1996) (**Figure 1**). The *OVCA2* gene contains 1012 bp, and is composed of 2 exons (184 bp and 828 bp) (**Figure 1**). Exon 2 is also exon 13 of *OVCA1/DPH2L* (**Figure 1**). However, translation of *OVCA1* does not proceed into the shared exon, and *OVCA2* and *OVCA1* are completely distinct proteins. The full cDNA sequence of *OVCA1* and *OVCA2* has been deposited into GenBank (accession numbers AF335321 and AF321875, respectively).

Analysis of OVCA1 and OVCA2 under conditions of growth arrest, apoptosis and differentiation.

Recent studies suggested that *OVCA1* was downregulated in response to cell differentiation, growth arrest and apoptosis induced by RA. Since the results were in contrast to our previous findings of dramatic growth suppression induced by overexpression of *OVCA1*, we elucidated the expression of *OVCA1* and *OVCA2* in response to RA and 4HPR. Three human cell lines, the lung cancer cell lines Calu-6 and A549, the promyelocytic leukemia cell line HL-60, and the mouse embryonic fibroblast cell line F9 were treated with RA and 4HPR over a period of 4 days. Calu-6 and A549 cells were treated with 10 μ M RA and 4HPR, HL-60 cells were treated with 1 μ M RA and 3 μ M 4HPR and F9 cells were treated with 10⁻⁷M RA and 1 μ M 4HPR. The effects of RA and 4HPR have been previously reported in these cell lines: In HL-60 cells RA promotes differentiation, followed by apoptosis and 4HPR induces apoptosis (Delia et al., 1993; Martin et al., 1990); F9 cells treated with RA and 4HPR undergo both differentiation and apoptosis (Atencia et al., 1994; Clifford et al., 1999); Calu-6 cells undergo apoptosis in response to RA and 4HPR and A549 cells are resistant to RA (Li et al., 1998; Liu et al., 2000; van der Leede et al., 1993).

In order to determine whether the RA and 4HPR treatments were affecting the growth properties of our cell lines, we performed direct cell counts (**Figure 2A**). All cell lines that were treated with the drugs showed a decrease in cell number compared to control, except A549 cells treated with RA which have previously been shown to be resistant to RA. Although it has been suggested that A549 cells are also resistant to 4HPR, as determined by FACS analysis (Liu et al., 2000), we saw an

approximate 40-50% decrease in cell number in A549 cells treated with 4HPR compared to control cells in 3 separate experiments. It is known that many cell lines which are resistant to RA are affected by 4HPR (Chiantore et al., 1999; Clifford et al., 1999; Reynolds et al., 2000; Sun et al., 1999), although there has not been a thorough investigation of the effects of 4HPR on A549 cells. We also analyzed HL-60 cells by FACS analysis. HL-60 cells showed a dramatic arrest in G_1/G_0 and an increased sub G_1/G_0 fraction indicating increased cell death (HL60: % G_1/G_0 21.6; %S 50.8; % G_2 10.4; %< G_1/G_0 12.3; HL60 RA: % G_1/G_0 66.7; %S 9.58; % G_2 3.58; %< G_1/G_0 20.2; HL60 4HPR: % G_1/G_0 46.6; %S 19.4; % G_2 5.93; %< G_1/G_0 28.4).

We analyzed the expression of OVCA1 and OVCA2 following RA and 4HPR treatment by Western blot analysis. Antibodies against amino acids 27-41 of OVCA2 were generated by injecting the peptide into rabbits and the anti-serum was immunoaffinity purified (referred to as TJ143). The anti-OVCA1 antibodies TJ132 and FC22 have been described previously (Bruening et al., 1999). In Calu-6 cells and HL-60 cells OVCA2 protein levels were downregulated by RA and 4HPR (**Figure 2B**). In F9 cells and A549 cells, OVCA2 was unaffected. OVCA1 protein levels were unaffected by RA and 4HPR in all these cell lines (**Figure 2B**). OVCA2 protein levels were unaffected by growth arrest induced by cell confluence for 3 days or low serum for 1 week in A549 cells, whereas OVCA1 levels were decreased slightly in serum deprived cells (**Figure 2C**). Overall, our results were not consistent with a previous report (Liu et al., 2000) and suggest that OVCA2, not OVCA1 may be regulated by RA and 4HPR.

OVCA2 has a Broad Tissue Distribution.

In order to further characterize *OVCA2* we analyzed *OVCA2* mRNA expression in a variety of tissues. Multiple tissue Northern blots were probed with the exon 2/13 of *OVCA1/2* or the unique exon 1 of *OVCA2* (**Figure 3**). As shown in **Figure 3A**, all tissues showed two bands (~2.4 kb and ~1.3 kb). When our blots were re-probed with an exon 1 probe of *OVCA2*, all tissues tested showed only the 1.3 kb band representing the *OVCA2* transcript, with testis, heart, skeletal muscle, liver and pancreas showing high mRNA expression (**Figure 3B**).

In addition, we analyzed OVCA2 protein expression in a number of cell lines and tissues. Western blot analysis using the anti-OVCA2 antibody TJ143 revealed that Cos-1 cells, transfected with a genomic DNA fragment containing the two exons of OVCA2 under the control of a CMV promoter, produced the predicted ~25 kDa protein (**Figure 4A**). The same results were obtained when Cos-1 cells were transfected with the OVCA2 cDNA (not shown), indicating that the mRNA transcribed from the genomic DNA was correctly spliced within the cells. The antibody also detected endogenous OVCA2 in various breast and ovarian cell lines (**Figure 4A**) and in a variety of human tissues (**Figure 4B**). Of the tissues analyzed, the kidney, liver, testis, placenta and thymus all showed high levels of OVCA2 (**Figure 4B**).

OVCA2 is Highly Evolutionarily Conserved

The OVCA2 protein consists of 227 amino acids (**Figure 5**). A BLAST search of GenBank/EMBL and Swissprot databases revealed that *OVCA2* does not match any known mammalian genes. However, one *C. elegans* and 4 yeast proteins were identified which showed up to 60% similarity and up to 45% identity to the amino acid sequence of OVCA2, and contained a similar number of amino acids (**Figure 5**). These sequences were described as putative dihydrofolate reductases (DHFRs), but they share more conserved domains with OVCA2 than with mammalian DHFRs (data not shown). A BLAST search of the EST database revealed full length mouse and partial rat OVCA2 homologues displaying 87% and 86% similarity, respectively, to the amino acid sequence of OVCA2. In addition, two plant ESTs (rice and arabidopsis) (up to 53% similar), and multiple human sequences were identified. A multiple sequence alignment of OVCA2 with all available non-human OVCA2 homologues (**Figure 5**) revealed at least 5 conserved domains, which presently have no known function, but which may be important new functional domains based on their evolutionary conservation. Zoo blots probed with the unique exon 1 of *OVCA2* demonstrated that all mammalian species tested have an *OVCA2* homologue (data not shown). Interestingly, when exon 2 of *OVCA2*, which is a non-coding exon of *OVCA1*, was used to probe these blots, both *OVCA2* and *OVCA1* bands were identified, suggesting that the genomic

arrangement of the two genes is conserved among many different species. This high degree of evolutionary conservation suggests that *OVCA2* may be very important for normal cellular function.

The Genetics Computer Group (GCG) package was used to evaluate functional motifs within the *OVCA2* amino acid sequence (**Figure 5**). Two protein kinase C phosphorylation sites (a.a. 18 and a.a. 178), two casein kinase-2 phosphorylation sites (a.a. 76 and a.a. 84), and a possible leucine zipper variant (a.a. 95) were identified, all of which are conserved within the available mouse and rat sequences. In addition, a MYB DNA binding motif was observed (a.a. 83), which is identical to the native MYB motif, except for a conservative amino acid change from tryptophan to phenylalanine. Interestingly, this domain contains one of the casein kinase-2 phosphorylation sites. No other functional groups were identified which could provide clues to the function of *OVCA2*.

OVCA2 protein model.

Sequence analysis using PSI-BLAST indicated that *OVCA2* is related to the N-terminal domain of some dihydrofolate reductases (DHFRs), notably DYR_SCHPO, a DHFR in yeast. This domain has a hydrolase fold that is found in alpha-beta hydrolases including esterases and lipases, and includes the three residues of the catalytic triad, Asp, Ser, His (**Figure 6**). The crystal structure of Protein Data Bank entry 1AUR (Kim et al., 1997) was used to build a model of *OVCA2* using the sidechain conformation prediction program SCWRL (Bower et al., 1997). The sequence identity between *OVCA2* and the crystal structure is only 13% but the same fold was identified with high confidence with three different programs, PSI-BLAST (Altschul and Koonin, 1998), 3d-pssm (Kelley et al., 2000) and Threader (Jones et al., 1992). The significance of this domain within the DHFRs, however, has yet to be reported.

DISCUSSION

We have found that *OVCA2* can be downregulated in cells in response to RA and 4HPR, but that *OVCA1* is unaffected. This is in contrast to a recent paper by Liu *et al* (2000) where it was reported

that *OVCA1/DPH2L* mRNA levels were decreased in several cancer cell lines after treatment with RA or 4HPR (Liu et al., 2000). The authors used mRNA differential display to uncover genes modulated by RA in human lung cancer cell lines and a clone was identified that was homologous to the 3'UTR of *OVCA1/DPH2L*. They performed Northern blot analysis with a probe to a 3' fragment of *OVCA1/DPH2L* which detected both a ~2.3kb transcript and a ~1.7kb transcript, which is consistent with our Northern blot data when probed with exon2/13 of *OVCA1/2*. We and Phillips *et al* have previously described the 2.4kb/2.3kb transcript to be *OVCA1/DPH2L* (Phillips et al., 1996; Schultz et al., 1996). However, Liu *et al* interpreted the ~1.7kb transcript to be a smaller transcript of *OVCA1/DPH2L*. We have now clarified that the 1.7kb/1.3kb transcript encodes for *OVCA2*, which is an entirely different protein from *OVCA1/DPH2L*.

We have found that *OVCA2* is downregulated in response to RA and 4HPR in Calu-6 cells and HL-60 cells. However *OVCA2* was not downregulated in F9 cells treated with either RA or 4HPR. This is not entirely surprising due to the differences in the cell types. F9 cells are mouse embryonic cells whereas Calu-6 and HL-60 cells are human cancer cell lines. We have evaluated the sequence of the *OVCA2* promoter for potential retinoic acid response elements (RAREs) and AP1 binding sites. Our initial screen of the first 10kbp of genomic sequence upstream of exon 1 failed to uncover any of the common RARE consensus sequences (De Luca, 1991) but did identify three putative AP1 binding sites. *OVCA2* may therefore be downregulated as a consequence of retinoid receptors' antagonizing AP1 activity (Salbert et al., 1993). Although we saw a decrease in cell number after treatment of A549 cells with 4HPR we did not see a concordant decrease in *OVCA2* expression. It is believed that 4HPR has both retinoid receptor dependent and independent effects and the independent effects give rise to growth inhibition in cell lines which are resistant to RA treatment (Clifford et al., 1999; Giandomenico et al., 1999; Sun et al., 1999). It is also interesting that *OVCA2* was not downregulated by other mechanisms of growth arrest such as confluence and low serum. This suggests that *OVCA2* may only be downregulated by a specific factor(s) in a

retinoid receptor-dependent pathway that is common to HL-60 and Calu-6 cells, but not in F9 nor A549 cells.

We have shown that over-expression of *OVCA1* reproducibly inhibits colony formation in several ovarian tumor cell lines and that stable expression of exogenous *OVCA1* expression is difficult to obtain which is consistent with but is not proof of a tumor suppressor function (Bruening et al., 1999). However, over-expression of *OVCA2* in a variety of tumor cell lines has no obvious effects on growth (Prowse and Godwin, unpublished data). The fact that *OVCA2* is downregulated in Calu-6 and HL-60 cells also suggests that *OVCA2* is not a tumor suppressor gene, but may still be involved in growth regulation in the cell. The MRAL, which we have mapped in ovarian tumors (Schultz et al., 1996), is in fact only 20kb and our mapping studies indicate there are only three genes in this region, *OVCA1* and *OVCA2*, which we have previously reported (Schultz et al., 1996) and *OVCA4* which is a testis specific gene (Godwin, unpublished data). It therefore seems likely that *OVCA1*, not *OVCA2*, is the tumor suppressor gene in this region. It is of interest that the HL-60, Calu-6 and A549 cell lines analyzed by Liu *et al* showed no *OVCA1* transcript by Northern blot analysis (Liu et al., 2000), but our analyses do show *OVCA1* protein in these cell lines. This could be due to analyzing different subpopulations of the cell lines and/or could reflect differences in post-transcriptional regulation of *OVCA1*. Their cell lines are of interest since the lack of *OVCA1* transcript suggests that *OVCA1* could be a tumor suppressor gene involved in the development of lung tumors and leukemias. Indeed, studies have shown that loss of heterozygosity (LOH) at 17p is one of the most frequent alterations in lung cancer (Konishi et al., 1998; Tsuchiya et al., 2000). In addition, LOH at 17p13.3 is more frequent than at 17p13.1, where *TP53* maps, and it appeared to occur in the absence of *TP53* mutation and/or 17p13.1 deletion (Konishi et al., 1998; Tsuchiya et al., 2000). It will be important to further investigate the role of *OVCA1* in the development of lung cancer and leukemias.

In summary, *OVCA2* is a novel gene identified on chromosome 17p13.3. *OVCA2* is composed of two exons: a unique exon 1, and an exon 2, which comprises part of the 3' untranslated region of *OVCA1*. Thus, the two genes are overlapping, but their protein products are completely distinct. Both *OVCA1* and *OVCA2* are highly conserved, suggesting they have important roles in the cell. The homology of *OVCA2* to alpha-beta hydrolases suggests that it may have some enzymatic activity, however further studies are required to determine the significance of this. Further analysis of the function(s) of *OVCA2* will help to determine *OVCA2*'s role in retinoid induced growth arrest, differentiation and apoptosis.

ACKNOWLEDGMENTS

This work was supported in part by National Institutes of Health Grants RO1 CA-70328 (to A.K.G.), the United States Army Medical Research Grant DAMD17-96-1-6088 (to A.K.G.), the Ovarian Cancer Research Fund (to AKG), a grant from the American Cancer Society (to R.L.D.), and by an appropriation from the Commonwealth of Pennsylvania.

REFERENCES

Altschul, S.F. and Koonin, E.V., Iterated profile searches with PSI-BLAST--a tool for discovery in protein databases. *Trends Biochem Sci*, **23**, 444-7. (1998).

Atencia, R., Garcia-Sanz, M., Unda, F. and Arechaga, J., Apoptosis during retinoic acid-induced differentiation of F9 embryonal carcinoma cells. *Exp Cell Res*, **214**, 663-7. (1994).

Berman, H.M., Westbrook, J., Feng, Z., Gilliland, G., Bhat, T.N., Weissig, H., Shindyalov, I.N. and Bourne, P.E., The Protein Data Bank. *Nucleic Acids Res*, **28**, 235-42. (2000).

Bower, M.J., Cohen, F.E. and Dunbrack, R.L., Prediction of protein side-chain rotamers from a backbone-dependent rotamer library: a new homology modeling tool. *J Mol Biol*, **267**, 1268-82. (1997).

Bruening, W., Prowse, A.H., Schultz, D.C., Holgado-Madruga, M., Wong, A. and Godwin, A.K., Expression of OVCA1, a candidate tumor suppressor, is reduced in tumors and inhibits growth of ovarian cancer cells. *Cancer Res*, **59**, 4973-83. (1999).

Chambon, P., Hansen, L.A., Sigman, C.C., Andreola, F., Ross, S.A., Kelloff, G.J. and De Luca, L.M., The retinoid signaling pathway: molecular and genetic analyses. *Semin Cell Biol*, **5**, 115-25. (1994).

Chiantore, M.V., Giandomenico, V. and De Luca, L.M., Carcinoma cell lines resistant for growth inhibition and apoptosis to retinoic acid are responsive to 4-hydroxy-phenyl-retinamide: correlation with tissue transglutaminase. *Biochem Biophys Res Commun*, **254**, 636-41. (1999).

Clifford, J.L., Menter, D.G., Wang, M., Lotan, R. and Lippman, S.M., Retinoid receptor-dependent and -independent effects of N-(4-hydroxyphenyl)retinamide in F9 embryonal carcinoma cells. *Cancer Res*, **59**, 14-8. (1999).

De Luca, L.M., Retinoids and their receptors in differentiation, embryogenesis, and neoplasia. *Faseb J*, **5**, 2924-33. (1991).

Delia, D., Aiello, A., Lombardi, L., Pelicci, P.G., Grignani, F., Formelli, F., Menard, S., Costa, A., Veronesi, U. and Pierotti, M.A., N-(4-hydroxyphenyl)retinamide induces apoptosis of malignant hemopoietic cell lines including those unresponsive to retinoic acid. *Cancer Res*, **53**, 6036-41. (1993).

DiSepio, D., Sutter, M., Johnson, A.T., Chandraratna, R.A. and Nagpal, S., Identification of the AP1-antagonism domain of retinoic acid receptors. *Mol Cell Biol Res Commun*, **1**, 7-13. (1999).

Dunbrack, R.L., Comparative modeling of CASP3 targets using PSI-BLAST and SCWRL. *Proteins, Suppl*, 81-7. (1999).

Dunbrack, R.L. and Cohen, F.E., Bayesian statistical analysis of protein side-chain rotamer preferences. *Protein Sci*, **6**, 1661-81. (1997).

Evans, T.R., Kaye, S.B., Hansen, L.A., Sigman, C.C., Andreola, F., Ross, S.A., Kelloff, G.J. and De Luca, L.M., Retinoids: present role and future potential. *Br J Cancer*, **80**, 1-8. (1999).

Giandomenico, V., Andreola, F., Rodriguez de la Concepcion, M.L., Collins, S.J. and De Luca, L.M., Retinoic acid and 4-hydroxyphenylretinamide induce growth inhibition and tissue transglutaminase through different signal transduction pathways in mouse fibroblasts (NIH 3T3 cells). *Carcinogenesis*, **20**, 1133-5. (1999).

Hansen, L.A., Sigman, C.C., Andreola, F., Ross, S.A., Kelloff, G.J. and De Luca, L.M., Retinoids in chemoprevention and differentiation therapy. *Carcinogenesis*, **21**, 1271-9. (2000).

Jones, D.T., Taylor, W.R. and Thornton, J.M., A new approach to protein fold recognition. *Nature*, **358**, 86-9. (1992).

Kelley, L.A., MacCallum, R.M. and Sternberg, M.J., Enhanced genome annotation using structural profiles in the program 3D-PSSM. *J Mol Biol*, **299**, 499-520. (2000).

Kim, K.K., Song, H.K., Shin, D.H., Hwang, K.Y., Choe, S., Yoo, O.J. and Suh, S.W., Crystal structure of carboxylesterase from *Pseudomonas fluorescens*, an alpha/beta hydrolase with broad substrate specificity. *Structure*, **5**, 1571-84. understanding of the molecular pathogenesis of this fatal disease. (1997).

Kitareewan, S., Spinella, M.J., Allopenna, J., Reczek, P.R. and Dmitrovsky, E., 4HPR triggers apoptosis but not differentiation in retinoid sensitive and resistant human embryonal carcinoma cells through an RARgamma independent pathway. *Oncogene*, **18**, 5747-55. (1999).

Konishi, H., Takahashi, T., Kozaki, K., Yatabe, Y., Mitsudomi, T., Fujii, Y., Sugiura, T. and Matsuda, H., Detailed deletion mapping suggests the involvement of a tumor suppressor gene at 17p13.3, distal to p53, in the pathogenesis of lung cancers. *Oncogene*, **17**, 2095-100. (1998).

Li, Y., Dawson, M.I., Agadir, A., Lee, M.O., Jong, L., Hobbs, P.D. and Zhang, X.K., Regulation of RAR beta expression by RAR- and RXR-selective retinoids in human lung cancer cell lines: effect on growth inhibition and apoptosis induction. *Int J Cancer*, **75**, 88-95. (1998).

Liu, G., Wu, M., Levi, G. and Ferrari, N., Down-regulation of the Diphthamide biosynthesis protein 2-like gene during retinoid-induced differentiation and apoptosis: implications against its tumor-suppressor activity. *Int J Cancer*, **88**, 356-62. (2000).

Martin, S.J., Bradley, J.G. and Cotter, T.G., HL-60 cells induced to differentiate towards neutrophils subsequently die via apoptosis. *Clin Exp Immunol*, **79**, 448-53. (1990).

Nagpal, S., Athanikar, J. and Chandraratna, R.A., Separation of transactivation and AP1 antagonism functions of retinoic acid receptor alpha. *J Biol Chem*, **270**, 923-7. (1995).

Phillips, N.J., Zeigler, M.R. and Deaven, L.L., A cDNA from the ovarian cancer critical region of deletion on chromosome 17p13.3. *Cancer Lett*, **102**, 85-90. (1996).

Phillips, N.J., Ziegler, M.R., Radford, D.M., Fair, K.L., Steinbrueck, T., Xynos, F.P. and Donis-Keller, H., Allelic deletion on chromosome 17p13.3 in early ovarian cancer. *Cancer Res*, **56**, 606-11. (1996).

Reynolds, C.P., Wang, Y., Melton, L.J., Einhorn, P.A., Slamon, D.J. and Maurer, B.J., Retinoic-acid-resistant neuroblastoma cell lines show altered MYC regulation and high sensitivity to fenretinide. *Med Pediatr Oncol*, **35**, 597-602. (2000).

Salbert, G., Fanjul, A., Piedrafita, F.J., Lu, X.P., Kim, S.J., Tran, P. and Pfahl, M., Retinoic acid receptors and retinoid X receptor-alpha down-regulate the transforming growth factor-beta 1 promoter by antagonizing AP-1 activity. *Mol Endocrinol*, **7**, 1347-56. (1993).

Salicioni, A.M., Xi, M., Vanderveer, L.A., Balsara, B., Testa, J.R., Dunbrack, R.L. and Godwin, A.K., Identification and structural analysis of human RBM8A and RBM8B: two highly conserved RNA-binding motif proteins that interact with OVCA1, a candidate tumor suppressor. *Genomics*, **69**, 54-62. (2000).

Schultz, D.C., Vanderveer, L., Berman, D.B., Hamilton, T.C., Wong, A.J. and Godwin, A.K., Identification of two candidate tumor suppressor genes on chromosome 17p13.3. *Cancer Res*, **56**, 1997-2002. (1996).

Schultz, D.C., Vanderveer, L., Buetow, K.H., Boente, M.P., Ozols, R.F., Hamilton, T.C. and Godwin, A.K., Characterization of chromosome 9 in human ovarian neoplasia identifies frequent genetic imbalance on 9q and rare alterations involving 9p, including CDKN2. *Cancer Res*, **55**, 2150-7. (1995).

Sun, S.Y., Li, W., Yue, P., Lippman, S.M., Hong, W.K. and Lotan, R., Mediation of N-(4-hydroxyphenyl)retinamide-induced apoptosis in human cancer cells by different mechanisms. *Cancer Res*, **59**, 2493-8. (1999).

Tsuchiya, E., Tanigami, A., Ishikawa, Y., Nishida, K., Hayashi, M., Tokuchi, Y., Hashimoto, T., Okumura, S., Tsuchiya, S. and Nakagawa, K., Three new regions on chromosome 17p13.3 distal to p53 with possible tumor suppressor gene involvement in lung cancer. *Jpn J Cancer Res*, **91**, 589-96. (2000).

van der Leede, B.M., van den Brink, C.E. and van der Saag, P.T., Retinoic acid receptor and retinoid X receptor expression in retinoic acid-resistant human tumor cell lines. *Mol Carcinog*, **8**, 112-22. 19104, USA. (1993).

FIGURE LEGENDS

Figure 1. Genomic organization of *OVCA1* (exons shown in black boxes) and *OVCA2* (exons shown in white boxes). *OVCA1* and *OVCA2* map to a 20kb minimum region of allelic loss in ovarian tumors, between the markers D17S28 and D17S5/30, at 17p13.3 (Schultz et al., 1996). The *OVCA1* and *OVCA2* genes overlap one another, and have one exon in common (exon 13 of *OVCA1*

and exon 2 of *OVCA2*). Since translation of *OVCA1* does not proceed into exon 13 in *OVCA1/exon 2* in *OVCA2*, the genes encode for completely distinct *OVCA1* and *OVCA2* proteins.

Figure 2. (A) Growth inhibition of cells treated with RA and 4HPR. Cells were seeded at equal density and were counted using a hemocytometer after 4 days of treatment with ethanol alone (vehicle control), RA or 4HPR. The relative cell number as a percentage of the control is shown for each cell line. (B) Analysis of *OVCA2* and *OVCA1* expression in various cell lines treated with RA and 4HPR compared to control cells (ethanol alone). 30 μ g of extracts from the indicated cell lines and treatments were separated by 12% SDS-PAGE and processed by Western blotting. The blots were probed with the anti-*OVCA2* antibody TJ143 or the anti-*OVCA1* antibody TJ132. For the analysis of *OVCA1* in F9 cells the anti-*OVCA1* antibody FC22 was used because it cross-reacts with mouse *Ovca1*. Anti- β -actin was used a loading control. (C) Analysis of the effects of confluence and low serum on *OVCA2* and *OVCA1* expression. A549 cells were growth arrested by culturing in 1% serum for 1 week or culturing for 3 days after confluence. 30 μ g of extracts from the indicated treatments were separated by 12% SDS-PAGE and processed by Western blotting. The blots were probed with the anti-*OVCA2* antibody TJ143 or the anti-*OVCA1* antibody TJ132. Anti- β -actin was used a loading control.

Figure 3. Tissue expression pattern of *OVCA1* and *OVCA2* mRNA. Blots containing 5 μ g of polyA⁺ selected mRNA from each of the indicated human tissues were hybridized with a ~830 bp cDNA probe corresponding to exon 13 of *OVCA1* and exon 2 of *OVCA2* (A) or a ~200 bp cDNA probe corresponding to exon 1 of *OVCA2* (B). Size standards are in kilobases.

Figure 4. (A) Characterization of *OVCA2* expression. 20 μ g of extracts from the indicated cell lines were separated by 12% SDS-PAGE and processed by Western blotting. The blot was probed with the anti-*OVCA2* antibody, TJ143. Lane *Cos-1/OVCA2*, extract of *Cos-1* cells that had been

transfected with pcDNA3-OVCA2; lanes *HIO-118*, *HIO-135*, *HIO-117*, extracts from SV40 Tag-immortalized human ovarian surface epithelial cell lines (HIO); lane *primary ovarian cell line*, extract from human ovarian surface epithelial cell line; lanes *A2780* and *SKOV3*, extracts from ovarian cancer cell lines; lane *MCF-7*, extract from breast cancer cell line. (B) OVCA2 expression in human tissues. 50µg of extracts from the indicated human tissues (Clontech) were separated by 12% SDS-PAGE and processed by Western blotting. The blot was probed with the anti-OVCA2 antibody TJ143.

Figure 5. Multiple sequence alignment of OVCA2 amino acid sequence and similar sequences from mouse, rat, *C.elegans*, *S.cerevisiae*, *S.pombe*, rice and arabidopsis. At least 5 conserved regions are evident. Two protein kinase C phosphorylation sites (PKC), two casein kinase-2 sites (CK2), a potential pseudo-leucine zipper motif, and a potential MYB DNA binding site (MYB-DNA) are all indicated.

Figure 6. Molecular model of OVCA2 shown as a ribbon diagram. The three residues of the catalytic triad conserved in alpha-beta hydrolases are shown as stick figures. The model was built from Protein Data Bank entry 1AUR (Kim et al., 1997).

Subject: Comments on Draft Report: Research Computing Information Technology Advisory Committee**Date:** Tue, 04 Sep 2001 12:10:24 -0400**From:** Michael Ochs <m_ochs@fcc.edu>**To:** am_skalka@fcc.edu**CC:** frank <fj_manion@fcc.edu>, p_harsche@fcc.edu, GD_Markham@fcc.edu,
RL_Dunbrack@fcc.edu, rr_hardy@fcc.edu, a_godwin@fcc.edu, E_Ross@fcc.edu,
m_ochs@fcc.edu

Ann,

While I was at the Bioinformatics Gordon conference, Frank forwarded to me a draft of a document on the role of IT in research at Fox Chase, dated August 8. The document nicely laid out the areas generating large sets of data at Fox Chase. I feel that this is an excellent start to dealing with the increasing need for IT in biological research. I wanted to add some additional thoughts, based on the Gordon conference and present work ongoing in the Bioinformatics Facility.

The approach of the draft document was based on the individual areas generating data. However, one of the main themes of the meeting was the integration of different data sources and analysis, which I felt was overlooked. In addition, the document seemed to treat Bioinformatics as only concerned with sequence homology, whereas the researchers at the meeting and our own ongoing work are aiming to integrate analysis across domains. Finally, another major theme both of the conference and of the meetings with the BRITE consortium of independent cancer centers basic research IT groups, which Frank and Bob Robbins from the Hutch brought together, is the requirement for institutions to work together as the problems have become far too large to be tackled by individual research groups.

A) Data Integration

After a discussion at lunch with Michael Waters from the National Center for Toxicogenomics concerning databases and what they are missing in terms of data analysis, I joined with a group he formed to discuss how to make databases work together. Adam Arkin from UC Berkeley discussed how his automated methods of data retrieval (necessary for his modelling work) have been thwarted by constantly changing interfaces (definitions of how to automatically retrieve data) and web page designs (which make finding key features in the response difficult). The group, which included the leaders from the EcoCyc and EcoReg databases, the Moirai databases from Washington University, and Marcus Wiedler (head of Bioinformatics for Bayer AG), is hoping to focus databases around a common core schema to aid automated data retrieval. In reality, most members seemed to feel that stable interfaces (i.e. programming definitions of how to get data) might be more feasible in the near future, though they are not the ideal system. This is an important consideration to our plans at Fox Chase, as we will certainly want to make sure we can retrieve data easily, without constantly expending efforts to update our retrieval subsystems. Also, it is possible that we will develop databases which we wish to serve to the outside community (e.g. Population Science databases and databases developed within the Communication SPORE).

B) Bioinformatics

Bioinformatics focuses on data handling and analysis in an integrated fashion, with planning for the future expansion of databases and tools. Within the document there is a sense that data analysis and retrieval will take place through web interfaces. While this seems reasonable at present, in the future the amount of data will overwhelm this approach. Instead the stable interfaces discussed in the previous section are needed and integrated data analysis needs to be planned. For example, when we decided to create BeoBLAST as a local resource, we

designed the system to allow not only access through the web page, but also automated access (we are submitting our paper on BeoBLAST this week and we hope other institutions will adopt it). This is critical as we move forward with microarray analysis, since we plan to tie the output of the microarray analysis directly into BLAST to return significant hits to cDNAs (which are often ESTs of unknown function) automatically. This in turn will later be tied into our automated annotation system (presently under design after Members expressed high interest last year). The automated system will use a minimal level of intelligence to perform such functions as taking an EST, retrieving a maximal consensus sequence from the TIGR database, and performing BLAST and PSI-BLAST on this sequence and any translated ORFs of some minimal length.

It is important to note that such methods are possible only when data analysis is viewed as an integrated whole, not limited by artificial boundaries based on data generation. Our present plan for handling microarray data, for instance, includes automated reading of the images using WaveRead, which we developed to automatically identify spots and grids in microarray images (we are submitting a revised manuscript for publication this week and Michael Waters is interested in testing it at the National Center for Toxicogenomics). The results will be passed to the analysis system, which presently handles ImaGene output instead, for normalization and then either standard statistical analysis or other more complex analysis (Self Organizing Maps, QT-Clust, and Bayesian Decomposition are planned initially). We plan to add simple visualization, however presently Excel or other files are returned to the researcher. Later we will be able to add proteomics data for more integrated analysis since the system is flexible. The maximum efficiency is gained by making the process seamless, which requires bioinformatics to play a role within each part of the process.

The plan within the document for the creation of a molecular modelling facility is an excellent example of where Fox Chase can leverage its significant intellectual investment to provide a valuable resource. I think this needs to be contrasted to the thought of larger modelling. Several examples of such modelling were presented at the Gordon conference. Cynthia Stokes of Entelos showed a very impressive model of a specific disease, modelled from the level of molecular interactions all the way through organismal response to mixed therapeutics. The model was able to predict rather well the clinical response of individuals in a trial. However Entelos has an extremely large budget and well over 100 scientists dedicated to these models. Masura Tomita of Keio University gave a corresponding example from academia. The E-Cell project at Keio University is attempting to create models of cells by determining all reaction constants in metabolic processes, all signalling mechanisms, all transcription and translation methods, and all other cellular processes. So far they have managed only a reduced minimal cellular model of a prokaryote of 127 genes (reduced from a real organism, *M. genitalium*, with 470 genes). This process is backed by \$120 million in funding from the prefecture as well as several million dollars per year in ongoing support. It is clear that Fox Chase cannot expect to dedicate these kinds of resources. Instead, in Bioinformatics we have focused so far on creation of analysis systems which can be tied to other resources for final analysis while incorporating simple experimental models of the biological systems under study. For example, the Bayesian Decomposition algorithm which I developed allows one to model the transcriptional response as part of the prior knowledge used mathematically within the analysis. Through discussions with Bob Perry and John Burch we have begun to include such details in the modelling. We will later add the ability to interface the analysis with models created either by hand or through the University of Connecticut's V-Cell system (a simplified E-Cell which allows modelling of signalling pathways and transcription).

C) Collaborations

What was very clear from both the Gordon conference, discussions within the BRITE group, and Frank's talks with Michael Liebman at Penn is that

no single academic group is likely to be able to handle the whole job alone. Instead, the interactions with other members of the community are going to play an increasingly large role in the success of any individual Bioinformatics group. As such I used the Gordon conference to initiate contacts with other academic groups. We have invited Toni Kazic from Washington University to talk on database design, including her attempt to define minimal units (semiotes) which can be used to construct consistent database schema. Marcus Wiedler from Bayer has offered us his open source database schema for microarray data, which includes integration of sequence search results and automated BLAST searches as well as standard MIAME data (though it still needs to clear internal Bayer hurdles prior to release). This should be useful regardless of the database system we adopt. I am presenting Michael Waters with information on Bayesian Decomposition and WaveRead, as the National Center for Toxicogenomics is interested in building high throughput systems and has been having problems with microarray image analysis. I have been invited by the program director, Robert Negm, to speak at a special meeting of NCI's Cancer Biomarkers Research Group on using microarray data to identify biomarkers. I am also providing John Smith of the University of Alabama with references and contacts in the visualization community. I will provide the BRITE group with a report on the Gordon conference and on likely places for future collaborations between BRITE and other institutions.

I believe that the integration, from data generation through quantitation and analysis to visualization and modelling, is what is needed to make the analysis of microarray and future high throughput data efficient. By continuing our work in this area and making contacts to leverage our work, we can position Fox Chase to both provide developments and to profit from advances as they occur. But it is important to note that Bioinformatics is essentially this integration throughout the process, so that avoiding artificial divisions based on the data source or on preexisting divisions within the Fox Chase infrastructure is important.

--
Michael Ochs, Ph.D.
Manager, Bioinformatics
Fox Chase Cancer Center
Philadelphia, PA



DEPARTMENT OF THE ARMY
US ARMY MEDICAL RESEARCH AND MATERIEL COMMAND
504 SCOTT STREET
FORT DETRICK, MARYLAND 21702-5012

REPLY TO
ATTENTION OF:

MCMR-RMI-S (70-1y)

29 May 02

MEMORANDUM FOR Administrator, Defense Technical Information
Center (DTIC-OCA), 8725 John J. Kingman Road, Fort Belvoir,
VA 22060-6218

SUBJECT: Request for Change in Distribution Statements

1. The U.S. Army Medical Research and Materiel Command has reexamined the need for the limitation assigned to technical reports written for Grant DAMD17-96-1-6088. Request the limited distribution statements for Accession Documents Number ADB249637 and ADB275131 be changed to "Approved for public release; distribution unlimited." These reports should be released to the National Technical Information Service.

2. Point of contact for this request is Ms. Judy Pawlus at DSN 343-7322 or by e-mail at judy.pawlus@det.amedd.army.mil.

FOR THE COMMANDER:

A handwritten signature in black ink, appearing to read "Phyllis M. Rinehart", is written over the typed name and title.

PHYLIS M. RINEHART
Deputy Chief of Staff for
Information Management